Implementing a Nuclear Power Plant Model for Evaluating Load-Following

Capability on a Small Grid

by

Samet Egemen Arda

A Thesis Presented in Partial Fulfillment
of the Requirements for the Degree
Master of Science

Approved April 2013 by the
Graduate Supervisory Committee:

Keith E. Holbert, Chair
John Undrill
Daniel Tylavsky

ARIZONA STATE UNIVERSITY

May 2013

ABSTRACT

A pressurized water reactor (PWR) nuclear power plant (NPP) model is introduced into Positive Sequence Load Flow (PSLF) software by General Electric in order to evaluate the load-following capability of NPPs.

The nuclear steam supply system (NSSS) consists of a reactor core, hot and cold legs, plenums, and a U-tube steam generator. The physical systems listed above are represented by mathematical models utilizing a state variable lumped parameter approach. A steady-state control program for the reactor, and simple turbine and governor models are also developed. Adequacy of the isolated reactor core, the isolated steam generator, and the complete PWR models are tested in Matlab/Simulink and dynamic responses are compared with the test results obtained from the H. B. Robinson NPP. Test results illustrate that the developed models represents the dynamic features of real-physical systems and are capable of predicting responses due to small perturbations of external reactivity and steam valve opening.

Subsequently, the NSSS representation is incorporated into PSLF and coupled with built-in excitation system and generator models. Different simulation cases are run when sudden loss of generation occurs in a small power system which includes hydroelectric and natural gas power plants besides the developed PWR NPP. The conclusion is that the NPP can respond to a disturbance in the power system without exceeding any design and safety limits if appropriate operational conditions, such as achieving the NPP turbine control by adjusting the speed of the steam valve, are met. In other words, the NPP can participate in the control of system frequency and improve the overall power system performance.

DEDICATION

To

my Mother and Father

ACKNOWLEDGEMENTS

TABLE OF CONTENTS

LIST OF TABLES

LIST OF FIGURES

x

CHAPTER 1

INTRODUCTION

1.1 Motivation

In today's world, nuclear energy plays an important role in electricity generation. In fact, 13.5% of the world's electricity need is provided by nuclear power reactors [1]. It offers carbon-free emission and sustainable energy, and these features make nuclear power more favorable than other generation types for a prospective solution to the world's increasing energy demand.

Based on a report released by the International Atomic Energy Agency (IAEA), the number of nuclear reactors in operation was 435, producing 369 GWe, throughout the world on the last day of 2011. Investigating this result demonstrates a decrease in nuclear electricity generation compared to the last year's report mainly due to the permanent shutdowns of 13 reactors during 2011. Four of the shutdowns took place in Japan because of the nuclear disaster in Fukishima considered as the biggest one after the Chernobyl disaster and the others were in Germany as an implementation of the country's energy policy [2].

Although the disaster in Japan brings the safety issue related to nuclear power to the world's attention once again, it seems utilization of nuclear power with its disadvantages is inevitable. This conclusion can be drawn by just looking at the number of nuclear reactors currently under construction all around the world which is 65 [3]. In addition, renewal of operating licenses of existing nuclear power plants (NPP) and even capacity updates to these power plants are continuing. One last note is that developing

1

countries also are stepping forward in order to have nuclear technology. While the Islamic Republic of Iran constructed and commissioned its first NPP in 2011, several countries including Turkey, the United Arab Emirates and Belarus are in contact and negotiating on an agreement about building NPPs with nuclear reactor vendors such as Russia and The Republic of Korea [2].

International Energy Outlook 2011 reveals that the usage of nuclear power for electricity production will continue to increase and an almost 10% growth is projected by the end of 2035 compared with the data of 2008. The case study utilized by the report factors in some uncertainties such as construction costs, uranium enrichment and safety regulations. Nonetheless, the expected increase in nuclear energy production shows no fluctuations but a nearly linear trend of growth (see Figure 1.1).
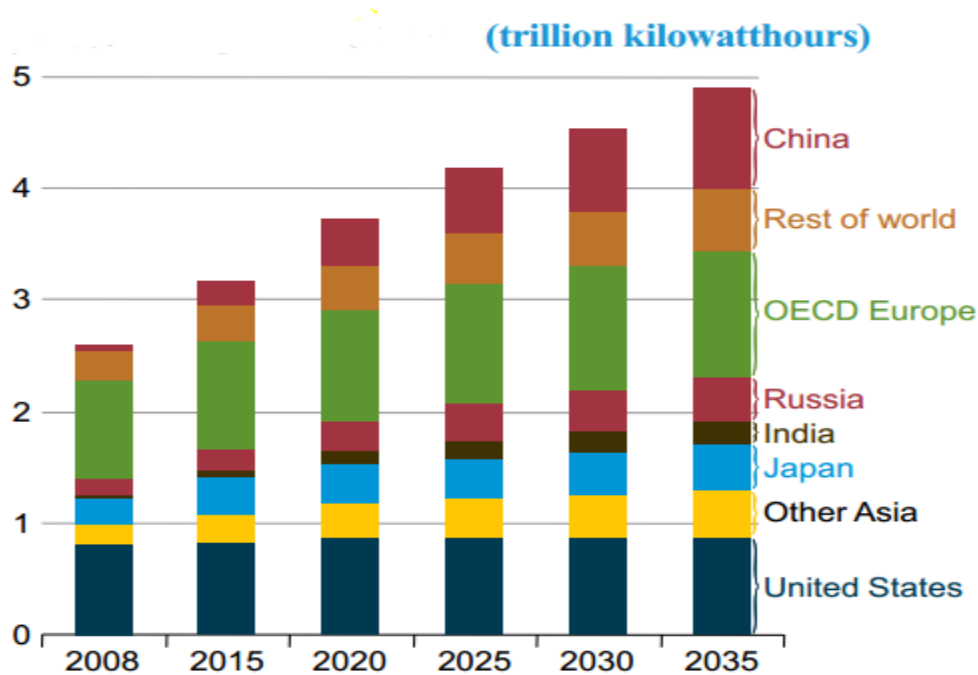
Figure 1.1 World net electricity generation by nuclear power by region [4].

Taking all the factors above into consideration, one can easily conclude that nuclear energy will be on the table in an environment where the energy planning of the future is discussed. The question then arises, is it really possible to operate NPPs as load-following power plants, for the purpose of having a more reliable power system, rather than just producing energy at a constant rate to meet base-load demand? The answer is yes and actually it is already the case in France and Germany. Before moving forward and investigating why these two countries want NPPs to change their output according to power demand, one should know that the main reason of having NPPs as base-load power plants is that they have high capital costs and low operating costs (low fuel costs), the opposite of oil-fired power plants having low capital costs and variable fuel costs. Thus, they are run continuously at flat rate, a decision based upon economics rather than safety limitations [5].

In France, almost 80% of electricity generation comes from nuclear energy with 58 active nuclear reactors. The present situation is a result of the 1973-1974 oil crisis. Since oil prices quadrupled during that time, in order to diminish the effects of such possible future crises on the economy and energy, the French government decided to increase nuclear energy production. That decision was driven by the considerable experience of the country in engineering and scarcity of natural resources. Now, the country is able to generate electricity with the lowest cost in Europe and the greenhouse gas emission has decreased considerably over the 30 years. The huge reliance on nuclear power forces France to use NPPs in a load-following operational mode. For example, electric heating is very common due to the cheap electricity, and temperature fluctuations

3

in winter changes the power demand of the grid a great deal which requires NPPs to adjust their output [6].

In Germany, 22% of the electricity generation is supplied by nuclear power. The governmental regulations are pushing the utilities to increase their renewable energy capacity and the target is to provide 30% of the electricity need of the country from renewable sources [5]. In this scenario, the impact of the intermittent electricity sources in the grid will be augmented meaning that sudden changes in power demand can occur any time. Hence in a power system having NPPs as one of the important participants, like the German power system, NPPs must be operated in the load-following mode to compensate the difference in the total power generation. Figure 1.2 shows how the electricity production of some of the NPPs in Germany changes throughout a day.
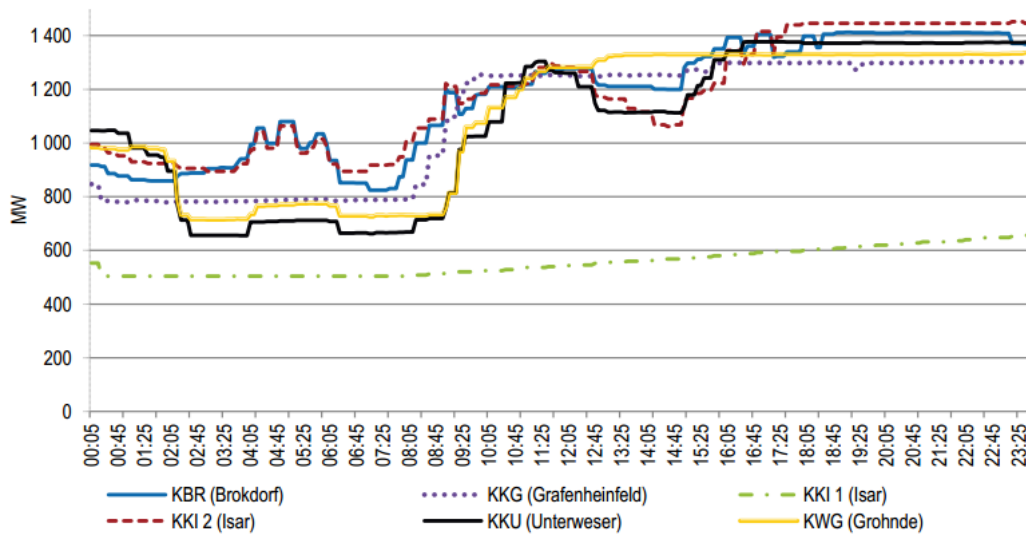
Figure 1.2 The load-following operation with some NPPs in Germany [7].

In this study, it is demonstrated that the load-following operation of a NPP is achievable without exceeding any design and safety limits. For this purpose, a

pressurized water reactor (PWR) NPP is utilized mainly due to the fact that PWRs are the

most widely used reactors in the world.

1.2 Research Objectives and Thesis Organization

The main objectives of this study are based upon the following:

- To establish a PWR NPP model for the 1300 MWe Palo Verde Nuclear
  Generating Station (PVNGS) that reasonably represents dynamic features of it
  with the help of a software package called Positive Sequence Load Flow (PSLF)
  by General Electric (GE);

- To verify whether the model is realistic or not by comparing the results gathered
  from other studies; and

- To evaluate the interaction between the established model and a power network,
  and compare the result to other electricity generation types from that standpoint.

Figure 1.3 gives a brief summary of this study by illustrating which components of a

PWR NPP are developed and which are directly taken from PSLF.
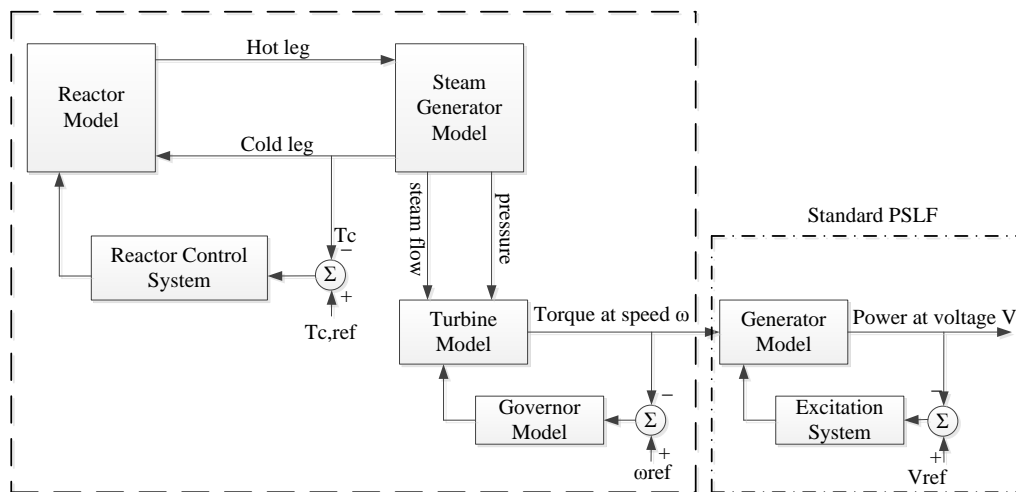
Figure 1.3 Block diagram of a PWR NPP

5

After this introduction, a review of relevant literature and a brief explanation about PSLF are presented in Chapter 2. While Chapter 3 describes the mathematical models of real physical systems in a PWR NPP, Chapter 4 is composed of testing the model in the simulation environment of Matlab/Simulink. The interaction of the model with a relatively small but reasonable power grid is placed in Chapter 5. Lastly, Chapter 6 reiterates the conclusions of the study and points out the areas beyond of the scope of this research and in which future work can be carried out.

CHAPTER 2

LITERATURE REVIEW

2.1 Introduction

The interest in understanding dynamic behavior of NPPs peaked in the 1970s as the computerized simulation techniques evolved. Since then developments in computer technology continued rapidly which made possible modeling real electrical networks and brought powerful power flow solution software into the market. However, only a few of the commercially available software have a model of a NPP to include in dynamic simulations.

Considering the above statement as the problem to which this study brings a solution, NPP modeling related previous studies are presented in Section 2.2. In Section 2.3, reasons for choosing PSLF are explained in addition to a short description of it.

2.2 Previous Studies on Modeling NPP

Before discussing prior works, it should be noted that the most common approach to model a PWR NPP is the state variable lumped parameter modeling approach and all works listed here utilize that method.

Zhao et al. [8-11] presented a number of papers about modeling PWR NPP specifically into the Power System Analysis Software Package (PSASP). All of these papers followed same order; first building the model, and then investigating its dynamic characteristics. Among those papers, [10] only developed isolated core model consisting of neutronics and core dynamics. Presenting test results for small perturbations on reactivity and core inlet temperature was followed by discussion on the effects of fission

product poisoning and negative temperature feedback. Reference [9] presented a NPP model comprised of steam generator, hot and cold legs, and reactor control system in addition to an isolated core model. Responses to a small reactivity change and to a decrease in operating power by 10% were illustrated in order to show the response of the model was concordant with self-stability, reaching a new stable operating point in the case of a change in reactivity without any reactor regulating system, and self-regulating, the ability to adjust the power output according to the power demand with no reactor control system, aspects of PWR NPPs. References [8] and [11] built the model in same manner with [9] but what made them different was extra simulation results gathered from a single machine infinite bus system when a three-phase short circuit fault was applied to one of the lines in the system.

Kerlin et al. [12] developed a mathematical model for the H. B. Robinson NPP producing 740 MWe (2200 MWth). The model included point kinetics, core heat transfer, piping and plenums, pressurizer, and the steam generator. Point kinetics described the reactor power by using six groups of delayed neutrons and reactivity feedback terms caused by fuel temperature, coolant temperature, and primary loop system pressure. Core thermodynamics were represented with nodal approximation in which every axial section used two coolant temperature nodes for every fuel temperature node because of advantages of this approximation over others such as the well-mixed and the arithmetic average approximation. The pressurizer was modeled with the help of mass, energy, and volume balances. Moreover, it was assumed that water-steam mixture in the pressurizer was always at saturated conditions. Finally, a control system for the pressurizer was also

implemented. For the steam generator, a simple model with the representation of primary fluid, tube metal, and secondary fluid lumps for the heat transfer process was used. All piping and plenums were defined with first-order lags while assuming that the heat was transferred without any losses. First, results for an isolated core when 7.1¢ ($ or ¢ are special units for reactivity which are defined to make the amount of reactivity easier to express) reactivity change occurred and isolated steam generator in the case of 1% increase in steam flow were presented. Following that, the response of the complete model to common step disturbances, such as changes in control rod or steam valve position, were compared with actual measurement results for validation of the theoretical model. A final note was made that the proposed model for the H. B. Robinson NPP was able to predict reactivity and steam valve perturbations well.

In his PhD dissertation, Ali [13] investigated the U-tube steam generator (UTSG) and introduced four different models ranging from a three-lump model of a simplified steam generating system to a fourteen-lump detailed model of a UTSG. Governing equations for each model are derived and explained step by step. Dynamic responses of all UTSG models for primary inlet temperature, feedwater temperature, and steam valve perturbations were presented, but only results for a 10% change in steam valve coefficient were utilized so as to make a comparison between the models. The detailed model was coupled with a model for a PWR and the frequency response of the combined system was compared with the experimental results obtained from dynamic tests conducted on the H.B. Robinson NPP. Thus, the adequacy of the detailed UTSG model

was checked. As a final check point, comparisons were made between the detailed model and two other models from previous studies.

Schultz [14] published a book entirely dedicated to control of NPPs. In Chapter 6, several programs for the control of a reactor were investigated by explaining the advantages of one over another program. The first one was the constant-average-temperature program whereby the average temperature of the primary coolant was constant regardless of the power output. It was also mentioned that this type of program was the one requiring the least amount of external control for reactors with negative temperature feedback. The second program kept reactor outlet temperature constant because of possible structural limitations (constant-outlet-temperature program). The last one was favored by the secondary steam system since it was to hold the steam pressure constant while letting primary coolant temperatures increase. A compromise program, basically a non-constant program meaning neither primary coolant average temperature nor steam pressure were constant, was introduced at the end of the theoretical discussion. The mathematical models for each control system were developed.

2.3 PSLF

PSLF is a load flow solution software package by GE. It allows studying power system transmission networks and equipment performance under both steady-state and dynamic conditions. PSLF is able to process large-scale simulations involving a large volume of data and can handle system models of up to 80,000 buses. The abundance of built-in models provides a comprehensive simulation environment. The most important feature, at least for this study, is that the user-defined programming can be achieved by a

programming language called EPCL which is designed mainly to work in conjunction with PSLF [15].

Taking the factors presented above into account, the reasons for choosing PSLF can be summarized in three main points:

1. With the user-defined programming in PSLF, the NPP model which will be developed in this study can be implemented into PSLF;

2. Combining the developed model with excitation and generator models in the software, the complete NPP model can be introduced into any power system for dynamic tests; and

3. The variety of options that built-in models provide makes possible a comparison between the NPP model and other types of power plants like hydroelectric, natural gas, and coal fired power plants.

CHAPTER 3

DEVELOPMENT OF MATHEMATICAL MODELS

In Figure 3.1, a PWR steam supply system is depicted with its major components. In this study, all components except coolant pumps and pressurizer, considering the scope of the thesis, will be modeled for dynamic simulation. In addition, two of the PWR steady-state control options and simple turbine and governor models are presented for the simulations that are run on the model of a small electrical grid.
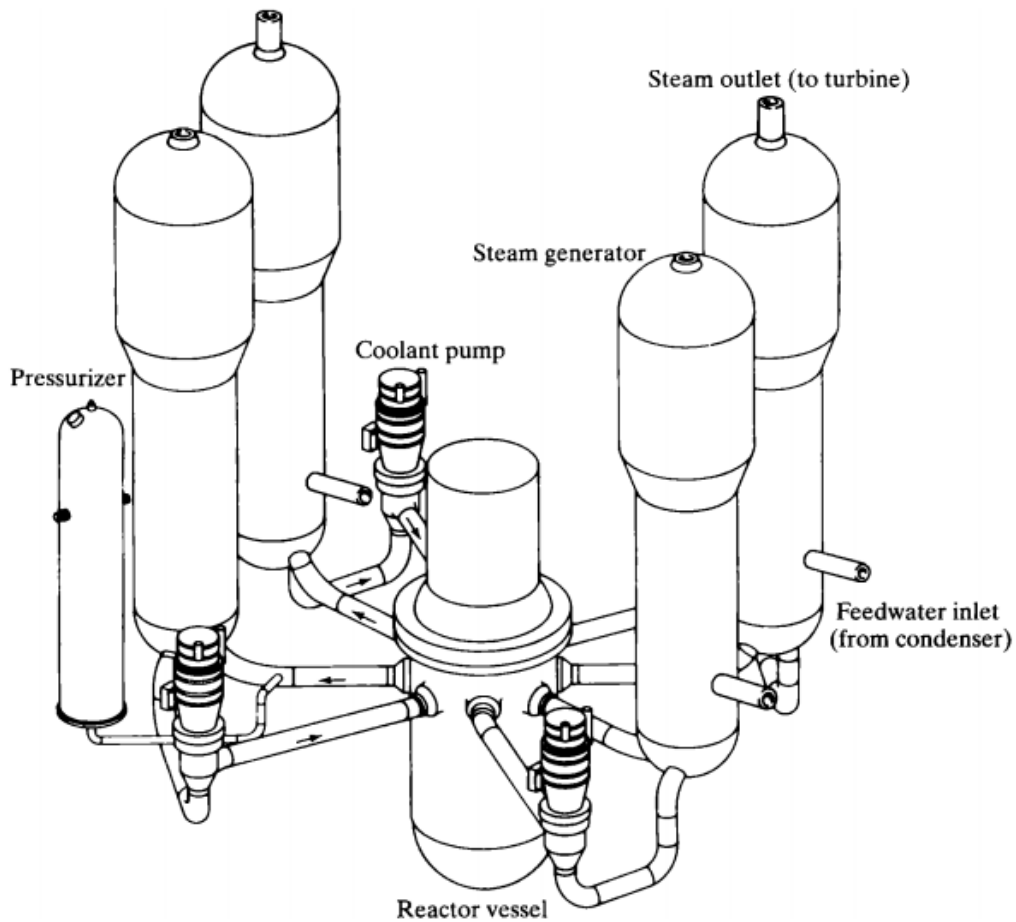
Figure 3.1 Schematic diagram of major components of a PWR [16].

12

3.1 Reactor Core

The reactor core will be modeled in two parts which are the neutron dynamics and

the reactor core fuel and coolant temperature models.

3.1.1 Neutron dynamics model

The point kinetics equations for neutrons describe reactor power, since it is

proportional to average neutron density in the reactor. The equations using a single

combined delayed neutron group are as follows [8]:

$$\frac{dP}{dt} = \frac{\rho(t) - \beta}{\Lambda} P(t) + \lambda C(t)$$

(3.1)

$$\frac{dC}{dt} = \frac{\beta}{\Lambda} P(t) - \lambda C(t)$$

where

$P(t)$ = reactor thermal power,
$C(t)$ = delayed neutron precursors,
$\rho(t)$ = reactivity,
β = effective delayed neutron fraction,
Λ = neutron generation time, and
λ = delayed neutron precursor decay constant.

One should note that reactivity is zero in steady-state while it can be few cents

during reactor power maneuvering

The reactivity term in the above consists of several other terms including

reactivity induced by control rods and feedback effects due to core fuel-coolant

temperatures and pressure

$$\rho = \beta \, \delta\rho_{ext} + \alpha_F \delta T_F + \alpha_C \delta T_C$$

(3.2)

where

$\delta\rho_{ext}$ = reactivity induced by control rods,
α_F = fuel temperature coefficient of reactivity,
δT_F = fuel temperature deviation,

13

α_C = coolant (moderator) temperature coefficient of reactivity,

δT_C = coolant temperature deviation.

After linearization, Equation (3.1) takes the form of

$$\frac{d\delta P}{dt} = \frac{-\beta}{\Lambda}\delta P + \lambda\delta C + \frac{\alpha_F P_0}{\Lambda}\delta T_F + \frac{\alpha_C P_0}{\Lambda}\delta T_C + \frac{\beta P_0}{\Lambda}\delta\rho_{exit}$$

$$\frac{d\delta C}{dt} = \frac{\beta}{\Lambda}\delta P - \lambda\delta C$$

(3.3)

3.1.2 Thermodynamics model

The heat transfer process in the core region will be represented by using Mann's model [17] that utilizes two coolant lumps for every fuel lump. This approach provides better physical representation than utilizing just one coolant lump in which generally the average coolant temperature is the mean value of inlet and outlet coolant temperatures. An illustration the Mann's model is provided in Figure 3.2.
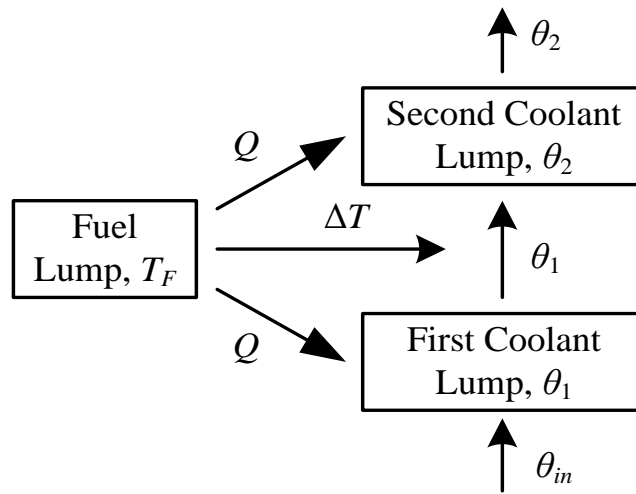
Figure 3.2 Schematic diagram of Mann's model for core dynamics.

A number of assumptions are made in order to simplify the development of the mathematical model:

14

- One-dimensional fluid flow model is utilized.

- Coolant lumps are considered to be well-stirred.

- The fuel-to-coolant heat transfer coefficient is assumed to be constant.

- For the fuel and the primary coolant, constant density and specific heat are assumed.

The governing equations for the thermodynamics model, using the assumptions stated above, with one fuel and two coolant lumps are obtained by performing an energy balance. The equation for the fuel lump is

$$\frac{d}{dt}(m_F c_F T_F) = fP(t) - (UA)_{FC}(T_F - T_{\theta 1}) \tag{3.4}$$

where

T_F = average fuel temperature,
c_F = specific heat of the fuel,
m_F = mass of the fuel,
f = fraction of the total power produced in the fuel,
U_{FC} = heat transfer coefficient from fuel to coolant,
A_{FC} = effective heat transfer surface area,
$T_{\theta 1}$ = temperature of first coolant lump.

The equations for the coolant lumps are

$$\frac{d}{dt}\left(\frac{m_C}{2}c_p T_{\theta 1}\right) = \frac{(1-f)}{2}P(t) + \left(U\frac{A}{2}\right)_{FC}(T_F - T_{\theta 1}) - (\dot{m}_C c_p)(T_{\theta 1} - T_{\theta in}) \tag{3.5}$$

$$\frac{d}{dt}\left(\frac{m_C}{2}c_p T_{\theta 2}\right) = \frac{(1-f)}{2}P(t) + \left(U\frac{A}{2}\right)_{FC}(T_F - T_{\theta 1}) - (\dot{m}_C c_p)(T_{\theta 2} - T_{\theta 1}) \tag{3.6}$$

where

m_C = mass of primary coolant in the core region,
c_p = specific heat of primary coolant,
$\dot{m}_C$ = mass flow rate of coolant in the core,
$T_{\theta in}$ = core inlet coolant temperature,

15

$T_{\theta 2}$ = temperature of second coolant lump,

The equations above can be rearranged so that related time constants become

apparent

$$\frac{dT_F}{dt} = \frac{f}{m_F c_F} P(t) - \frac{1}{\tau_F}(T_F - T_{\theta 1}) \tag{3.7}$$

$$\frac{dT_{\theta 1}}{dt} = \frac{(1-f)}{m_C c_p} P(t) + \frac{1}{\tau_C}(T_F - T_{\theta 1}) - \frac{2}{\tau_R}(T_{\theta 1} - T_{\theta in}) \tag{3.8}$$

$$\frac{dT_{\theta 2}}{dt} = \frac{(1-f)}{m_C c_p} P(t) + \frac{1}{\tau_C}(T_F - T_{\theta 1}) - \frac{2}{\tau_R}(T_{\theta 2} - T_{\theta 1}) \tag{3.9}$$

where

τ_C = coolant heat transfer time constant $= m_C c_p / (UA)_{FC}$

τ_F = fuel heat transfer time constant $= m_F c_F / (UA)_{FC}$

τ_R = coolant residence time in the core $= m_C / \dot{m}_C$

Values of these time constants for PVNGS are presented in Table 3.1 and all parameters

related to the reactor core are tabulated in Appendix B.1.

Table 3.1 Time constants for thermodynamics model

Variable	Value
τ_C	7.170 sec
τ_F	4.376 sec
τ_R	0.674 sec

3.2 Plenums

In order to have a better representation of the dynamic response of the NPP, one

should model the reactor core upper (exit) and lower (inlet) plenums, and steam generator

16

inlet and outlet plenums. The heat balance in first-order differential equation form for the

reactor upper plenum is

$$\frac{d}{dt}\left(m_{C,RXU} c_p T_{RXout}\right) = \dot{m}_C c_p \left(T_{\theta 2} - T_{RXout}\right) \tag{3.10}$$

$$\frac{dT_{RXout}}{dt} = \frac{1}{\tau_{RXU}} \left(T_{\theta 2} - T_{RXout}\right) \tag{3.11}$$

where

$\quad m_{C,RXU}$ = mass of the primary coolant in the reactor core upper plenum,

$\quad T_{RXout}$ = reactor vessel outlet temperature,

$\quad \tau_{RXU}$ = coolant residence time in the reactor core upper plenum.

Since the other plenums follow the same pattern, only the model for reactor core

upper plenum is explicitly stated in this section.

3.3 Hot and Cold Legs

Temperature models for the hot and cold legs can be also expressed by the first-

order lag.

$$\frac{d}{dt}\left(m_{C,HL} c_p T_{HL}\right) = \dot{m}_{C,HL} c_p \left(T_{RXout} - T_{HL}\right) \tag{3.12}$$

$$\frac{d}{dt}\left(m_{C,CL} c_p T_{CL}\right) = \dot{m}_{C,CL} c_p \left(T_{PO} - T_{CL}\right) \tag{3.13}$$

Rearranging the above equations yields

$$\frac{dT_{HL}}{dt} = \frac{1}{\tau_{HL}} \left(T_{RXout} - T_{HL}\right) \tag{3.14}$$

$$\frac{dT_{CL}}{dt} = \frac{1}{\tau_{CL}} \left(T_{PO} - T_{CL}\right) \tag{3.15}$$

where

$\quad m_{C,HL}$ = primary coolant mass in the hot leg,

$\quad T_{HL}$ = temperature of hot leg,

17

$\dot{m}_{C,HL}$ = coolant mass flow in the hot leg,

$m_{C,CL}$ = primary coolant mass in the cold leg,

T_{CL} = temperature of cold leg,

$\dot{m}_{C,CL}$ = coolant mass flow in the cold leg,

τ_{HL} = coolant residence time in the hot leg,

τ_{CL} = coolant residence time in the cold leg.

Before leaving this section, all time constants related to piping and plenums are listed in Table 3.1. The related parameters for the calculation of these time constants are shown in Appendix B.2.

Table 3.2 Time constants for plenums, hot and cold legs

Location	Value
Reactor outlet plenum (τ_{RXU})	2.517 sec
Reactor inlet plenum (τ_{RXL})	2.145 sec
Hot leg (τ_{HL})	0.234 sec
Cold leg (τ_{CL})	1.310 sec
Steam generator outlet plenum (τ_{SGO})	0.726 sec
Steam generator inlet plenum (τ_{SGI})	0.659 sec

3.4 Steam Generator

The steam generator model is the most complicated one due to two-phase flow in the secondary side. As a result, developing the model for it requires more effort. Bearing that in mind, the assumptions used for the steam generator model are listed below:

- One-dimensional fluid flow model is utilized for both the primary and secondary coolants.

- Perfect feedwater control is assumed.

18

- For the primary coolant, constant density and specific heat are assumed.

- Thermal conductivity of the tube metal is assumed to be constant.

- Heat transfer coefficients are assumed to be constant during transients.

- Thermodynamic properties of saturated water and steam are considered to be linear functions of pressure close to the steady-state operating level.

As demonstrated in Figure 3.3, most of the lower part of a steam generator is occupied by tube bundles, and the upper region is equipped with moisture separators ensuring that a high quality steam passes through turbines.
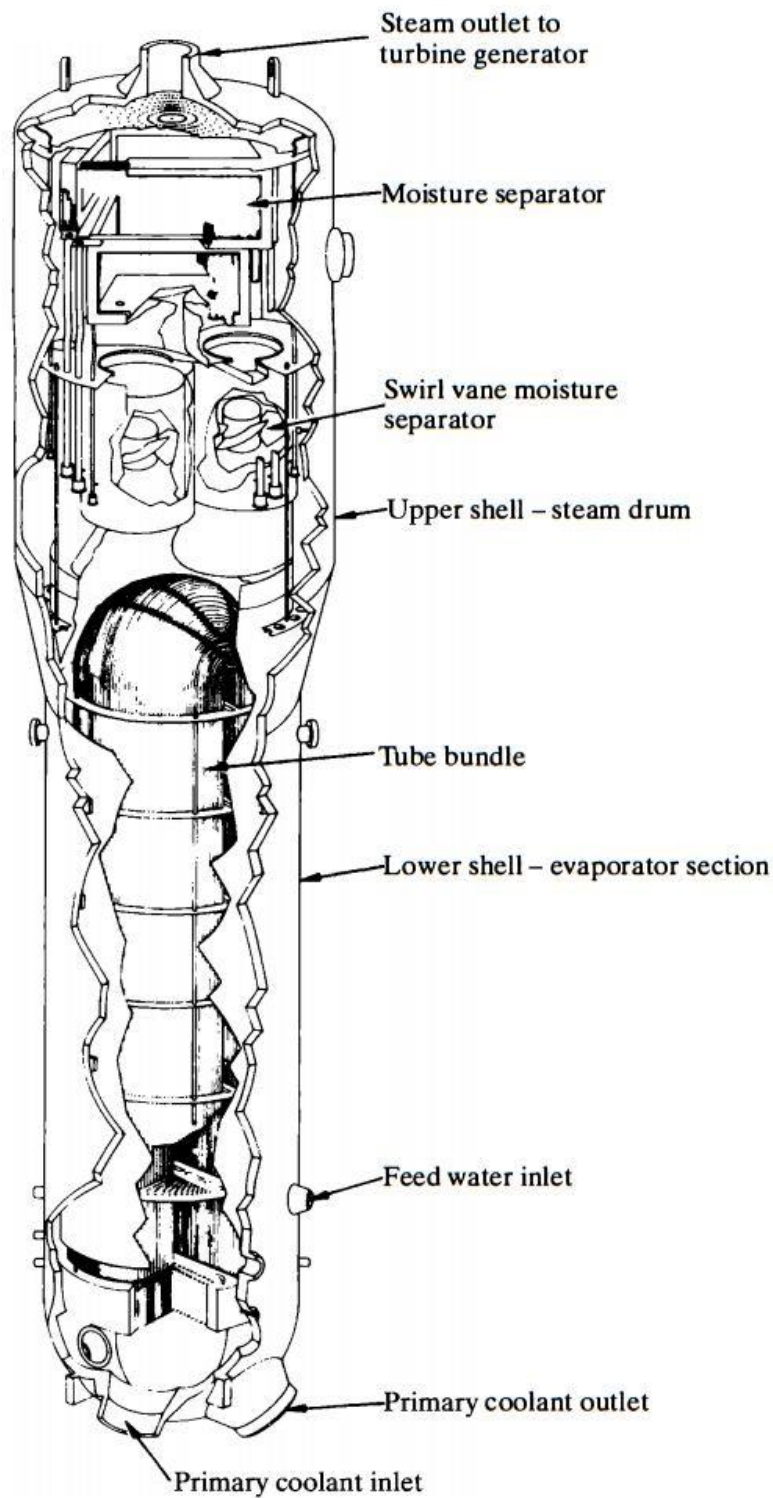
Figure 3.3 Details of a vertical U-tube steam generator (Westinghouse Electric Corporation).

20

Before defining equations for the UTSG, it is important to understand the physical processes within the UTSG since it contains both primary and secondary coolant. Starting with primary coolant, it enters from the bottom, as shown in Figure 3.4, and mixes within the inlet plenum. Then, it flows through tubes, reaches the outlet plenum from where it leaves the steam generator via outlet nozzles. Feedwater, on the other hand, enters the steam generator above the tube bundle and pours down. Then, it moves towards the upper region by flowing across the tubes where heat transfer from primary coolant to secondary coolant occurs. Some portion of the feedwater turns into saturated steam and leaves the steam generator after passing through the moisture separators. A supporting diagram of this process is presented in Figure 3.4. The U-tube steam generator is also known as a recirculation type steam generator.
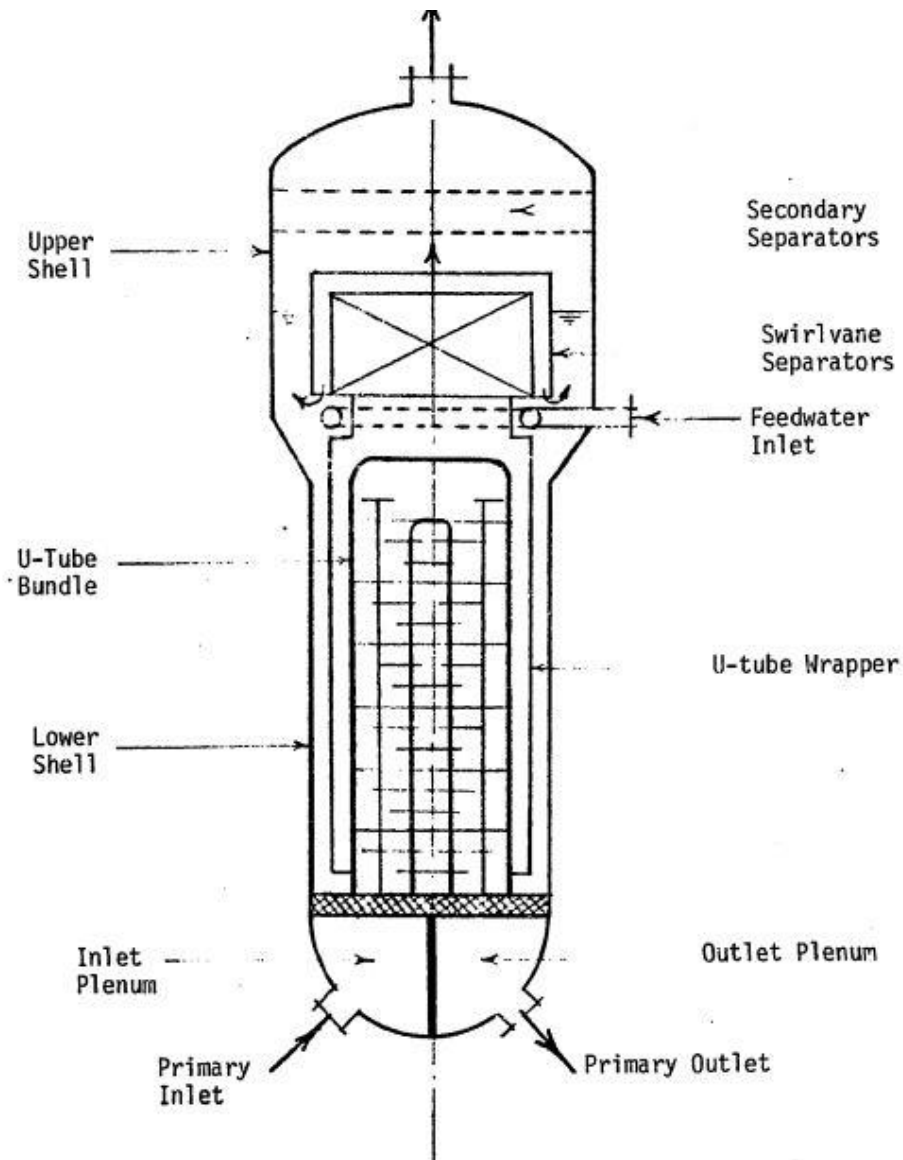
Figure 3.4 U-tube steam generator schematic diagram.

In order to have a better representation of the U-tube metal bundle, it is divided

into two parts (see Figure 3.5). The resulting model for the steam generator discussed

here has five lumps: two for the primary coolant, two for the tube metal, and one for the

secondary coolant [13].
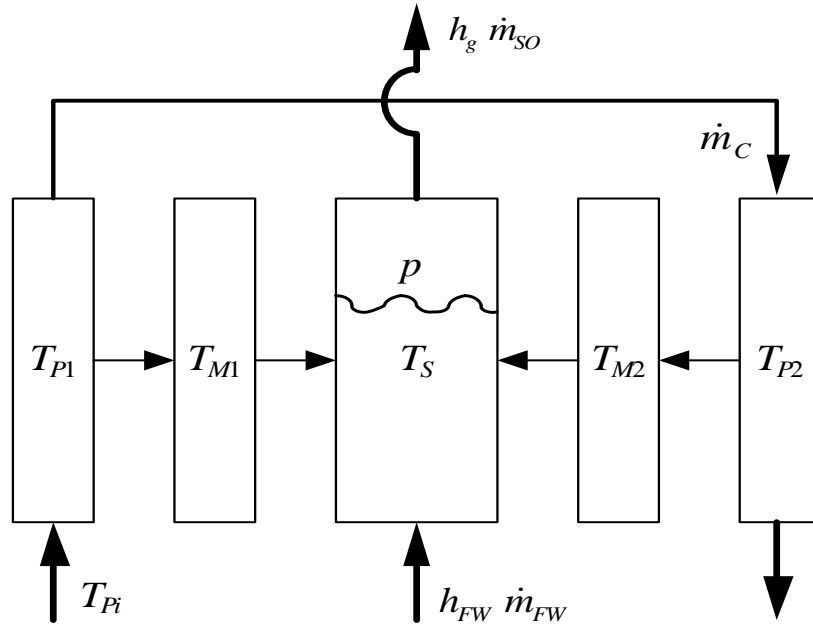
Figure 3.5 Schematic diagram for the steam generator model.

3.4.1 Primary coolant lump 1

A heat balance for primary coolant lump 1 (PRL1) yields

$$\frac{d}{dt}\left(m_{P1}c_pT_{P1}\right)=\dot{m}_Cc_p\left(T_{PI}-T_{P1}\right)-\left(U_{pm}S_{pm}\right)_1\left(T_{P1}-T_{M1}\right) \qquad (3.16)$$

where

m_{P1} = mass of primary coolant in PRL1,

T_{P1} = bulk mean temperature of the primary coolant in PRL1,

T_{PI} = temperature of the primary water entering the steam generator,

U_{pm} = effective heat transfer coefficient between primary coolant lumps and tube metal lumps,

S_{pm} = effective heat transfer surface area between primary coolant lumps and tube metal lumps,

T_{M1} = average temperature of the tube metal lump 1 (MTL1).

Assuming the specific heat and density of primary coolant will not change, the

energy balance equation can be written as

23

$$\frac{dT_{P1}}{dt} = \frac{1}{\tau_{P1}} T_{PI} - \left(\frac{1}{\tau_{PM1}} + \frac{1}{\tau_{P1}} \right) T_{P1} + \frac{1}{\tau_{PM1}} T_{M1} \qquad (3.17)$$

where

$$\tau_{P1} = \frac{m_{P1}}{\dot{m}_C} = \text{residence time of primary coolant in PRL1,}$$

$$\tau_{PM1} = \frac{m_{P1} c_p}{\left(U_{pm} S_{pm} \right)_1} = \text{time constant for PRL1 to MTL1 heat transfer.}$$

3.4.2 Primary coolant lump 2

Similar to PRL1, a heat balance is performed for primary coolant lump 2 (PRL2).

$$\frac{d}{dt} \left(m_{P2} c_p T_{P2} \right) = \dot{m}_C c_p \left(T_{P1} - T_{P2} \right) - \left(U_{pm} S_{pm} \right)_2 \left(T_{P2} - T_{M2} \right) \qquad (3.18)$$

where

m_{P2} = mass of primary coolant in PRL2,

T_{P2} = bulk mean temperature of primary coolant in PRL2,

T_{M2} = average temperature of the tube metal lump 2 (MTL2).

Introducing related time constants, Equation (3.18) takes the form of

$$\frac{dT_{P2}}{dt} = \frac{1}{\tau_{P2}} T_{P1} - \left(\frac{1}{\tau_{PM2}} + \frac{1}{\tau_{P2}} \right) T_{P2} + \frac{1}{\tau_{PM2}} T_{M2} \qquad (3.19)$$

where

$$\tau_{P2} = \frac{m_{P2}}{\dot{m}_C} = \text{residence time of primary coolant in PRL2,}$$

$$\tau_{PM2} = \frac{m_{P2} c_p}{\left(U_{pm} S_{pm} \right)_2} = \text{time constant for PRL2 to MTL2 heat transfer.}$$

3.4.3 Tube metal lump 1

A heat balance with the assumption of constant tube metal density and specific

heat is

$$\frac{d}{dt} \left(m_{M1} c_M T_{M1} \right) = \left(U_{pm} S_{pm} \right)_1 \left(T_{P1} - T_{M1} \right) - \left(U_{ms} S_{ms} \right)_1 \left(T_{M1} - T_S \right) \qquad (3.20)$$

24

where

m_{M1} = mass of MTL1,

c_M = specific heat of tube metal,

U_{ms} = effective heat transfer coefficient between tube metal lumps and
secondary coolant lump,

S_{ms} = effective heat transfer area between tube metal lumps and
secondary coolant lump,

T_S = bulk mean temperature of secondary coolant lump.

Applying perturbation variables and time constants into Equation (3.20) changes

the relation into

$$\frac{d\delta T_{M1}}{dt} = \frac{1}{\tau_{MP1}}\delta T_{P1} - \left(\frac{1}{\tau_{MS1}} + \frac{1}{\tau_{MP1}}\right)\delta T_{M1} + \frac{1}{\tau_{MS1}}\delta T_S \qquad (3.21)$$

where

$\tau_{MP1} = m_{M1}c_M / \left(U_{pm}S_{pm}\right)_1$ = time constant for MTL1 to PRL1 heat transfer,

$\tau_{MS1} = m_{M1}c_M / \left(U_{ms}S_{ms}\right)_1$ = time constant for MTL1 to secondary coolant
lump (SCL) heat transfer.

It can be assumed that the steam temperature equals the saturation temperature at

that specific pressure since the secondary lump consists of a liquid-vapor mixture in

equilibrium. Then, any change in pressure will end up causing a change in the saturation

temperature (see Appendix A). Taking this factor into account

$$\frac{d\delta T_{M1}}{dt} = \frac{1}{\tau_{MP1}}\delta T_{P1} - \left(\frac{1}{\tau_{MS1}} + \frac{1}{\tau_{MP1}}\right)\delta T_{M1} + \frac{1}{\tau_{MS1}}\left(\frac{\partial T_{SAT}}{\partial p}\right)\delta p \qquad (3.22)$$

where

T_{SAT} = saturation temperature,

p = steam pressure,

$\partial T_{SAT}/\partial p$ = slope of the linear approximation of the change in saturation
temperature respect to steam pressure.

25

3.4.4 Tube metal lump 2

The same procedure is followed to obtain the expression for MTL2.

$$\frac{d}{dt}\left(m_{M2}c_M T_{M2}\right) = \left(U_{pm}S_{pm}\right)_2\left(T_{P2}-T_{M2}\right) - \left(U_{ms}S_{ms}\right)_2\left(T_{M2}-T_S\right) \qquad (3.23)$$

$$\frac{d\delta T_{M2}}{dt} = \frac{1}{\tau_{MP2}}\delta T_{P2} - \left(\frac{1}{\tau_{MS2}}+\frac{1}{\tau_{MP2}}\right)\delta T_{M2} + \frac{1}{\tau_{MS2}}\left(\frac{\partial T_{SAT}}{\partial p}\right)\delta p \qquad (3.24)$$

where

m_{M2} = mass of MTL2,

$\tau_{MP2} = m_{M2}c_M / \left(U_{pm}S_{pm}\right)_2$ = time constant for MTL2 to PRL2 heat transfer,

$\tau_{MS2} = m_{M2}c_M / \left(U_{ms}S_{ms}\right)_2$ = time constant for MTL2 to SCL heat transfer.

Time constants introduced for the steam generator are tabulated in Table 3.3.

Appendix B.3 consists of the required parameters for the calculation of these constants.

Table 3.3 Time constants for steam generator model

Variable	Value
τ_{P1}	1.2815 sec
τ_{PM1}	1.2233 sec
τ_{P2}	1.2815 sec
τ_{PM2}	0.5826 sec
τ_{MP1}	0.3519 sec
τ_{MS1}	0.3519 sec
τ_{MP2}	0.1676 sec
τ_{MS2}	0.1676 sec

3.4.5 Secondary coolant lump

The presence of a steam-water mixture in the secondary coolant lump requires

performing mass and volume balances in addition to energy balance.

26

Mass Balance:

$$\text{Liquid phase: } \frac{dm_{SW}}{dt} = \dot{m}_{FI} - \dot{m}_{SG} \tag{3.25}$$

$$\text{Vapor phase: } \frac{dm_{SS}}{dt} = \dot{m}_{SG} - \dot{m}_{SO} \tag{3.26}$$

where

m_{SW} = liquid mass in the secondary lump,

$\dot{m}_{FI}$ = feedwater inlet flow,

$\dot{m}_{SG}$ = vapor generation rate,

m_{SS} = vapor mass in the secondary lump,

$\dot{m}_{SO}$ = steam outlet flow.

Volume Balance:

The total volume of the secondary lump in the steam generator remains constant

meaning the change over time is zero.

$$\frac{dV_{SW}}{dt} + \frac{dV_{SS}}{dt} = \frac{dV_{ST}}{dt} = 0 \tag{3.27}$$

where,

V_{SW} = liquid volume in the secondary lump,

V_{SS} = vapor volume in the secondary lump,

V_{ST} = total volume of SCL.

Saturated conditions allow expressing the volume of the steam and water in SCL with

related specific volumes,

$$V_{SW} = m_{SW} \cdot \upsilon_f \tag{3.28}$$
$$V_{SS} = m_{SS} \cdot \upsilon_g \tag{3.29}$$

where υ_f and υ_g are the specific volumes of saturated liquid and vapor, respectively.

Combining the last three equations yields

$$\frac{d}{dt}\left(m_{SW} \cdot \upsilon_f\right) + \frac{d}{dt}\left(m_{SS} \cdot \upsilon_g\right) = 0 \tag{3.30}$$

27

$$v_f \frac{dm_{SW}}{dt} + m_{SW} \frac{dv_f}{dt} + v_g \frac{dm_{SS}}{dt} + m_{SS} \frac{dv_g}{dt} = 0 \qquad (3.31)$$

Assuming that the specific volume of saturated liquid will not change during a transient

and using the relationship $\frac{dv_g}{dt} = \left(\frac{\partial v_g}{\partial p}\right)\frac{dp}{dt}$, Equation (3.31) can be written as

$$\frac{dp}{dt} = -\frac{1}{m_{SS} \frac{\partial v_g}{\partial p}} \left(v_f \frac{dm_{SW}}{dt} + v_g \frac{dm_{SS}}{dt} \right) \qquad (3.32)$$

Using the relationships in Equations (3.25) and (3.26), and assuming that perfect

feedwater control is applied which means $\dot{m}_{FI} = \dot{m}_{SO}$, Equation (3.32) can be modified.

$$\frac{dp}{dt} = -\frac{1}{m_{SS} \frac{\partial v_g}{\partial p}} \left[v_f \left(\dot{m}_{FI} + \dot{m}_{SG} \right) + v_g \left(\dot{m}_{SG} - \dot{m}_{SO} \right) \right] \qquad (3.33)$$

$$\frac{dp}{dt} = -\frac{1}{m_{SS} \frac{\partial v_g}{\partial p}} \left[v_{fg} \left(\dot{m}_{SG} - \dot{m}_{SO} \right) \right] \qquad (3.34)$$

where $v_{fg} = v_g - v_f$.

Finally, if the steam flow rate is just a function of steam pressure, in other words,

if the critical flow is utilized

$$\dot{m}_{SO} = C_L \cdot p \qquad (3.35)$$

where C_L is the steam valve coefficient. The pressure rate of change is now

$$\frac{dp}{dt} = -\frac{1}{m_{SS} \frac{\partial v_g}{\partial p}} \left[v_{fg} \left(\dot{m}_{SG} - C_L \cdot p \right) \right] \qquad (3.36)$$

28

Heat Balance:

$$\frac{d}{dt}\left(m_{SW}e_f + m_{SS}e_g\right) = \left(U_{ms}S_{ms}\right)_1\left(T_{M1} - T_S\right) + \left(U_{ms}S_{ms}\right)_2\left(T_{M2} - T_S\right)$$

$$+ \dot{m}_{FI}c_{pi}T_{FI} - \dot{m}_{SO}h_g \quad (3.37)$$

where

e_f = internal energy of saturated liquid,

e_g = internal energy of saturated vapor,

c_{pi} = specific heat of feedwater,

T_{FI} = temperature of feedwater entering the steam generator, and

h_g = specific enthalpy of saturated vapor.

Internal energies of water and steam at saturation conditions can be replaced with enthalpy values which are function of steam pressure in the secondary side. Changing the heat balance equation according to the statement above yields

$$m_{SW}\frac{dh_f}{dt} + h_f\frac{dm_{SW}}{dt} + m_{SS}\frac{dh_g}{dt} + h_g\frac{dm_{SS}}{dt} =$$

$$\left(U_{ms}S_{ms}\right)_1\left(T_{M1} - T_S\right) + \left(U_{ms}S_{ms}\right)_2\left(T_{M2} - T_S\right) + \dot{m}_{FI}c_{pi}T_{FI} - \dot{m}_{SO}h_g \quad (3.38)$$

where h_f is the specific enthalpy of the saturated liquid.

Keeping in mind that the properties of liquid and vapor are dependent on pressure, and utilizing the mass balance equations again

$$\left(m_{SW}\frac{\partial h_f}{\partial p} + m_{SS}\frac{\partial h_g}{\partial p}\right)\frac{dp}{dt} = \left(U_{ms}S_{ms}\right)_1\left(T_{M1} - T_S\right) + \left(U_{ms}S_{ms}\right)_2\left(T_{M2} - T_S\right)$$

$$+ \dot{m}_{FI}c_{pi}T_{FI} - h_g\left(\dot{m}_{SG} - \dot{m}_{SO}\right) - h_f\left(\dot{m}_{FI} - \dot{m}_{SG}\right) - \dot{m}_{SO}h_g \quad (3.39)$$

Rearranging the last 4 terms in Equation (3.39) by reconsidering that feedwater is adjusted to match steam flow $\left(\dot{m}_{FI} = \dot{m}_{SO}\right)$

$$-h_g\left(\dot{m}_{SG} - \dot{m}_{SO}\right) - h_f\left(\dot{m}_{SO} - \dot{m}_{SG}\right) = -\left(h_g - h_f\right)\left(\dot{m}_{SG} - \dot{m}_{SO}\right) = -h_{fg}\left(\dot{m}_{SG} - \dot{m}_{SO}\right)$$

$$-h_{fg}\left(\dot{m}_{SG}-\dot{m}_{SO}\right)=-h_{fg}\left[-\left(\frac{m_{SS}}{\upsilon_{fg}}\frac{\partial\upsilon_g}{\partial p}\right)\frac{dp}{dt}\right] \qquad (3.40)$$

$$-\dot{m}_{SO}h_g+\dot{m}_{SO}c_{pi}T_{FI}=-\dot{m}_{SO}\left(h_g-c_{pi}T_{FI}\right) \qquad (3.41)$$

Let's combine Equations (3.40) and (3.41) with the original heat balance equation

$$K\frac{dp}{dt}=\left(U_{ms}S_{ms}\right)_1\left(T_{M1}-T_S\right)+\left(U_{ms}S_{ms}\right)_2\left(T_{M2}-T_S\right)-\dot{m}_{SO}\left(h_g-c_{pi}T_{FI}\right) \qquad (3.42)$$

where

$$K=\left(m_{SW}\frac{\partial h_f}{\partial p}+m_{SS}\frac{\partial h_g}{\partial p}-m_{SS}\frac{h_{fg}}{\upsilon_{fg}}\frac{\partial\upsilon_g}{\partial p}\right)$$

After introducing perturbation variables, the equation takes the form of

$$K\frac{d\delta p}{dt}=\left(U_{ms}S_{ms}\right)_1\left(T_{M1}-\frac{\partial T_{SAT}}{\partial p}\delta p\right)+\left(U_{ms}S_{ms}\right)_2\left(T_{M2}-\frac{\partial T_{SAT}}{\partial p}\delta p\right)$$
$$-\dot{m}_{SO}\left(\frac{\partial h_g}{\partial p}\delta p-c_{pi}\delta T_{FI}\right)-\delta\dot{m}_{SO}\left(h_g-c_{pi}T_{FI}\right) \quad (3.43)$$

Substituting the linearized version of the equation for critical flow assumption

$\delta\dot{m}_{SO}=\delta C_L\cdot p+C_L\cdot\delta p$, the final expression is obtained for SFL

$$K\frac{d\delta p}{dt}=\left(U_{ms}S_{ms}\right)_1\left(T_{M1}-\frac{\partial T_{SAT}}{\partial p}\delta p\right)+\left(U_{ms}S_{ms}\right)_2\left(T_{M2}-\frac{\partial T_{SAT}}{\partial p}\delta p\right)$$
$$-\left[\dot{m}_{SO}\left(\frac{\partial h_g}{\partial p}\right)+C_L\left(h_g-c_{pi}T_{FI}\right)\right]\delta p-p\left(h_g-c_{pi}T_{FI}\right)\delta C_L+\dot{m}_{SO}c_{pi}\delta T_{FI} \quad (3.44)$$

3.5 Reactor Control System

The control of the reactor can be managed by various methods. Only two of them are discussed in this study.

3.5.1 Constant-average-temperature program

In this method, it is desired to keep the average temperature of the primary coolant in the core constant no matter what the thermal power output is. In other words while the hot log temperature increases, the cold leg temperature decreases for the operating conditions from zero power to full power. The disadvantage of this program is that large variations in steam pressure and temperature occur, assuming the steam valve position is fixed, which is not preferred by the secondary system. However, it is preferred by the reactor since in the case of a power change the moderator temperature coefficient of reactivity does not have a large impact on reactivity. Furthermore, the constant-average-temperature program minimizes required pressurizer size because the volume of the water in the NSSS basically does not change. Figure 3.6 provides a summary of the constant-average-temperature program.
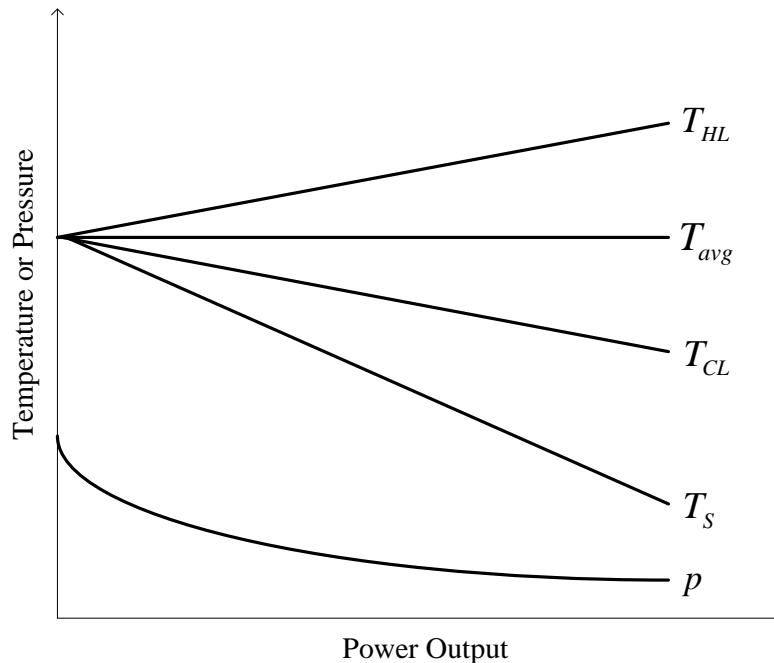
Figure 3.6 Characteristics of constant-average-temperature program [14].

31

The control action is achieved by a proportional-integral (PI) controller and the equation generating the signal for control rod drive is

$$\rho = K_{avg}\left[\left(T_{avg,ref} - T_{avg}\right) + \frac{1}{\tau}\int\left(T_{avg,ref} - T_{avg}\right)dt\right] \tag{3.45}$$

where

T_{avg} = the average temperature of the primary coolant,

$T_{avg,ref}$ = reference value for the average temperature,

K_{avg} = slope of the equation relating the average temperature to reactivity, and

τ = time compensation or tuning parameter.

3.5.2 Sliding-average-temperature program

For this slightly different method, the cold leg temperature is kept constant which lets the average and hot leg temperatures increase with an increase in the power output. The advantage of this program over the constant-average- temperature program is that the change in the steam pressure according to the power level is diminished. This program is also termed as a compromise program or non-constant program since it is intended to provide a balance between the needs of the primary and secondary systems. The relationship between temperatures and steam pressure for the program is illustrated in Figure 3.7.
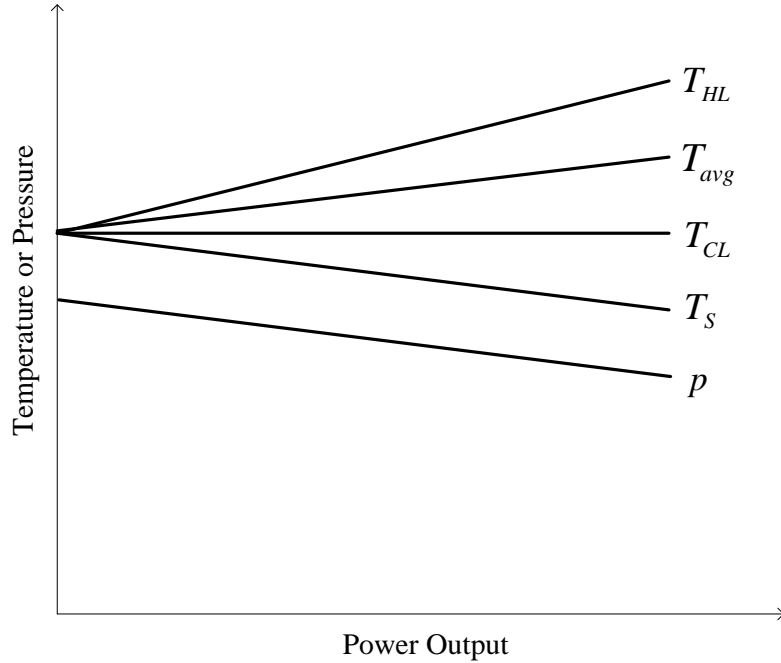
Figure 3.7 Characteristics of sliding-average-temperature program [18].

In parallel manner, the equation for the control rod drive signal is

$$\rho = K_{CL}\left[\left(T_{CL,ref} - T_{CL}\right) + \frac{1}{\tau}\int\left(T_{CL,ref} - T_{CL}\right)dt\right] \tag{3.46}$$

where

$T_{CL,ref}$ = the reference value for the cold leg temperature,

K_{CL} = slope of the equation relating the cold leg temperature to reactivity

3.6 Turbine and Governor Models

Since the developed PWR model is introduced into PSLF, turbine and governor

models are needed.

3.6.1 Turbine

The turbine model introduced here basically describes the method of acquiring the

heat content of the steam flowing through the secondary system. This heat content

(mechanical power) is a function of both steam flow and saturation pressure (see Figure

33

3.8) which is assumed to be steam pressure as discussed in previous sections. Then the resulting equation is

$$P_{Mech} = \eta_{Turb} \, \dot{m}_{SO} \, \Delta h \qquad (3.47)$$

where

P_{Mech} = mechanical power,

η_{Turb} = turbine power coefficient,

Δh = change in enthalpy due to change in steam pressure.

Steam Pressure →

Turbine Model → Mechanical Power

Steam Flow →
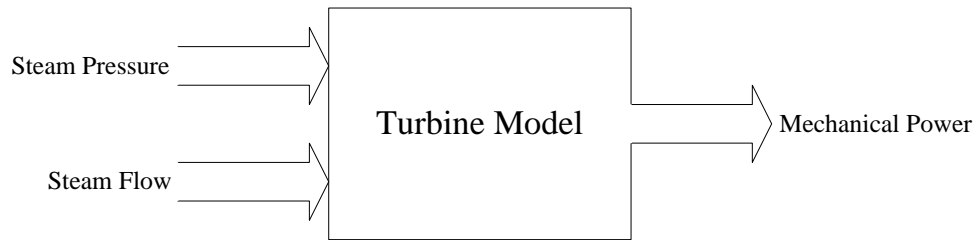
Figure 3.8 Schematic diagram of the turbine model.

The efficiency of the turbine is calculated by utilizing the full power operation parameters for the Palo Verde Nuclear Generating Station which are presented in Appendix B.4.

3.6.2 Governor

A simple governor model that controls the steam valve opening with respect to generator shaft speed is also introduced in this study so that the proposed PWR model is able respond to a disturbance occurring in the electric network. The block diagram of the model is illustrated in Figure 3.9. w_{ref} and w represent reference and actual values of the shaft speed respectively. While R is the permanent droop, v_s is the valve stroke and T_1 is the associated time constant with it.
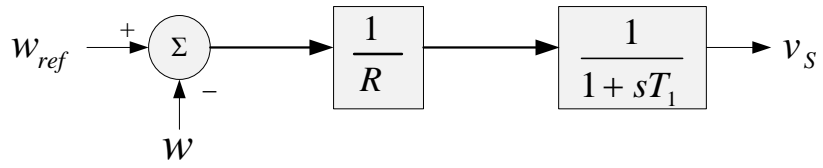
Figure 3.9 Block diagram of the governor model.

CHAPTER 4

TESTING THE DYMAMIC MODELS IN MATLAB/SIMULINK

In this chapter, mathematical models discussed in the previous chapter are tested

and evaluated with the help of Matlab/Simulink v7.7 by applying common disturbances

to them. For comparison, the same order in Reference [12] is followed. First, the dynamic

simulation results for the isolated core and steam generator models are presented, and

then the response of the combination of these two models with piping and plenums which

form the PWR steam supply system is presented. In Appendix C, figures for the complete

model from Matlab/Simulink are provided.

4.1 Isolated Core Model

In order to test the isolated core model, small perturbations to reactivity and core

inlet coolant temperature are applied separately, and changes in the reactor thermal power

and the core fuel and coolant temperatures are demonstrated.

4.1.1 Control rod movement

A 1¢ increase in the reactivity due to control rod withdrawal is applied to the

model at time = 10 sec. This action causes an increase in the fission rate and neutron flux

and, correspondingly, an initial rise in reactor thermal power, as shown in Figure 4.1.
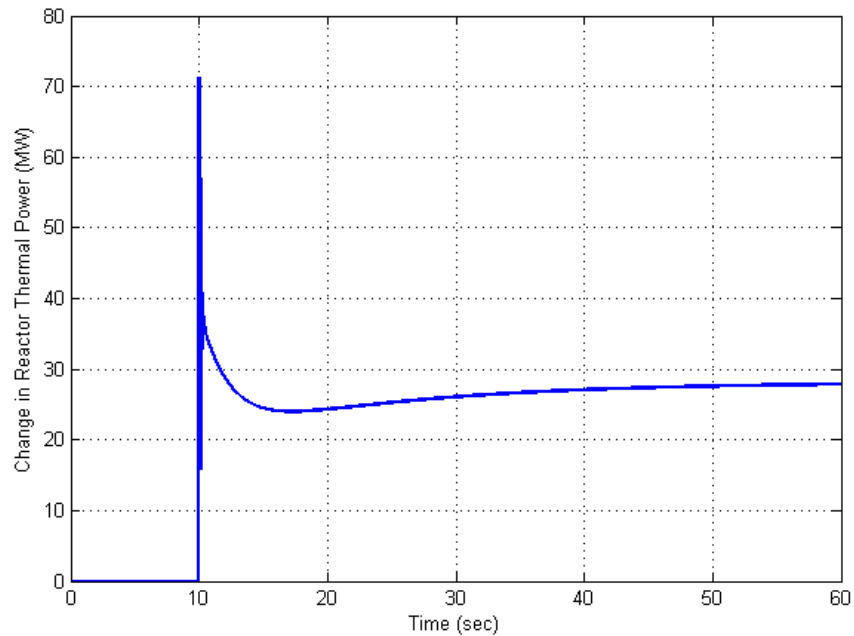
Figure 4.1 Deviation of the reactor thermal power for 1¢ reactivity increase.

Following the increased power generation, the fuel temperature increases and more heat is transferred from the fuel region to primary coolant in the core. The steady-state fuel (T_F) and core coolant ($T_{\theta2}$ and $T_{\theta1}$) temperatures rise by 4.3 °F, 0.4 °F, and 0.2 ºF, respectively, as shown in Fig. 4.2. These temperature changes drive the negative reactivity feedback mechanisms and the total reactivity starts decreasing, as seen in Figure 4.3. This behavior illustrates the inherent stability feature of a PWR. The resulting change in the reactor thermal power at the new stable operating condition is +28 MWth.
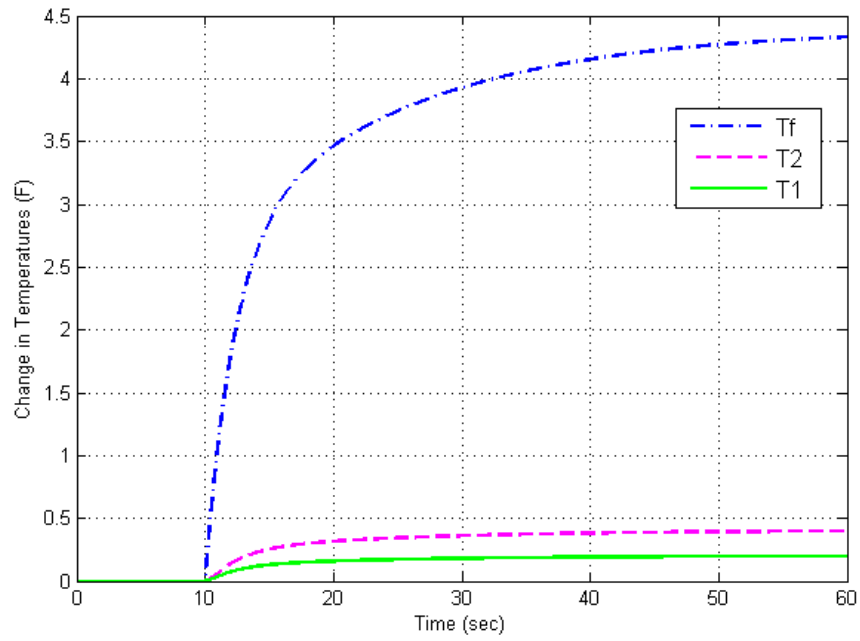
Figure 4.2 Deviation of the fuel and the core coolant temperatures for 1¢ reactivity
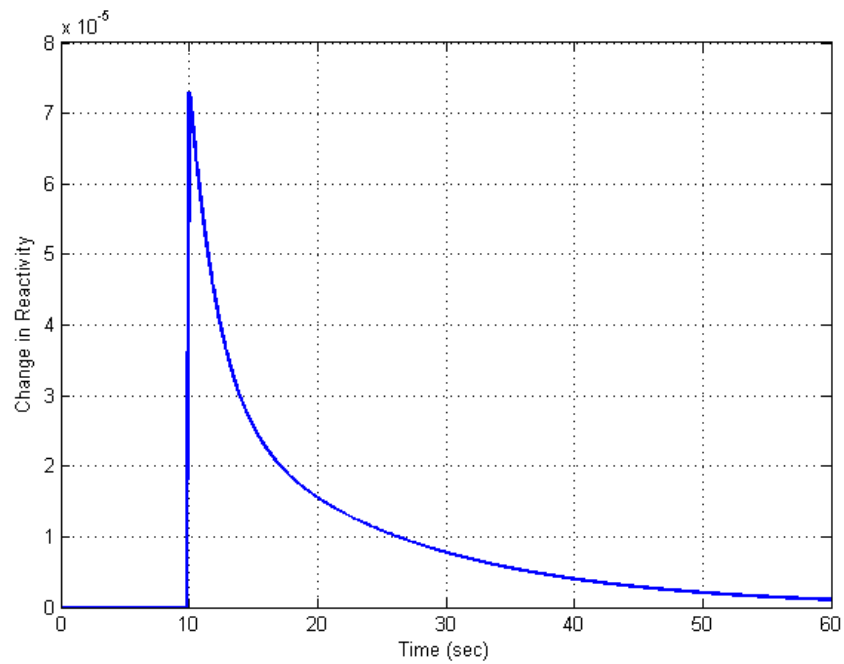
increase.

Figure 4.3 Change in total reactivity for 1¢ reactivity increase.

4.1.2 Coolant inlet temperature change

For the second scenario, a 1 ºF increase in the core inlet coolant temperature is applied to the model, again, at time = 10 sec. Due to this perturbation, the core coolant node 1 and exit temperatures increase. On the other hand, the reactivity decreases due to negative temperature coefficients, which leads to a sharp decrease in the reactor thermal power. As a result, the fuel temperature falls meaning the heat transfer from fuel to coolant region decreases, and the increase in the coolant temperatures stops. When a new stable point is reached, the difference in the core thermal power compared to the initial condition is -42.7 MW as depicted in Figure 4.4. The fuel temperature dips 5.6 °F while the rises in the core coolant node 1 and exit temperatures are 0.69 °F and 0.39 °F as seen in Figure 4.5
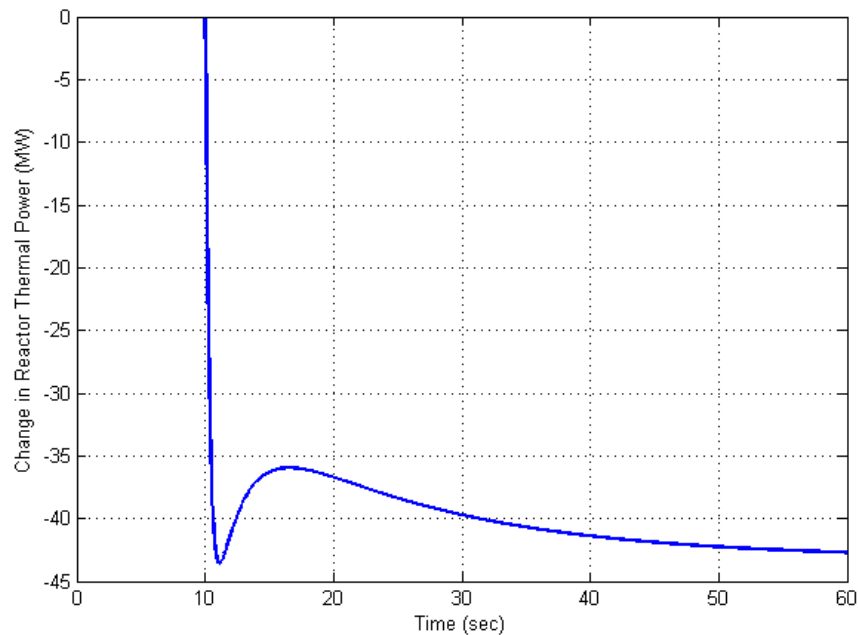
Figure 4.4 Deviation of the reactor thermal power for 1°F increase in the core inlet coolant temperature.
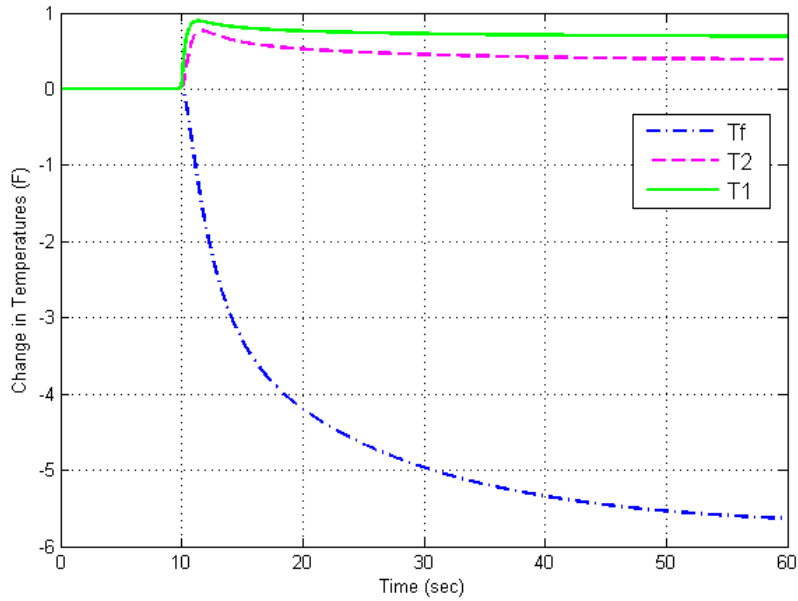
Figure 4.5 Deviation of the fuel and the core coolant temperatures for 1°F increase in the core inlet coolant temperature.

4.2 Isolated Steam Generator Model

Testing the isolated steam generator model is achieved by introducing positive step disturbances to temperature of the primary coolant in the steam generator inlet plenum and to steam valve position.

4.2.1 Coolant inlet temperature change

When an increase of 10 °F in the temperature of the primary coolant in the steam generator inlet plenum occurs at time = 5 sec, temperatures of primary coolant (T_{P1} and T_{P2}) in the steam generator increase. Consequently, more heat is transferred from the primary side to the tube metal. In a parallel manner, a rise in both of the tube metal lump temperatures (T_{M1} and T_{M2}) is observed (see Figure 4.6) and hence more heat is

40

transferred from the tube metal to the secondary side. Finally, steam production is

elevated which increases the steam pressure as seen in Figure 4.7.
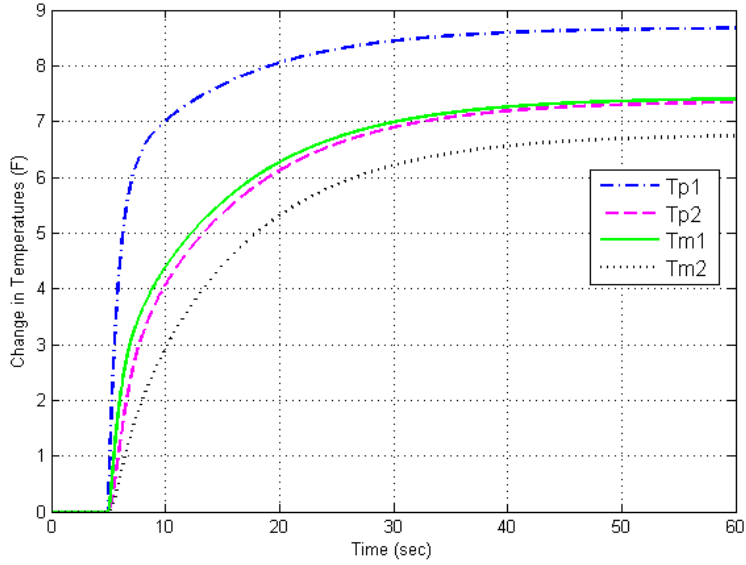
Figure 4.6 Temperature profiles for 10 °F increase in the steam generator inlet plenum
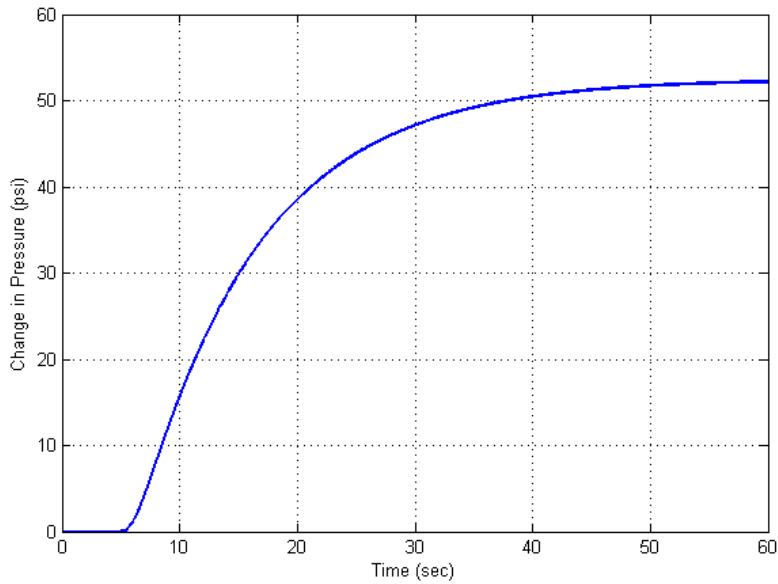
temperature.

Figure 4.7 Change in steam pressure for 10 °F increase in steam generator inlet plenum

temperature.

4.2.2 Steam valve position change

In the case of a 10% increase in steam valve opening at t = 5 sec, more steam must be produced in order to balance the disturbance caused by the change. This action causes the steam pressure to drop implying a decrease in the steam temperature. As the difference between secondary side and tube metal temperatures increases, heat transfer to the secondary side is elevated. Extracting more heat results in a decline in the temperatures of primary and tube metal lumps. Figures 4.8 and 4.9 show the changes of the key variables of the steam generator model as explained above.
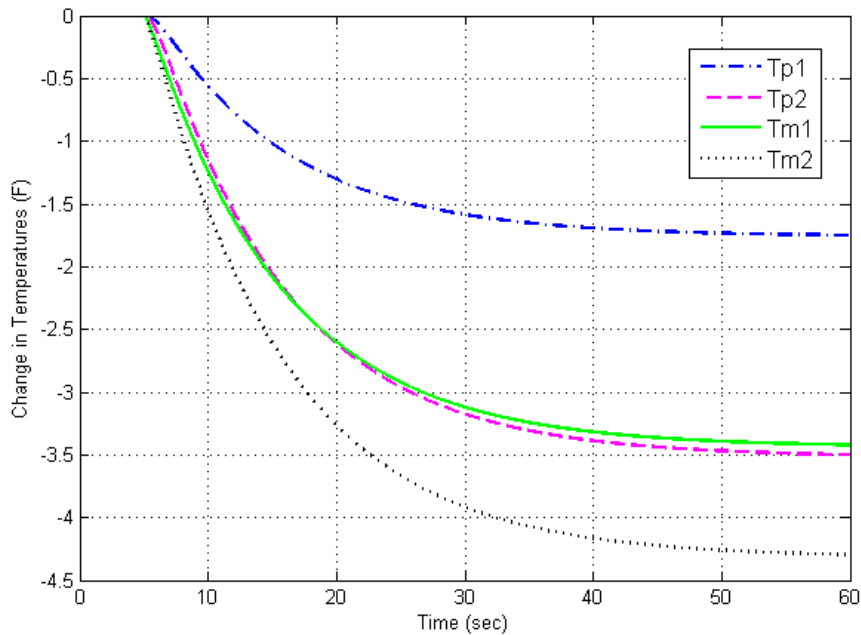
Figure 4.8 Steam generator temperature profiles for 10% increase in steam valve opening.
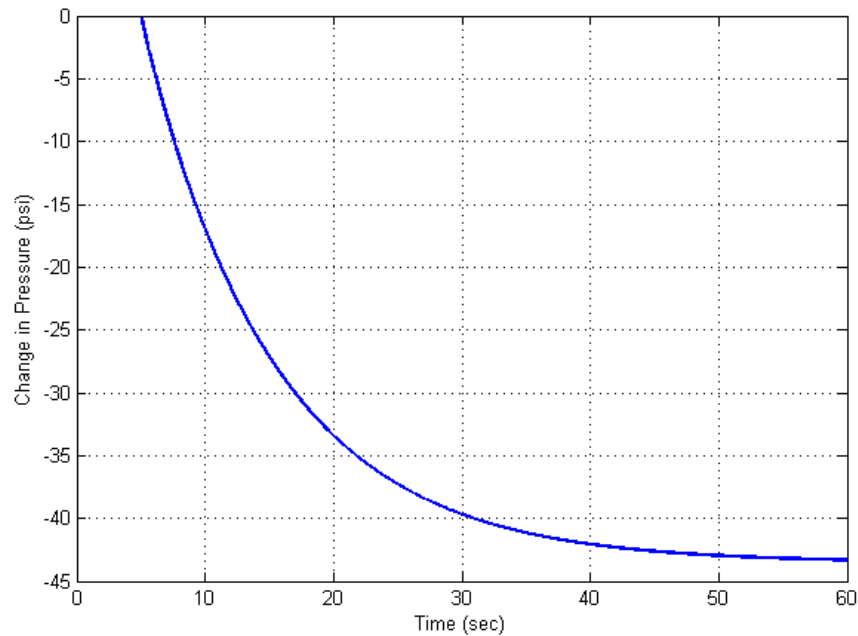
Figure 4.9 Change in steam pressure for 10% increase in steam valve opening.

4.3 Complete PWR Model

The complete model of the PWR is tested by applying small disturbances to the position of the control rods and the steam valve. The purpose of doing so is that the effects of a change in the reactor on the steam generator are demonstrated which helps to evaluate the model, and vice versa.

4.3.1 Control rod movement

For the first case, a 1¢ reactivity increase is introduced to the system at time = 10 sec. Similar to the isolated core model case, this perturbation causes an increase in the fission rate and neutron flux and, thereby, an initial rise in the reactor thermal power, as seen in Figure 4.10. The main difference between Figures 4.1 and 4.10 is due to the eventual increase in the core-inlet temperature (constant for the isolated core model).

43
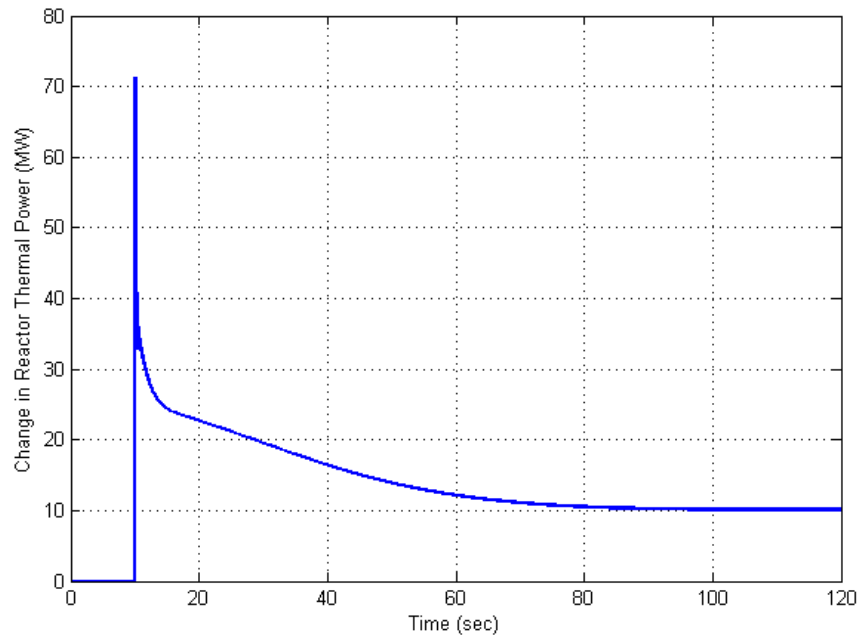
Figure 4.10 Change in reactor thermal power for 1¢ reactivity increase.

Then, the rise in the fuel temperature ends up transferring more heat to the primary coolant. Deviations of the fuel and the core coolant temperatures are respectively 2 °F (T_F), 0.56 °F ($T_{\theta 2}$), 0.49 ºF ($T_{\theta 1}$), and, 0.41 ºF ($T_{\theta in}$) as shown in Figure 4.11. Effects of negative feedback due to the fuel and core coolant temperature coefficients on the total reactivity are presented in Figure 4.12. Another important parameter to investigate is the steam pressure. Considering the fact that there is no change in steam valve position any rise in reactor thermal power must cause a growth in steam pressure since steam generation increases. Figure 4.13 shows the increase in the steam pressure.

44
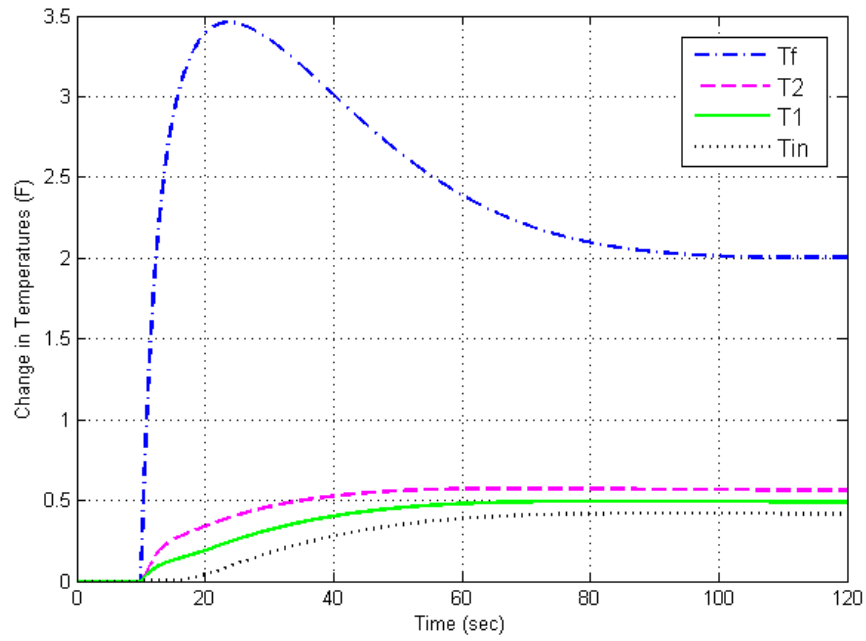
Figure 4.11 Change in fuel and core coolant temperatures for 1¢ reactivity increase.
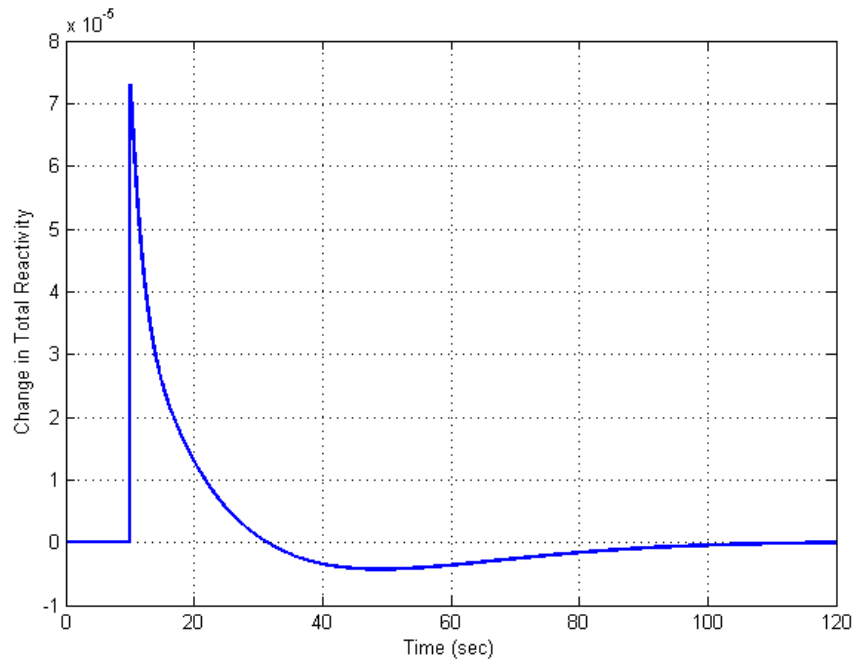
Figure 4.12 Change in total reactivity for 1¢ reactivity increase.
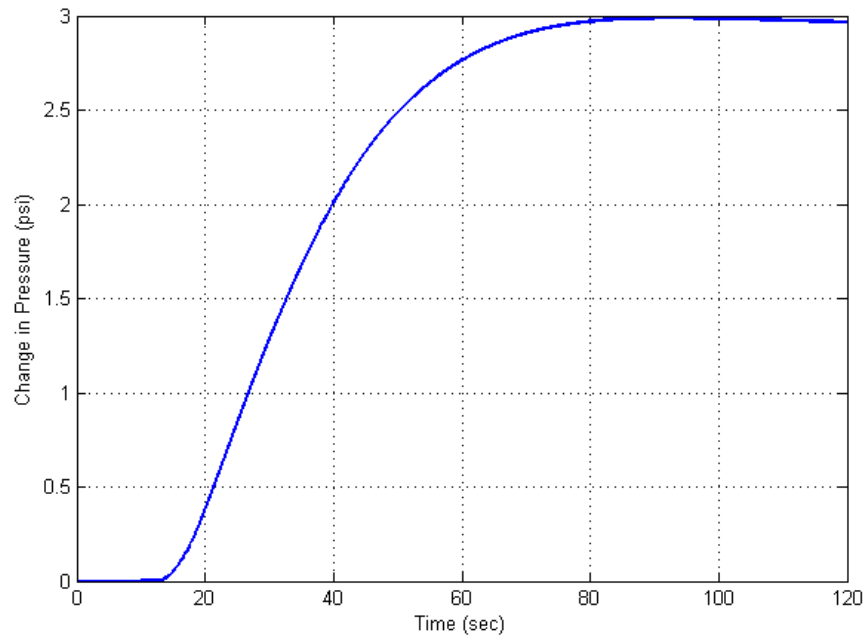
Figure 4.13 Change in steam pressure for 1¢ reactivity increase.

4.3.2 Steam valve position change

For the second case, a 1% increase in steam valve opening at t = 10 sec is introduced. Similar to the isolated steam generator model case, a drop is observed in the steam pressure as shown in Figure 4.14.
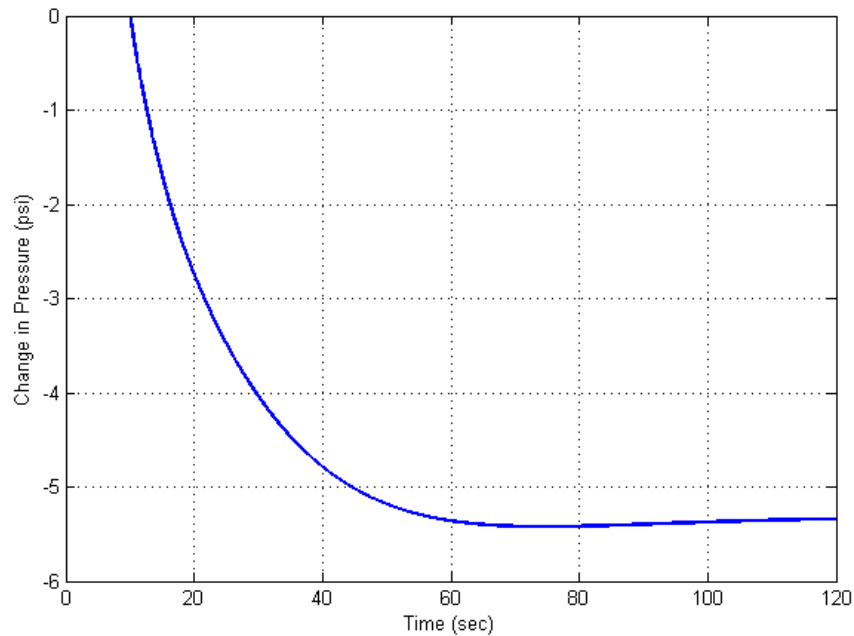
Figure 4.14 Change in steam pressure for 1% increase in steam valve opening.

The rise in demand for steam reduces the primary coolant temperatures in the steam generator meaning that core inlet temperature also initially decreases. Due to the negative temperature feedback effect, reactivity increases, and correspondingly the reactor thermal power rises (see Figure 4.15). It should be noted that since the signal for the increase in thermal power is originated in the steam generator, there is a time delay and a sharp increase does not happen in this case.

Figure 4.16 shows the resulting 2.8 °F increase in the fuel temperature, and decreases of primary coolant temperatures which are 0.19 °F ($T_{\theta 2}$), 0.34 °F ($T_{\theta 1}$), and 0.49 °F ($T_{\theta in}$).
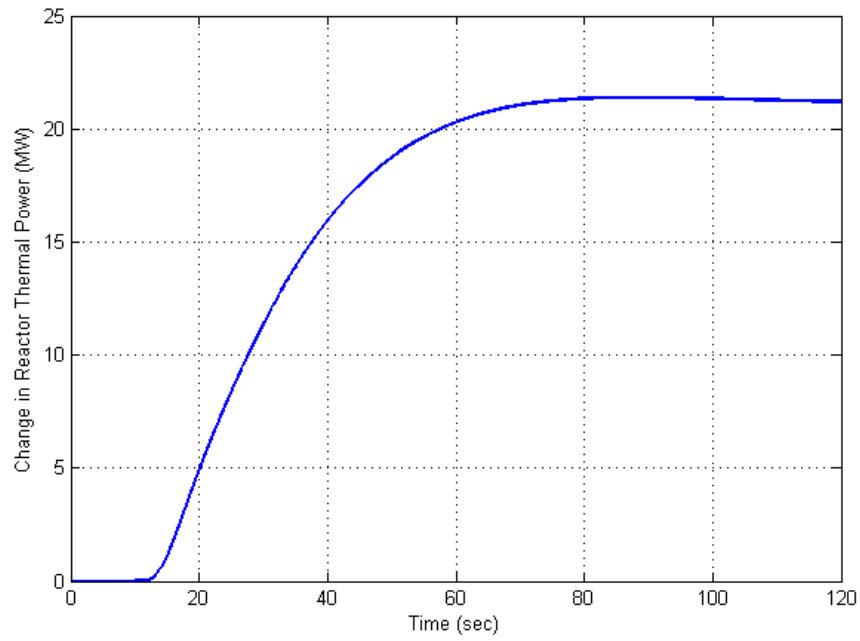
Figure 4.15 Change in reactor thermal power for 1% increase in steam valve opening.
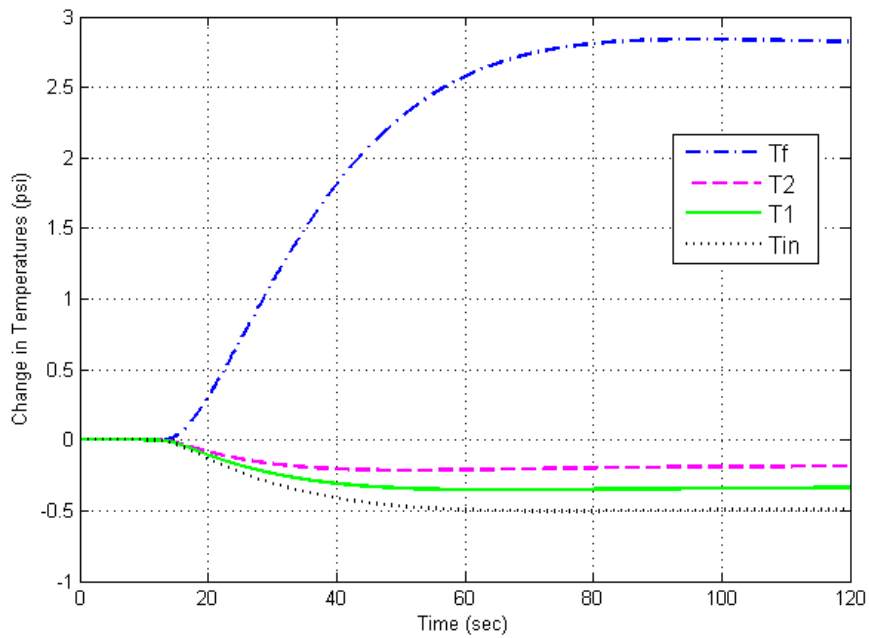
Figure 4.16 Change in fuel and core coolant temperatures for 1% increase in steam valve

opening.

48

4.4 Complete PWR Model with Reactor Control System

The sliding-average-temperature control system is added to the complete PWR model and tested. As explained in Chapter 3, the cold leg temperature must be constant for all operating power levels.

The steam valve is opened by 1% at time = 10 sec by which the effect of control system on the PWR can be observed. The decrease in the cold leg temperature due to the transient causes the control system to respond and the control rods are withdrawn so that thermal power generated in the core increases. Following that the hot leg temperature increases as depicted in Figure 4.17. Since the rise in the demand for more steam to the turbine is supplied by the withdrawal of the control rods, the cold leg temperature begins to increase, after the initial drop, which continues until it reaches the pre-transient steady-state value.
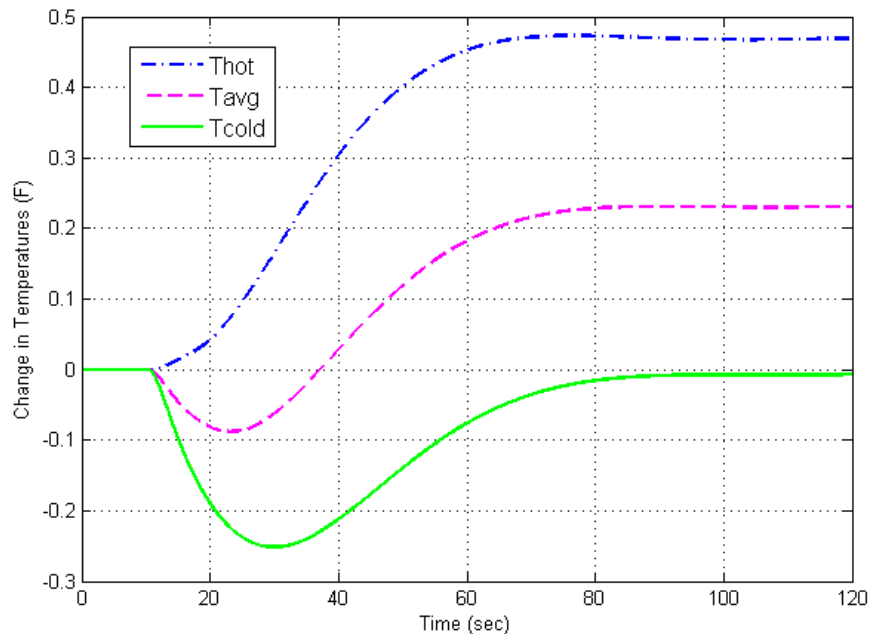
Figure 4.17 Change in primary coolant temperatures.

49

The other observation is that the drop in the steam pressure shrinks as compared to the dynamic simulation from the previous section in which the same perturbation is applied. While the change in steam pressure without the control system, after transient decays away, is -5.3 psi, the control action limits the deviation from the initial value to -1.9 psi as shown in Figure 4.18.
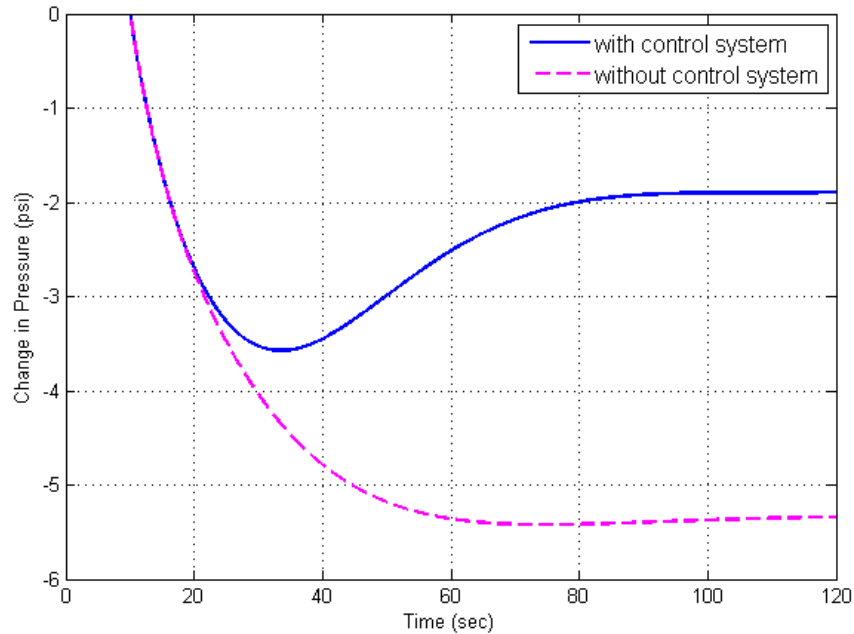
Figure 4.18 Effect of control system on steam pressure.

4.5 Complete PWR Model Coupled with Turbine Model

Finally, the turbine model is introduced into the system. As a rule of thumb, the thermal efficiency of a light water reactor, whether it is a boiling water reactor or a PWR, is about 33%. Considering this fact, the model is tested by applying a +1% change in steam valve position. The reactor thermal power increases by +33.2 MW at the new steady-state, while the deviation of the NPP output power from the initial value is +11

MW which yields a thermal efficiency of 33.1%. The related simulation results are shown in Figure 4.19.
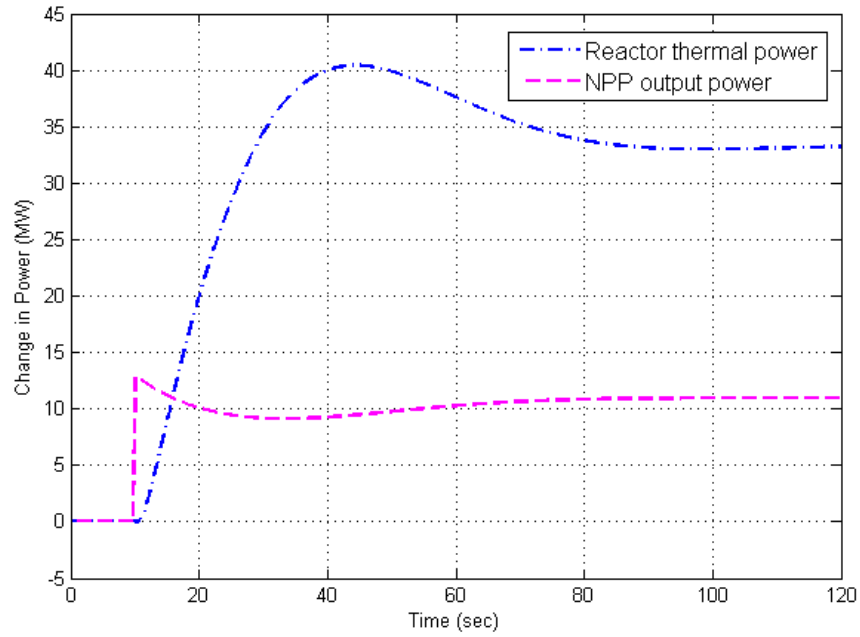
Figure 4.19 Change in reactor thermal and NPP output power for 1% increase in steam valve opening.

CHAPTER 5

IMPLEMENTING THE NPP MODEL IN PSLF

In this chapter, the developed NPP model is introduced into PSLF and dynamic simulations are performed for the purpose of examining the interaction between the NPP model and an electrical network.

In order to achieve this objective:

- First, a simple representation of Turkey's electric grid is introduced.

- Then the load flow solution is obtained by PSLF.

- Built-in dynamic models in PSLF and the NPP model are assigned to the related power generation methods described in the grid.

- Various simulations are run in the PSLF dynamic environment.

Figure 5.1 shows the microcosm model of the Turkish power system having a total generation of just over 50,000 MW. In the system, the generation consists of 21,000 MW of gas turbines, 30,000 MW of hydro units, and 1,300 MW of the NPP. The related PSLF code for the power system is presented in Appendix D.1.
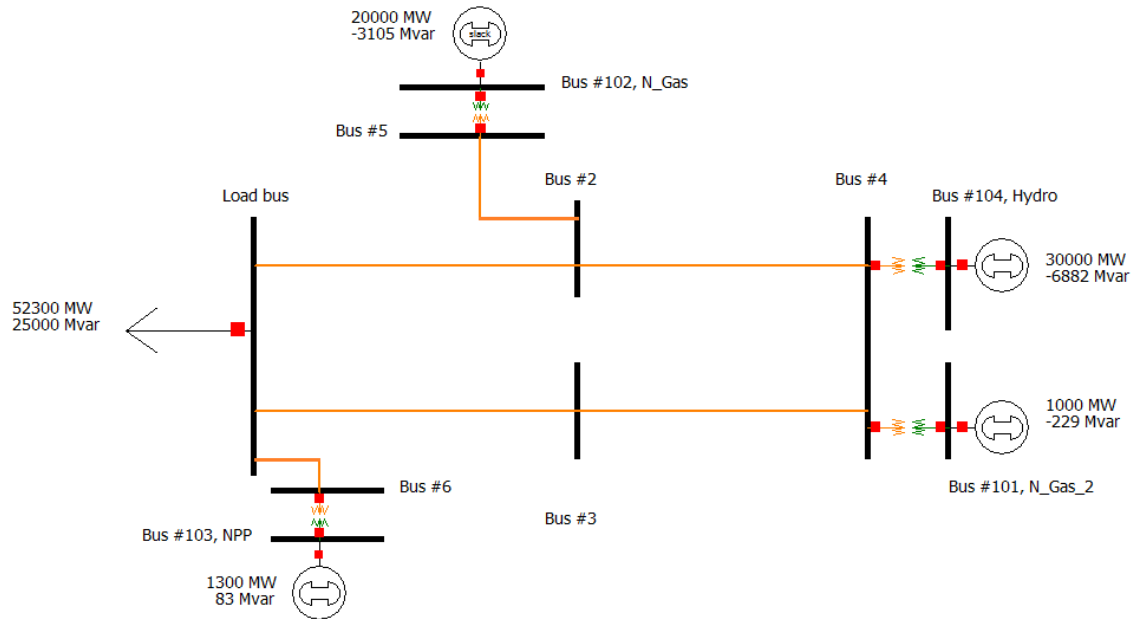
Figure 5.1 The network model representing Turkey's electricity grid.

After obtaining the load flow data by using the grid model in PSLF, a dynamic data file is created (see Appendix D.2). In that file, built-in turbine, governor, generator, and excitation system models are utilized for natural gas (NGP) and hydroelectric power plants (HPP). For the NPP, generator and excitation system models from PSLF are coupled with the PWR, turbine, governor, and reactor control system models described in this study. The developed models for the Matlab/Simulink dynamic environment in the previous chapter are transformed according to steps explained in PSLF manual. The resulting PSFL code for the models is shown in Appendix D.3.

The simulations are carried out under three major categories when a 1,000 MW loss of generation occurs in the power system at t = 5 sec.

5.1 Effect of NPP Turbine Control

A very simple NPP turbine control is achieved by limiting the rate of change in steam valve opening. The effect of the control for different steam valve opening rates,

53

unlimited, 0.5% p.u./sec, and 0.2% p.u./sec, are presented below. For all of these three

cases gas turbines in the system are run at their maximum and the sliding-average-

temperature control for the reactor is active.

Before examining the results, each case is defined in Table 5.1 for simplicity. The

obtained results from simulations are presented in Figures 5.2, 5.3, 5.4, and 5.5.

Table 5.1 Definition of NPP turbine control cases

Case Number	NPP Steam Valve Opening Rate	Color of Graph Line
1	Unlimited	Blue
2	0.005 p.u./sec	Red
3	0.002 p.u./sec	Green
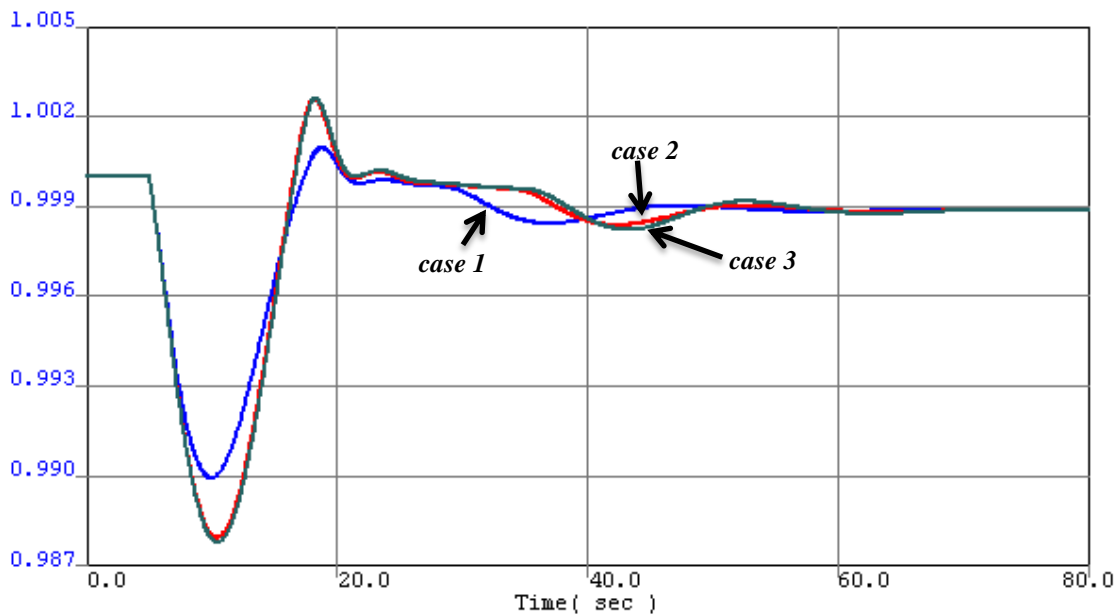
Figure 5.2 Change in the system frequency (p.u.).
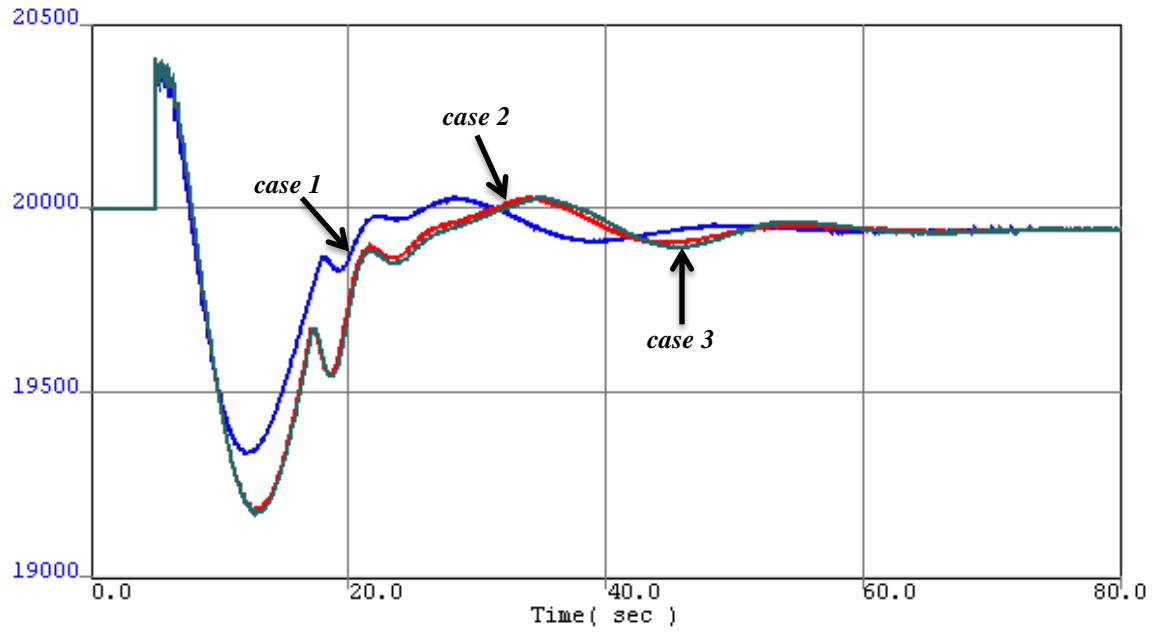
Figure 5.3 Change in the electrical power output (MW) of the NGP.
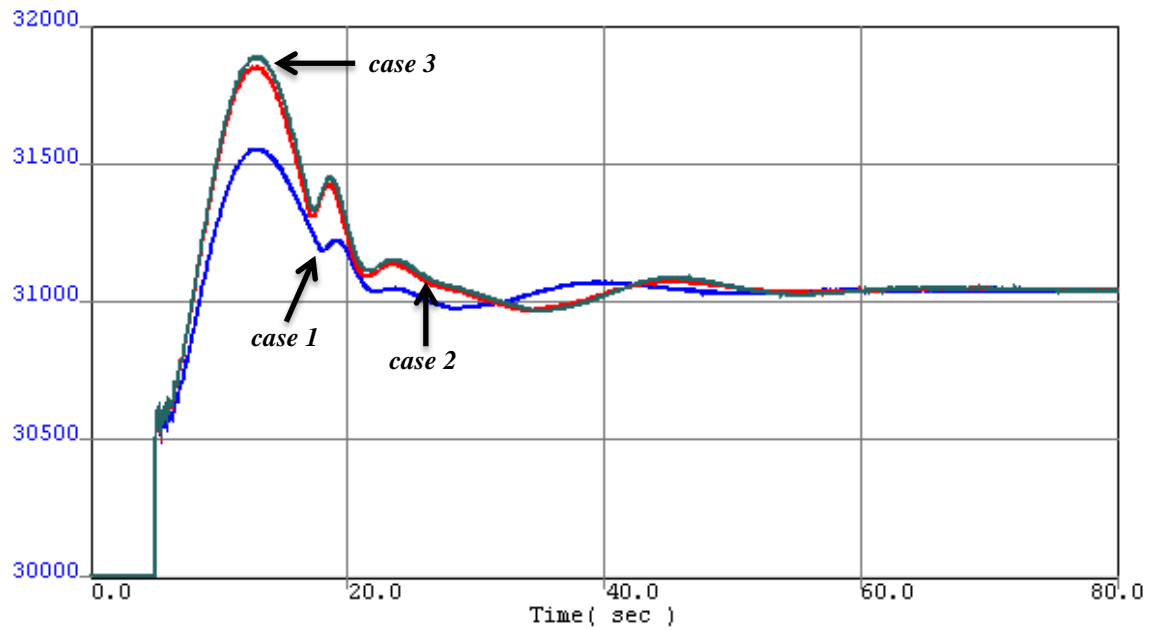
Figure 5.4 Change in the electrical power output (MW) of the HPP.

55
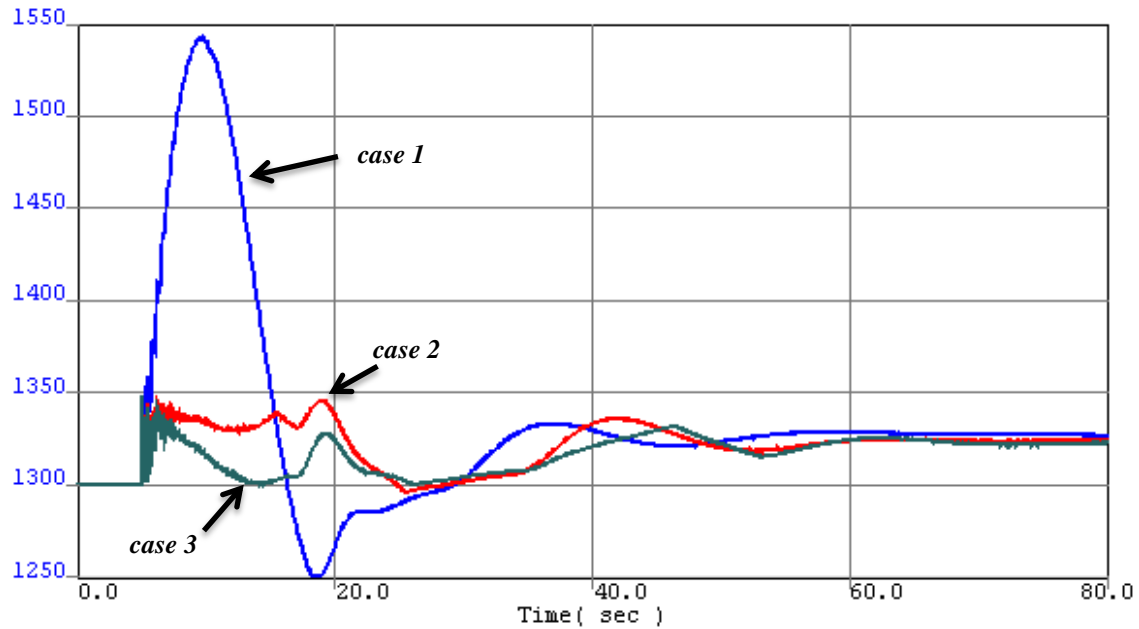
Figure 5.5 Change in the electrical power output (MW) of the NPP.

For *case 1*, when the disturbance occurs, the NGP with 20,000 MW output tries to respond to the change. However, since it is already running at its maximum, the temperature limit is reached and the speed of the gas turbine starts to decelerate meaning that electrical output of the plant is decreasing. Then the required generation must be supplied by the NPP and HPP. Thus, the output of the HPP increases but not as fast as a NGP. The NPP also responds and since there is no limitation on steam valve opening rate, a rapid change, +243 MW, is observed and then the generation decreases until it reaches 1,250 MW. From the operational point view of a NPP, such fast changes are not allowed due to safety and design limitations. When the new stable level is reached, electrical outputs of the HPP, NGP, and NPP are, respectively, 31,040 MW, 19,939 MW, and 1,325 MW in this case. The system frequency dips 0.5 of Hz during transient and reaches 49.95 Hz after transient.

If the steam valve opening rate is set to 0.005 p.u./sec, *case 2*, the NPP cannot increase its generation as it is in *case 1*. The increase is spread over time and the maximum value of the electrical power is 1,345 MW. Following that, the initial decrease in the NGP output and the initial increase in the HPP output are bigger than the results of the previous case since the HPP must supply the difference in generation which takes more time compared to *case 1*. While the final output value of the NPP decreases about 1 MW, the other plants almost keep the same values as in *case 1*. The initial drop of the system frequency is 0.6 Hz due to an increase in response time for this case while the new steady state value is 49.95 Hz again.

In the last case, the rate of change in steam valve position is 0.002 p.u./sec. Because of the strict limitation on the steam valve, almost all of the difference between the generation and the load is provided by the HPP during the transient. That is the reason why the initial increase in the electricity generation of the HPP is greater than the values in previous cases. The difference in the NPP output between *case 2* and *case 3* is that less steam flow is delivered to the turbine, again, due to slow steam valve opening rate. This means that the effect of the disturbance is felt slower. Thus, the reactor cannot respond as it does in *case 2* explaining the decrease, after the initial jump, in the electrical power of the NPP (see Appendix E for supporting figures). On the other hand, frequency of the grid and the generation of the NGP follow similar patterns with *case 2*. The biggest change in all output values of the power plants, at the new steady-state level, occurs again in the NPP with a 1 MW additional decrease (1,323 MW).

5.2 Grid Operation Issues

In the previous section, the initial power output of the NGP was at its maximum value and constant. In order to observe the effects of different operational modes, the NPP steam valve opening rate is kept constant at 0.005 p.u./sec while the initial steady-state power level of the NGP is decreased for each case with the total load in the power system. The sliding-average-temperature control for the reactor is still active for all cases. Table 5.2 provides a summary of how each case is set up. Simulation results for all three cases are shown in Figures 5.6, 5.7, 5.8, and 5.9.

Table 5.2 Definition of grid operation cases

Case Letter	NGP Output	Color of Graph Line
a	20,000 MW	Blue
b	19,500 MW	Red
c	19,000 MW	Green
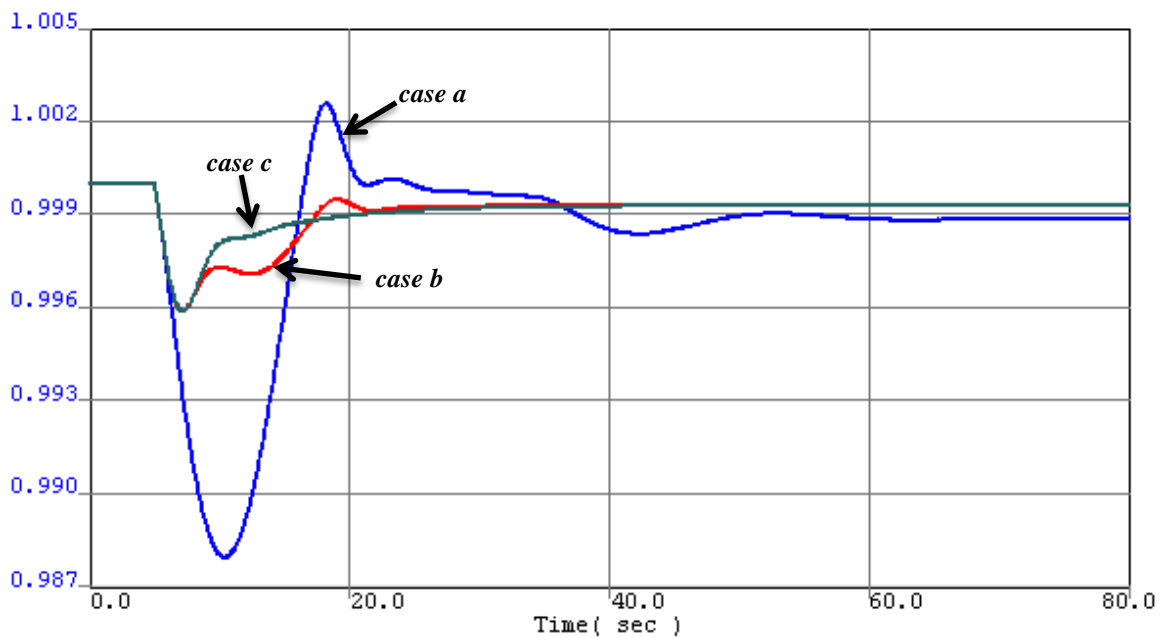
Figure 5.6 Change in the system frequency (p.u.).

58
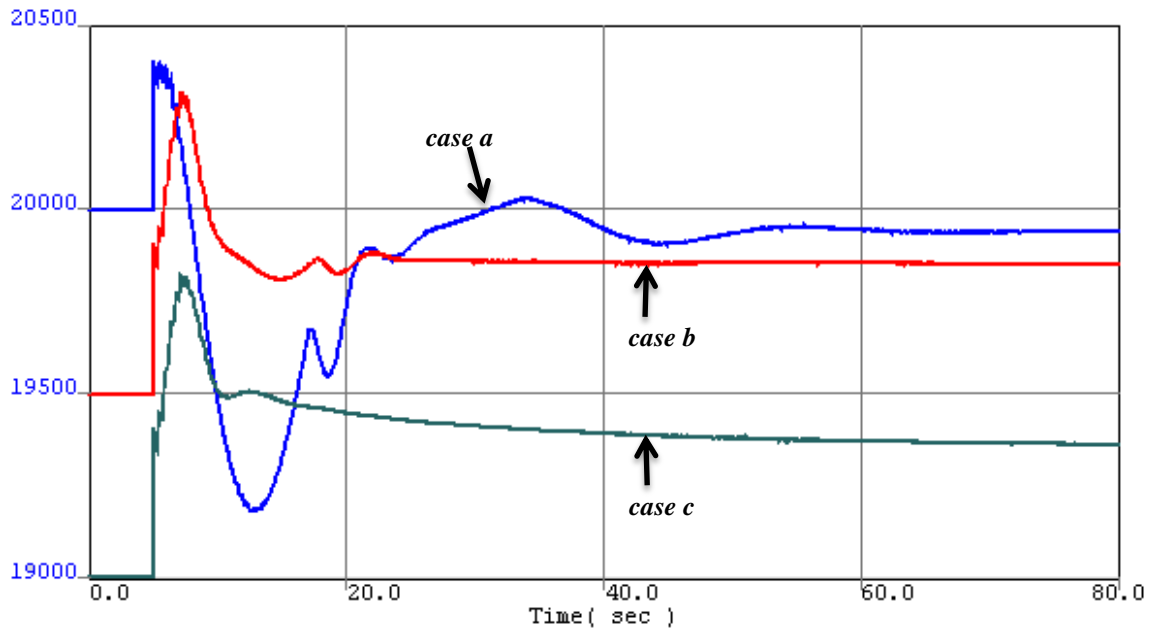
Figure 5.7 Change in the electrical power output (MW) of the NGP.
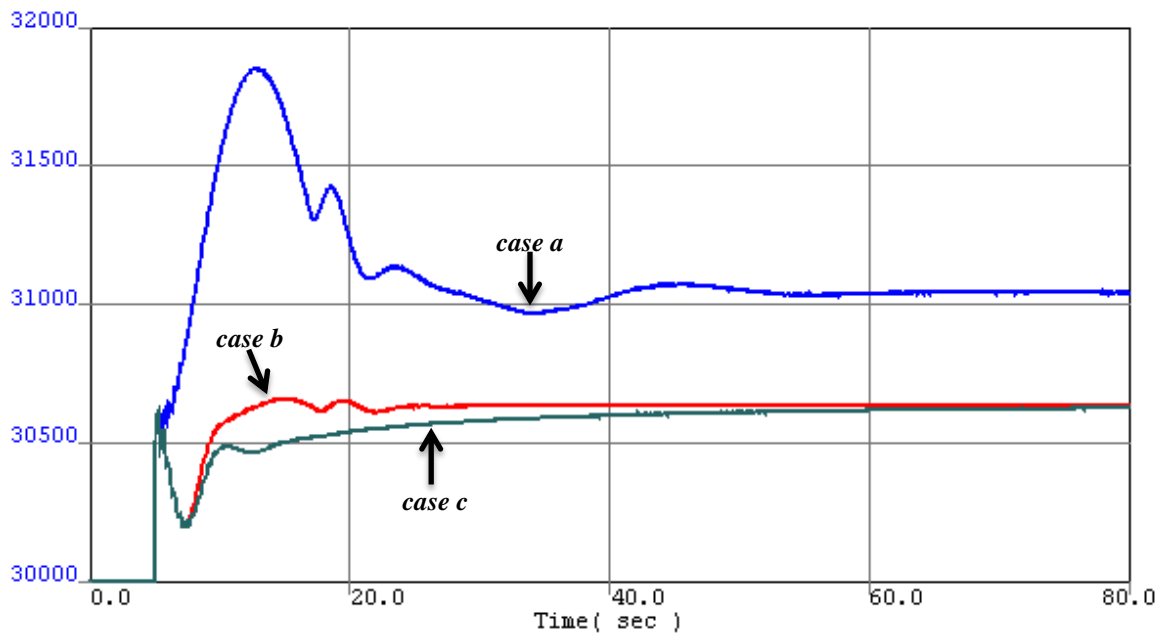
Figure 5.8 Change in the electrical power output (MW) of the HPP.

59
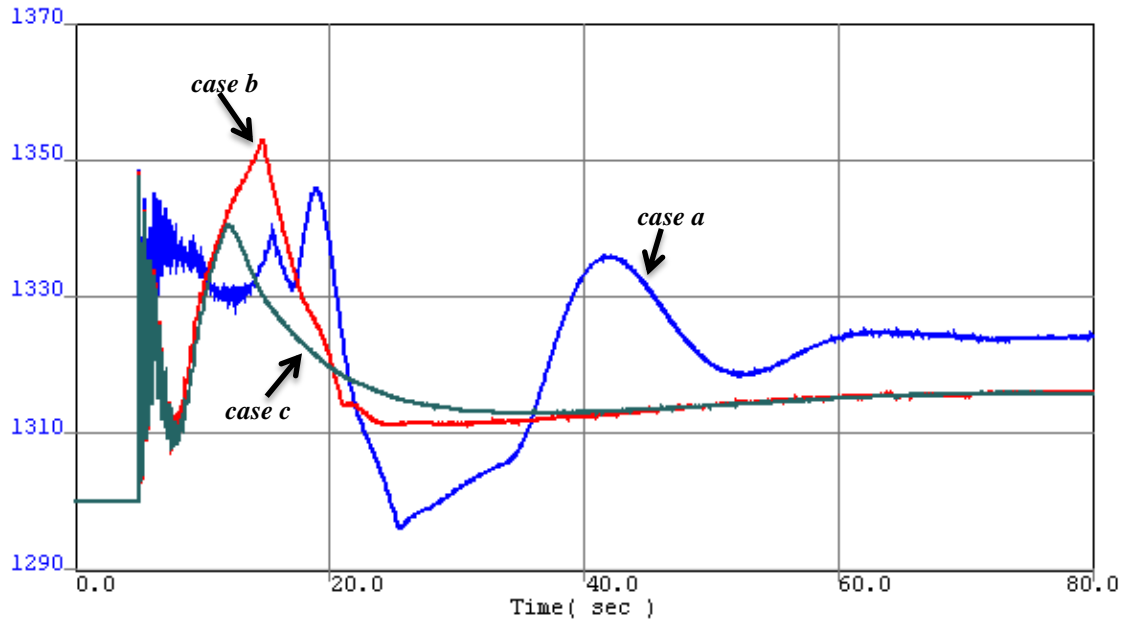
Figure 5.9 Change in the electrical power output (MW) of the NPP.

As it is obvious, *case a* is identical with *case 2* in the previous section. Thus, all comments made for *case 2* are also valid for *case a*.

If the output of the NGP is 19,500 MW when the load increases suddenly by 1,000 MW, *case b*, then the gas turbines are capable of responding. Since this is the fastest generation type in the system, an increase in the NGP generation is observed, initially, while the outputs of the NPP and the HPP decline after a quick jump. Approximately five seconds later, their outputs start increasing. Power plant generation levels at the new steady-state are 30,635 MW (hydro), 19,850 MW (natural gas), and 1,316 MW (nuclear). Comparing these results with *case a* in which the NGP is not able to assist; the deficiency in generation is dispelled by the participation of all power plants. In addition, the initial decrease in the system frequency diminishes and becomes 0.2 Hz instead of 0.6 Hz. An improvement in the final value of the system frequency is also achieved and the new value is 49.965 Hz (49.95 in *case a*).

In the last case, due to the increase in generation reserve of the NGP, it can contribute more during the transient, meaning that generation levels of the NPP and the HPP at the same time instant are lower than the values in *case b* as depicted in Figures 5.7 and 5.8. Consequently, as the share of the NGP is bigger in this case, implying that the overall system offsets the effect of the disturbance quicker, the oscillation in the grid frequency during the transient is eliminated, and the final value is 49.965 Hz.

5.3 Effect of Reactor Control System

Up to now, the reactor control system is active for dynamic simulations. It is time to investigate its impact on the nuclear steam supply system (NSSS) and the electrical network. Bearing that in mind, two cases are presented in both of which the NGPs are run at a power level of 19,500 MW and the NPP steam valve opening rate is kept constant at 0.005 p.u./sec. On the other hand, as expected, the sliding-average-temperature control is on for only one of the cases. Further details are provided in Table 5.3. The results for key parameters in the NPP are demonstrated in Figures 5.10, 5.11, 5.12, and 5.13.

Table 5.3 Definition of reactor control impact cases

Case Letter	Reactor Control System	Color of Graph Line
i	On	Blue
ii	Off	Red
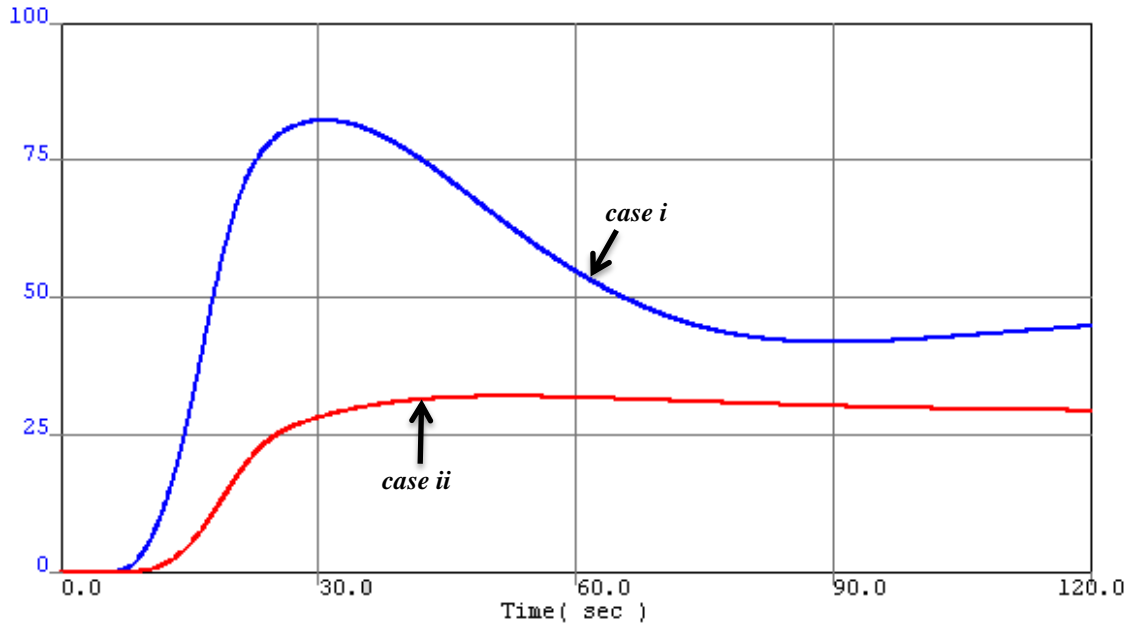
Figure 5.10 Change in the reactor thermal power (MW).
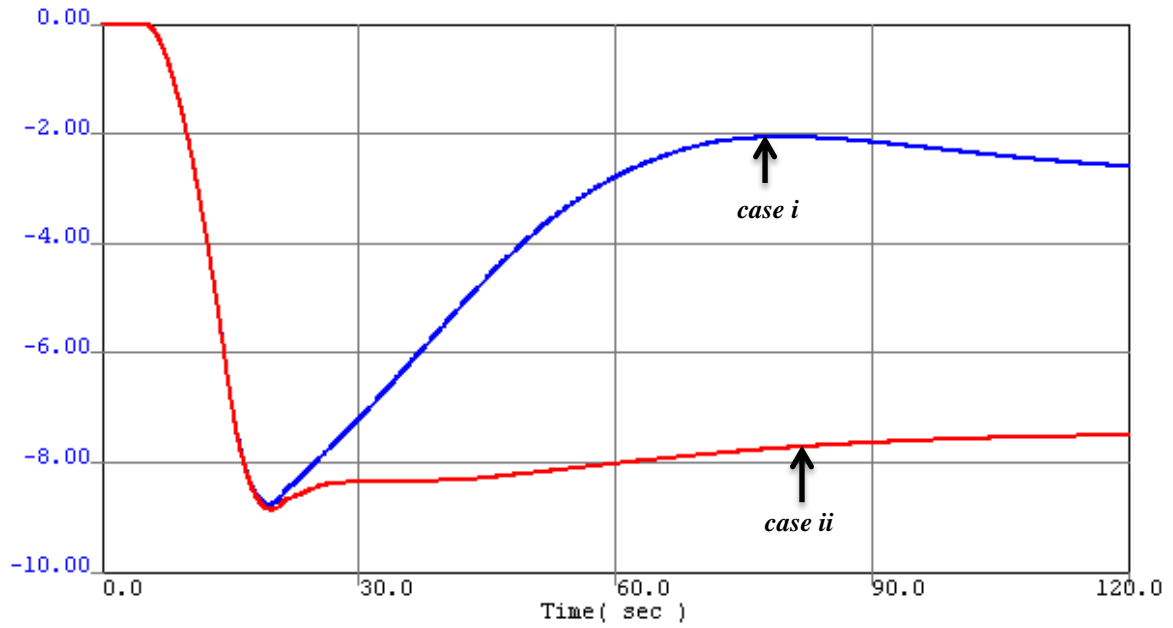
Figure 5.11 Change in steam pressure (psi).
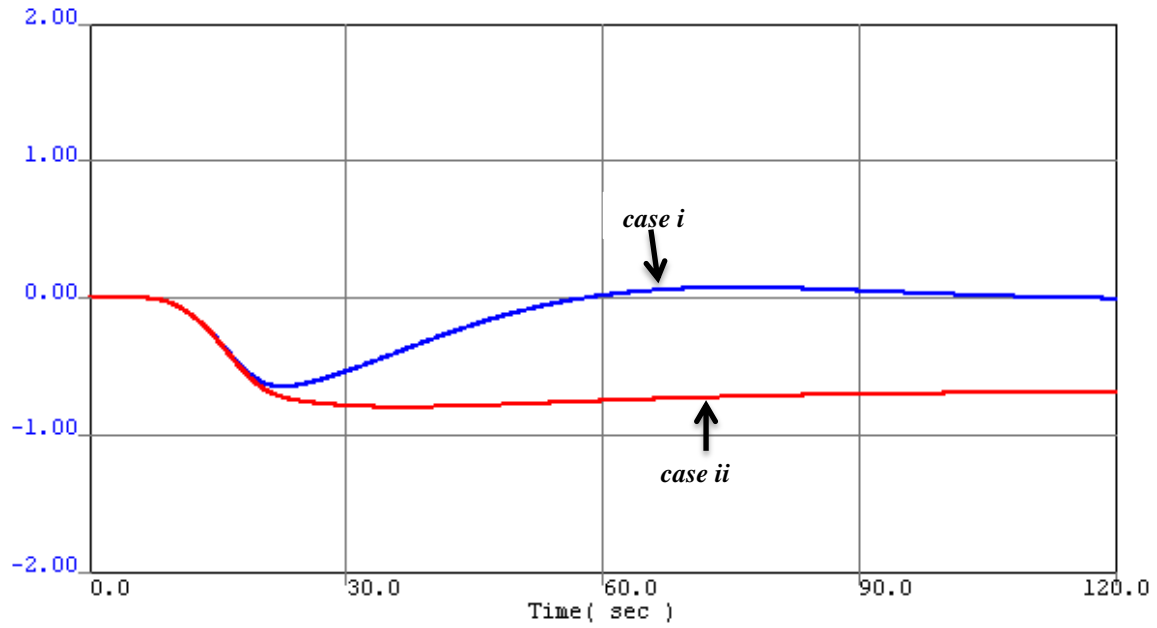
Figure 5.12 Change in the cold leg temperature (ºF).
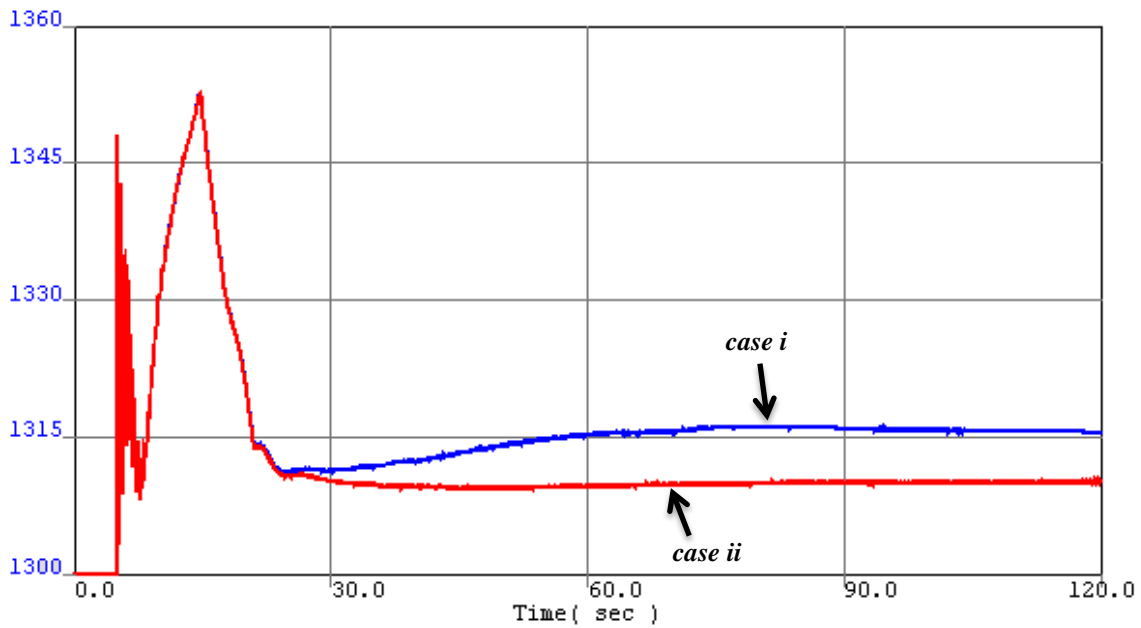
Figure 5.13 Change in the electrical power output (MW) of the NPP.

In *case i*, the change in the cold leg temperature triggers the reactor control system and the corresponding reactivity insertion is realized by control rods movement.

Following that, the reactor thermal power starts increasing. Thus, more heat is transferred to the primary coolant causing the hot leg temperature to increase. While the primary coolant is passing through the steam generator, it transfers part of its heat content in the steam generator explaining the increase in the steam pressure as shown in Figure 5.11. Then, one cycle is completed and the coolant reaches the cold leg with a rise in its temperature. This process is repeated until the change in the cold leg temperature becomes zero. When the system achieves a new stable operating condition after about 120 seconds, the deviations from initial values for the reactor thermal power and the steam pressure are +45 MW and -2.5 psi, respectively.

In the case of no reactor control, however, the NSSS relies on its self-regulating behavior, meaning that the decrease in the temperature of the cold leg activates the negative feedback mechanisms. This passive control action is slower and cannot provide an improvement in the cold leg and steam pressure conditions which deteriorate because of a disturbance occurring outside the reactor. It only stabilizes the system. That is the reason why the decreases in both of the parameters are higher than the previous case.

The electrical output of the NPP is same for both of the cases during the initial transient but the withdrawal of the control rods by the reactor control system brings the power level up. The steady-state value of the NPP generation is about 1,315 MW for *case i* whereas it stays around 1,310 MW in *case ii*.

5.4 Summary

Based on the results in Chapter 5, the reactor control system is vital for keeping key variables of the NSSS, such as primary coolant temperature and steam pressure, in a desired range when the system encounters a disturbance occurring in the electrical network. In addition, the turbine control prevents huge fluctuations in the reactor thermal power which can cause the reactor to trip. Finally, operating conditions of the network also have an impact on the NPP. As seen in Section 5.2, an increase in the generation reserve allows the NGP to respond to a change in the load. Since it is the fastest generation type in the system, the effect of a disturbance is dispelled quicker and the burden on other power plants during the initial transient decreases significantly.

CHAPTER 6

CONCLUSIONS AND FUTURE WORK

6.1 Research Summary

In the U.S., NPPs are operated at a constant power level over a fuel cycle in order
to meet the base load. On the other hand, some countries including France and Germany
let NPPs change their output according to fluctuations in power demand. As a
consequence of the growth of renewable energy sources in the power system of the U.S.,
a load-following operational mode for NPPs might be an option for accommodating these
intermittent sources properly in the system while ensuring the power system frequency
limits.

Considering the absence of a NPP model in PSLF and the need for an
investigation into the above possibility, a model representing the Palo Verde Nuclear
Generating Station is developed in this study. The NSSS is composed of the reactor core,
plenums, hot and cold legs, and steam generator models. Since one of the main objectives
of the study is to investigate the interaction between the NPP and a small electric grid, a
reactor control system, and simple turbine and governor models are also introduced. In
Chapter 4, with the help of Matlab/Simulink, dynamic responses from the isolated core
and steam generator are presented first. Then, the complete PWR model, a combination
of the above models with plenums, hot and cold legs, is tested. Following that, the test
results of the PWR representation with a reactor control system and a turbine model are
demonstrated, respectively. In Chapter 5, the PWR is introduced into PSLF and coupled
with built-in generator model and excitation system to form a NPP. Different simulation

cases are run in the PSLF dynamic simulation environment when the NPP is part of an electrical network.

6.2 Main Results of the Study

A detailed PWR model is developed into Matlab/Simulink in this study. Investigation into the components of the model and the model itself are carried out by applying small perturbations to the input parameters. Comparison between the obtained test results and the results from References [12] and [13] yields that the introduced PWR representation is realistic, and able to predict reactivity and steam valve perturbations. After the validation, a NPP model based on the developed PWR for the Palo Verde Nuclear Generating Station is introduced into PSLF. Different simulation cases are run in Chapter 5 in order to evaluate the impacts of reactor and NPP turbine controls, and grid operation issues on the overall behavior of the electric power system. The results indicate that choosing the right operational limits enables the NPP to respond to a disturbance occurring in the electrical network without exceeding its design and safety limits some of which are given in Appendix B. In other words, the NPP can contribute to system frequency control and bolster the network performance.

6.3 Future Work

The NPP model presented in this study can be extended in several directions. Possible areas in which future work may be carried out are

- A pressurizer model can be developed since the sliding-average-temperature program chosen for the NPP model causes the volume of primary coolant to change according to operating power level.

- The nonlinear terms of the governing equations for the models that are not utilized in the study might be included.

- Primary and secondary coolant flows, which are assumed to be constant, can be modeled.

- The dynamic simulation results from Chapter 5 are a starting point for evaluating the role of NPPs in the control of system frequency and power flows. Thus more detailed analysis, specifically by using models of real electrical networks, is required to understand thoroughly the extent to which a grid related event has impacts on the key variables of the NSSS.

REFERENCES

[1]   World Nuclear Association, "Nuclear Power in the World Today," [Online]. Available: http://www.world-nuclear.org/info/inf01.html [Accessed: 07 Sept. 2012].

[2]   "Nuclear Technology Review 2012," *56th IAEA General Conference*, Vienna, Austria, August 2012, pp. 5-7.

[3]   International Atomic Energy Agency, "Nuclear Power Reactors in the World 2012 edition," [Online]. Available: http://wwwpub.iaea.org/books/iaeabooks/8954/Nuclear-Power-Reactors-in-the-World-2012-Edition [Accessed: 10 Sept. 2012].

[4]   U.S. Energy Information Administration, International Energy Outlook 2011, U.S. Department of Energy, DOE/EIA-0484(2011), p. 88.

[5]   B. Gjorgiev and M. Čepin, "Nuclear power plant load following: problem definition and application," in *Proc. 20th Int. Conf. Nuclear Energy for New Europe 2011*, Bovec, Slovenia, September 2011, pp. 506-515.

[6]   World Nuclear Association, "Nuclear Power in France," [Online]. Available: http://www.world-nuclear.org/info/inf40.html [Accessed: 13 Jan. 2013].

[7]   NEA (2011), Technical and Economic Aspects of Load-following with Nuclear Power Plants, OECD/NEA online report available at: www.oecd-nea.org/ndd/reports/2011/load-following-npp.pdf.

[8]   J. Zhao, P. Wu, and D. Liu, "User-defined modeling of pressurized water reactor nuclear power plant based on PSASP and analysis of its characteristics," in *Proc. 2009 Asia-Pacific Power and Energy Engineering Conf.*, Wuhan, China.

[9]   L. Xiong, D. Liu, B. Wang, P. Wu, J. Zhao, X. Shi, "Dynamic characteristics analyse [sic] of pressurized water reactor nuclear power plant based on PSASP," in *Proc. 2009 4th IEEE Conf. on Industrial Electronics and Applications*, pp. 3629-3634.

[10]   X. Shi, P. Wu, D. Liu, L. Xiong, J. Zhao, Y. Zhang, "Modeling and dynamic analysis of nuclear power plant reactor based on PSASP," in *Proc. 2009 Asia-Pacific Power and Energy Engineering Conf.*, Wuhan, China.

[11]   L. Xiong, D. Liu, X. Shi, J. Zhao, and P. Wu, "Research and analyse [sic] for pressurized water reactor model into power system dynamic simulation," in *Proc. 2009 Asia-Pacific Power and Energy Engineering Conf.*, Wuhan, China.

[12]   T. W. Kerlin, E. M. Katz, J. G. Thakkar, and J. E. Strange, "Theoretical and experimental dynamic analysis of the H. B. Robinson nuclear plant," *Nuclear Technology*, vol. 30, pp. 299-316, Sept. 1976.

[13]   M. R. A. Ali, "Lumped parameter, state variable dynamic models for U-tube circulation type nuclear steam generators," Ph.D. dissertation, Dept. Nuc. Eng., Univ. Tennessee, Knoxville, 1976.

[14]   M. A. Schultz, *Control of Nuclear Reactors and Power Plants*, New York: McGraw-Hill, 1955, pp. 128-179.

[15]   Positive Sequence Load Flow software (PSLF), General Electric, 2012.

[16]   J. R. Lamarsh, and A. J. Baratta, *Introduction to Nuclear Engineering*, 3rd ed., New Jersey: Prentice Hall, 2001.

[17]   T. W. Kerlin, "Dynamic Analysis and Control of Pressurized Water Reactors," *Control and Dynamic Systems, Advances in Theory and Applications*, edited by C.T. Leondes, Academic Press, vol. 14, 1978, pp. 103-212.

[18]   " Westhinghouse Technology Systems Manual Section 1.2," [Online]. Available: pbadupws.nrc.gov/docs/ML1122/ML11223A195.pdf [Accessed: 12 Feb. 2013].

[19]   N. Venkatesh, "Validation of noise analysis techniques for evaluating the moderator temperature coefficient in pressurized water reactors," M.S. thesis, School of Elect., Comput., and Energy Eng., Arizona State Univ., Tempe, Arizona, 1993.

[20]   Y. E. Kim, J. W. Park, and J. Cleveland, "Thermophysical properties database of materials for light water and heavy water reactors," International Atomic Energy Agency, Vienna, Austria, Tech. Rep. IAEA-TECDOC-1496, Jun. 2006.

[21]   "Inconel 600 technical data," [Online]. Available: http://www.hightempmetals.com/techdata/hitempInconel600data.php [Accessed: 12 Feb. 2013].

[22]   "Inconel alloy 600," [Online]. Available: http://www.specialmetals.com/documents/Inconel%20alloy%20600%20(Sept%20 2008).pdf [Accessed: 11 Feb. 2013].

[23]   M. M. El-Wakil, *Powerplant Technology*, New York: McGraw-Hill, 2002, pp. 766-773.

APPENDIX A

LINEAR APPROXIMATION FOR PROPERTIES OF

SATURATED LIQUID AND VAPOR

As seen in Chapter 3, the development of the steam generator model requires using the thermodynamic properties of saturated liquid and vapor. These properties are obtained, in this study, by utilizing polynomial fitting. In order to have reasonably accurate values, the method is applied over the pressure range 850-1250 psia considering the normal operating transients of steam generator and the steady-state value of steam pressure at full power level which is 1070 psia for the Palo Verde Nuclear Generating Station. The data for the calculation are provided by the steam tables in Reference [22]. Figures A.1 through A.4 show the related plots from Microsoft Excel. The resulting values giving the rate of change for each property are

$$\frac{\partial T_{SAT}}{\partial p} = 0.1176 \text{ °F/psi}$$

$$\frac{\partial \upsilon_g}{\partial p} = \text{-0.000464 ft}^3\text{/lbm/psi}$$

$$\frac{\partial h_g}{\partial p} = \text{-0.0385 Btu/lbm/psi}$$

$$\frac{\partial h_f}{\partial p} = 0.1508 \text{ Btu/lbm/psi}$$
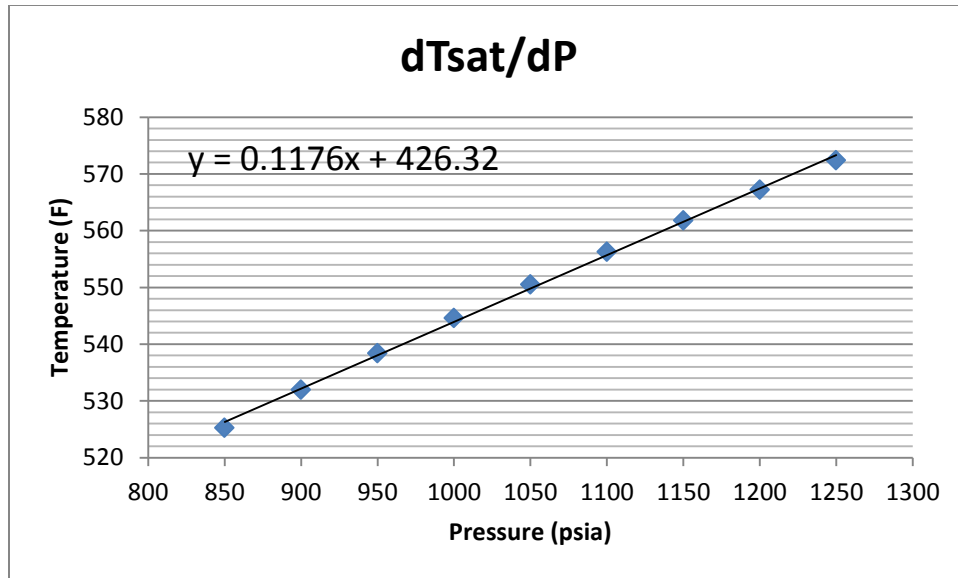
Figure A.1 Change in T_{SAT} with pressure.
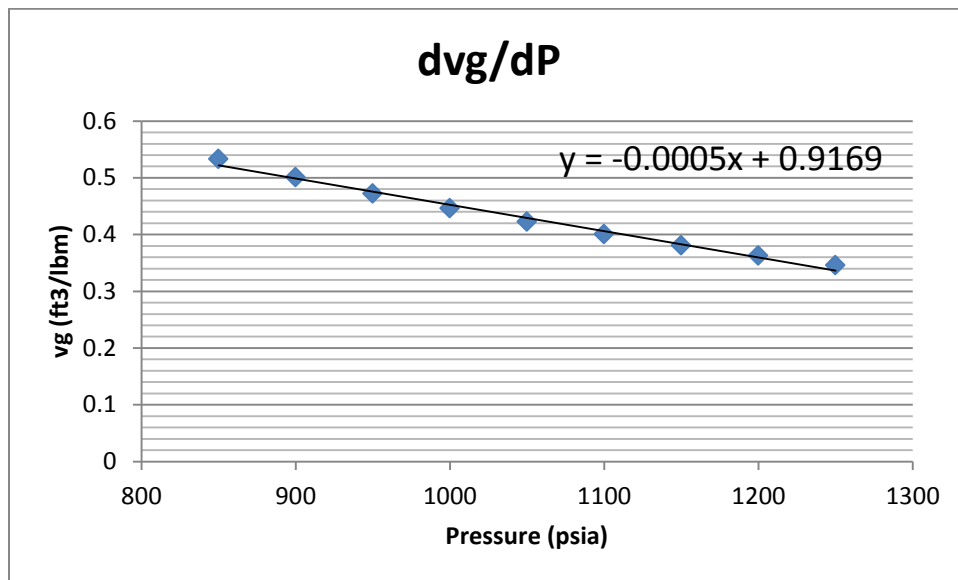
Figure A.2 Change in υ_g with pressure.
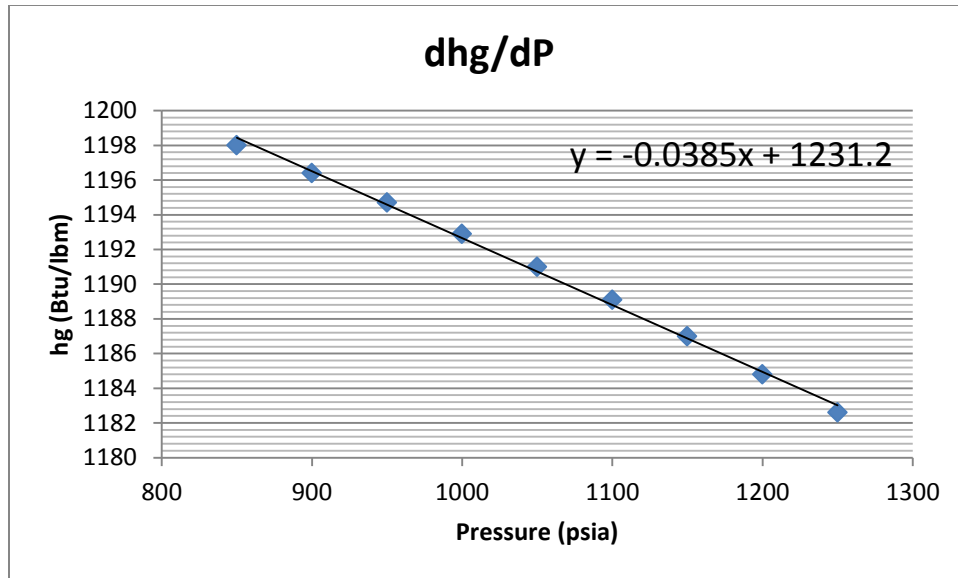
Figure A.3 Change in h_g with pressure.
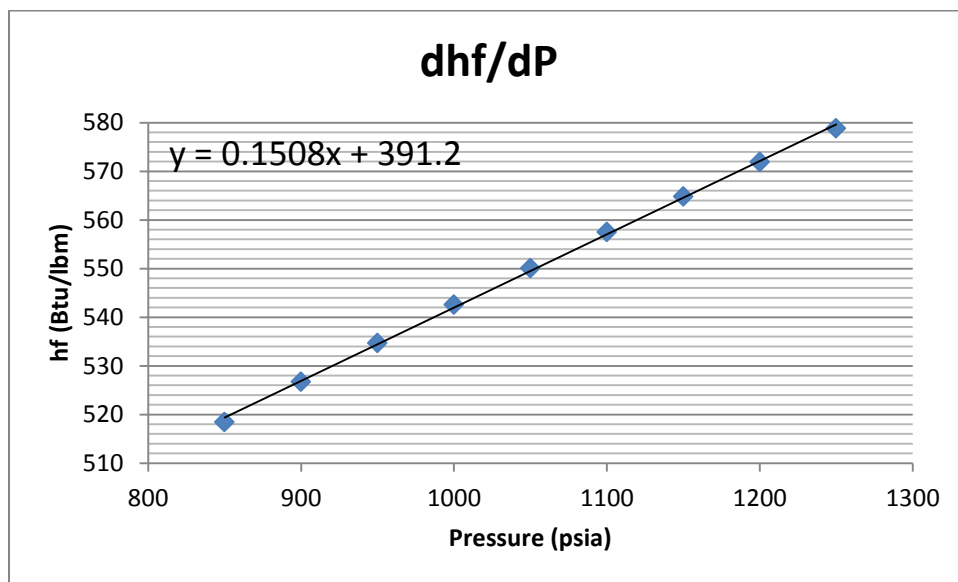
Figure A.4 Change in h_f with pressure.

APPENDIX B

MODEL PARAMETERS AND EVALUATION OF COEFFICIENTS

B.1 Reactor Core

Table B.1 Reactor core parameters for the Palo Verde Nuclear Generating Station

Variable	Description	Value	Source
P_0	Initial thermal power level	3800 MWth	FSAR-I 1.3-2
β	Delayed neutron fraction	0.0073	PV FILE A-49
Λ	Neutron generation time	30 μs	FSAR-I 1.3-6
λ	Delayed neutron precursor decay constant	0.1 s^{-1}	Reference [16]
a_F	Fuel temperature coefficient of reactivity	-1.2×10^{-5}/ °F	FSAR-I 1.3-6
a_C	Coolant temperature coefficient of reactivity	-1×10^{-4}/ °F	FSAR-I 1.3-6
T_F	Average fuel temperature	1160 °F	Reference [19]
c_F	Specific heat of fuel	0.1056 Btu/lbm·°F	Reference [20]
m_F	Total fuel mass	257.1×10^3 lbm	PV FILE A-44
f	Fraction of total power produced in fuel	0.975	FSAR-I 1.3-2
U_{FC}	Fuel-to-coolant heat transfer coefficient	325.588 Btu/hr·ft^2·°F	Reference [19]
A_{FC}	Effective heat transfer area	68,600 ft^2	FSAR-I 1.3-3
V_C	Volume of coolant in core	715.741 ft^3	Reference [19]
ρ_W	Density of water (2000 psia & 600 °F)	42.92 lbm/ft^3	Reference [16]
c_p	Specific heat of water (2000 psia & 600 °F)	1.448 Btu/lbm·°F	Reference [16]
$\dot{m}_C$	Primary coolant flow in core	164×10^6 lbm/hr	FSAR-I 1.3-2
T_{avg}	Average core coolant temperature	594 °F	FSAR-I 1.3-2

As the developed models are tested in Matlab/Simulink, final versions of the governing equations in *s* domain are presented in this section. Taking the Laplace transform of Equations (3.2) and (3.3), and performing some algebraic manipulation yields

$$\delta P(s)\left(s+\frac{\beta}{\Lambda}\right)=\lambda\delta C(s)+\frac{P_o}{\Lambda}\delta\rho(s) \tag{B.1}$$

$$\delta C(s)(s+\lambda)=\frac{\beta}{\Lambda}\delta P(s) \tag{B.2}$$

$$\delta\rho(s)=\beta\,\delta\rho_{ext}(s)+\alpha_F\delta T_F(s)+\alpha_C\delta T_C(s) \tag{B.3}$$

Following the same procedure, the equations for the thermodynamics model can be expressed as

$$\delta T_F(s)(\tau_F s+1)=\frac{f\,\tau_F}{m_F c_F}\delta P(s)+\delta T_{\theta 1} \tag{B.4}$$

$$\delta T_{\theta 1}(s)\left(\frac{\tau_C\tau_R}{\tau_R+2\tau_C}s+1\right)=\frac{(1-f)}{m_C c_p}\left(\frac{\tau_C\tau_R}{\tau_R+2\tau_C}\right)\delta P(s)+\left(\frac{\tau_R}{\tau_R+2\tau_C}\right)\delta T_F(s)+\left(\frac{2\tau_C}{\tau_R+2\tau_C}\right)\delta T_{\theta in}(s) \tag{B.5}$$

$$\delta T_{\theta 2}(s)\left(\frac{\tau_R}{2}s+1\right)=\frac{(1-f)}{m_C c_p}\left(\frac{\tau_R}{2}\right)\delta P(s)+\left(\frac{\tau_R}{2\tau_C}\right)\delta T_F(s)+\left(\frac{2\tau_C-\tau_R}{2\tau_C}\right)\delta T_{\theta 1}(s) \tag{B.6}$$

B.2 Plenums, Hot and Cold Legs

Table B.2 Model parameters for the Palo Verde Nuclear Generating Station

Variable	Description	Value	Source
ρ_W	Density of water (2000 psia & 620 °F)	40.93 lbm/ft^3	Reference [16]
c_p	Specific heat of water (2000 psia & 620 °F)	1.62 Btu/lbm·°F	Reference [16]
V_{SGI}	Total volume of steam generator inlet plenum (each)	366 ft^3	SYSTEM 80 4.4-43
$\dot{m}_{C,SG}$	Primary coolant flow in SG	82x10^6 lbm/hr	FSAR-I 1.3-9
ρ_W	Density of water (2000 psia & 560 °F)	46.04 lbm/ft^3	Reference [16]
c_p	Specific heat of water (2000 psia & 560 °F)	1.278 Btu/lbm·°F	Reference [16]
V_{SGO}	Total volume of steam generator outlet plenum (each)	358 ft^3	SYSTEM 80 4.4-43
V_{HL}	Volume of hot leg (each)	130 ft^3	SYSTEM 80 4.4-43
T_{HL}	Temperature of hot leg at full power	621.2 °F	FSAR-I 1.3-7
	Design temperature (max)	650 °F	
$\dot{m}_{C,HL}$	Primary coolant flow in hot leg	82x10^6 lbm/hr	SYSTEM 80 4.4-43
V_{CL}	Volume of cold leg (each)	323 ft^3	SYSTEM 80 4.4-43
T_{CL}	Temperature of cold leg at full power	564.5 °F	FSAR-I 1.3-7
$\dot{m}_{C,CL}$	Primary coolant flow in cold leg	41x10^6 lbm/hr	SYSTEM 80 4.4-43
V_{RXU}	Total volume of reactor core upper plenum	2115 ft^3	SYSTEM 80 4.4-43
V_{RXL}	Total volume of reactor core lower plenum	2871 ft^3	SYSTEM 80 4.4-43

B.3 Steam Generator

Table B.3 Steam generator parameters for the Palo Verde Nuclear Generating Station

Variable	Description	Value	Source
V_{SG}	Total volume of active tubes in steam generator (each)	1390 ft^3	SYSTEM 80 4.4-43
ρ_W	Density of water (2000 psia & 600 ºF)	42.92 lbm/ft^3	Reference [16]
c_p	Specific heat of water (2000 psia & 600 ºF)	1.448 Btu/lbm·ºF	Reference [16]
d_{out}	Outside diameter of tubes	0.75 in	SYSTEM 80 Table 5.4.2-1
t	Tube thickness	0.042 in	SYSTEM 80 Table 5.4.2-1
ρ_{IN}	Density of INCONEL alloy 600	0.304 lbm/in^3	Reference [21]
c_M	Specific heat of INCONEL alloy 600 (580 ºF)	0.1205 Btu/lbm·ºF	Reference [22]
m_{SW}	Liquid mass in secondary coolant lump (SCL)	334,000 lbm	SYSTEM 80 Table 11.1.8-1
$V_{SW}\big/V_{SS}$	Ratio of liquid and vapor volume in SCL	0.48	Reference [12]
υ_f	Specific volume of saturated liquid (1070 psia)	0.0218 ft^3/lbm	Reference [23]
υ_g	Specific volume of saturated vapor (1070 psia)	0.4114 ft^3/lbm	Reference [23]
h_g	Specific enthalpy of saturated vapor (1070 psia)	1189 Btu/lbm	Reference [23]
h_f	Specific enthalpy of saturated liquid (450 ºF)	430.2 Btu/lbm	Reference [23]
h_{fg}	$h_g - h_f$ (1070 psia)	635 Btu/lbm	Reference [23]
υ_{fg}	$\upsilon_g - \upsilon_f$ (1070 psia)	0.39 ft^3/lbm	Reference [23]
T_{FI}	Feedwater inlet temperature at full power	450 ºF	SYSTEM 80 Table 4.4-9
T_S	Steam temperature at full power	552.9 ºF	FSAR-I 1.3-9
	Design temperature	575 ºF	
p	Steam pressure at full power	1070 psia	FSAR-I 1.3-9
	Design pressure	1270 psia	
	Zero load steam pressure	1170 psia	

Following the same procedure, Equations (3.17) and (3.19), representing primary coolant lumps, can be written in the s domain as follows:

$$\delta T_{P1}(s)\left(\frac{\tau_{P1}\tau_{PM1}}{\tau_{P1}+\tau_{PM1}}s+1\right)=\left(\frac{\tau_{PM1}}{\tau_{P1}+\tau_{PM1}}\right)\delta T_{PI}(s)+\left(\frac{\tau_{P1}}{\tau_{P1}+\tau_{PM1}}\right)\delta T_{M1}(s) \quad \text{(B.7)}$$

$$\delta T_{P2}(s)\left(\frac{\tau_{P2}\tau_{PM2}}{\tau_{P2}+\tau_{PM2}}s+1\right)=\left(\frac{\tau_{PM2}}{\tau_{P2}+\tau_{PM2}}\right)\delta T_{P1}(s)+\left(\frac{\tau_{P2}}{\tau_{P2}+\tau_{PM2}}\right)\delta T_{M2}(s) \quad \text{(B.8)}$$

For tube metal lumps, Equations (3.22) and (3.24) can also be written in the s domain as follows:

$$\delta T_{M1}(s)\left(\frac{\tau_{MS1}\tau_{MP1}}{\tau_{MS1}+\tau_{MP1}}s+1\right)=\left(\frac{\tau_{MS1}}{\tau_{MS1}+\tau_{MP1}}\right)\delta T_{P1}(s)+\left(\frac{\tau_{MP1}}{\tau_{MS1}+\tau_{MP1}}\right)\left(\frac{\partial T_{SAT}}{\partial p}\right)\delta p(s) \quad \text{(B.9)}$$

$$\delta T_{M2}(s)\left(\frac{\tau_{MS2}\tau_{MP2}}{\tau_{MS2}+\tau_{MP2}}s+1\right)=\left(\frac{\tau_{MS2}}{\tau_{MS2}+\tau_{MP2}}\right)\delta T_{P2}(s)+\left(\frac{\tau_{MP2}}{\tau_{MS2}+\tau_{MP2}}\right)\left(\frac{\partial T_{SAT}}{\partial p}\right)\delta p(s) \quad \text{(B.10)}$$

The final expression is already introduced in Chapter 3 for the secondary coolant lump. However, after some algebraic manipulations, the equation takes the form of

$$\delta p(s)\left(\frac{K}{Y}s+1\right)=\frac{(U_{ms}S_{ms})_1}{Y}\delta T_{M1}(s)+\frac{(U_{ms}M_{ms})_2}{Y}\delta T_{M2}(s)-\frac{p(h_g-h_f(T_{FI}))}{Y}\delta C_L(s) \quad \text{(B.11)}$$

where

$$h_f(T_{FI})\cong c_{pi}T_{FI}$$

$$Y=\left[(U_{ms}S_{ms})_1+(U_{ms}S_{ms})_2\right]\left(\frac{\partial T_{SAT}}{\partial p}\right)+\dot{m}_{SO}\left(\frac{\partial h_g}{\partial p}\right)+C_L\left(h_g-h_f(T_{FI})\right)$$

$\dot{m}_{SO}c_{pi}\delta T_{FI}\cong 0$, since the temperature of the secondary coolant is assumed to be constant.

B.4 Reactor Control System, Turbine and Governor Models

Table B.4 Parameters for the reactor control system, turbine and governor models

Variable	Description	Value	Source
$T_{avg,ref}$	Reference value for the average temperature	$(T_{HL} + T_{CL})/2 = 594\,°F$	Calculated
K_{avg}	Slope of the equation relating T_{avg} to reactivity	$0.0205\,\rho\,/\,°F$	Calculated
τ	Tuning parameter	20 sec	
$T_{CL,ref}$	Reference value for the cold leg temperature	564.5 °F	
K_{CL}	Slope of the equation relating T_{CL} to reactivity	$0.0241\,\rho\,/\,°F$	Calculated
p_C	Main condenser pressure	1.72 psia	FSAR-I 1.3-7 Table 10.1-1
h_g	Specific enthalpy of saturated vapor (1070 psia)	1189 Btu/lbm	Reference [23]
x	Steam quality	0.7^1	Calculated
h_x	Specific enthalpy with quality x	793 Btu/lbm	Calculated
Δh	Change in enthalpy $(h_g - h_x)$	397 Btu/lbm	Calculated
η_{Turb}	Turbine power coefficient	0.65	Calculated
w_{ref}	Reference value of the shaft speed	1 p.u.	
R	Permanent droop	0.05 Hz/MW	
T_1	Valve stroke time constant	0.2 sec	
$\dot{m}_{SO}$	Total steam outlet flow at full power	17.18×10^6 lbm/hr	SYSTEM 80 Table 5.4.2-1

---

[1] Steam exit quality is calculated by utilizing ideal Rankine cycle.

APPENDIX C

MATLAB/SIMULINK FIGURES FOR COMPLETE PWR MODEL
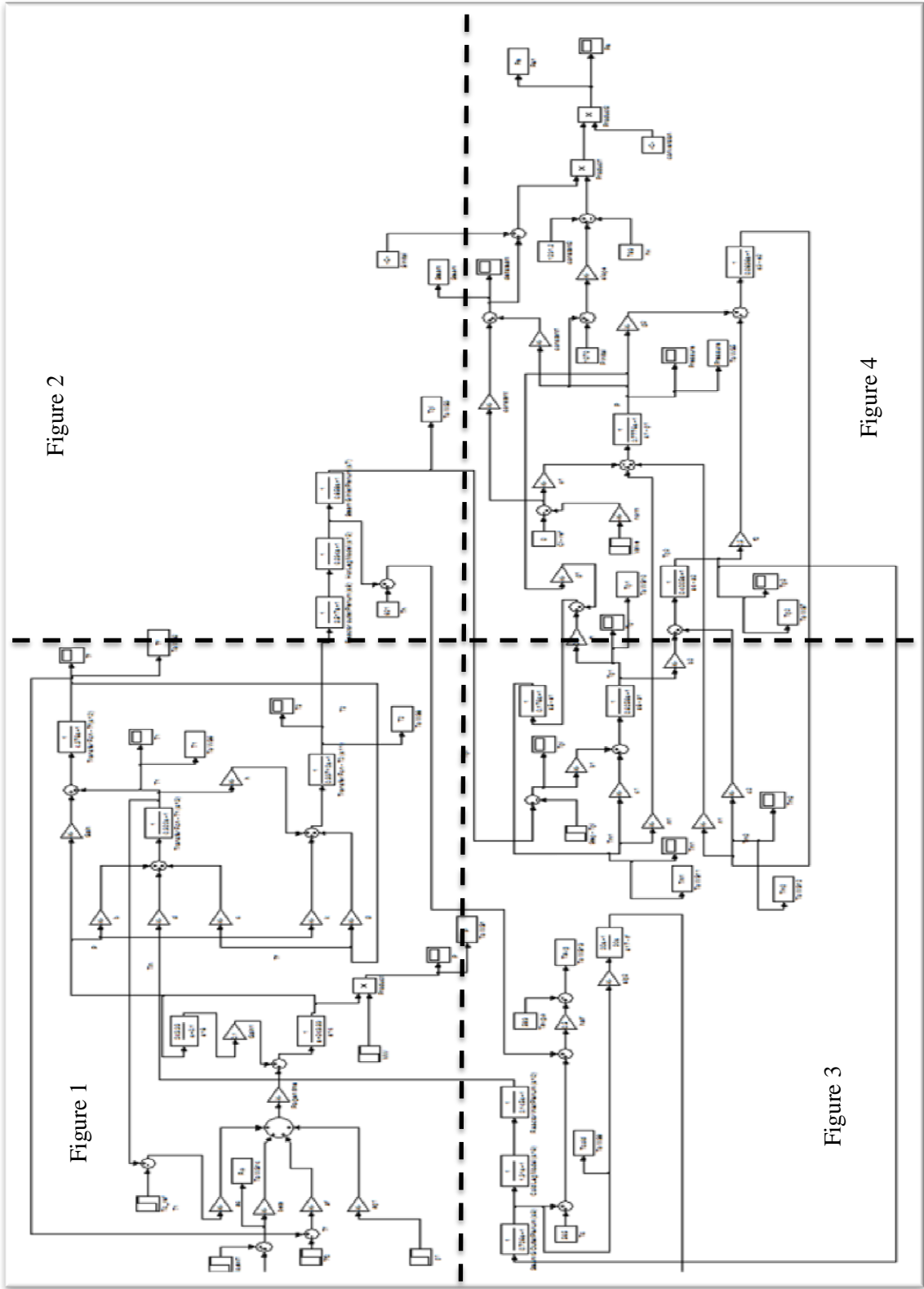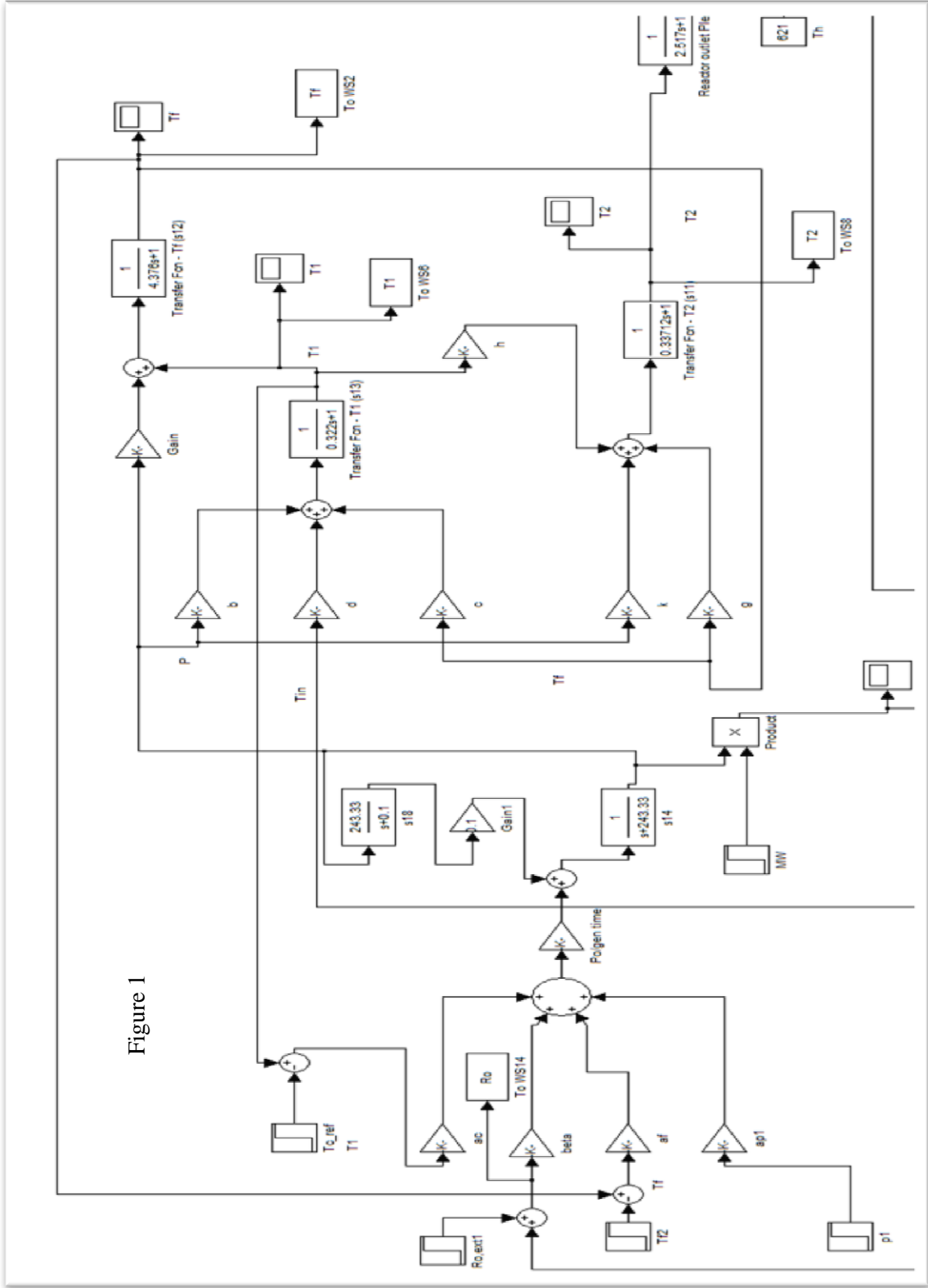
Figure 1

Figure 2

Figure 3

Figure 4

83

Figure 1

84
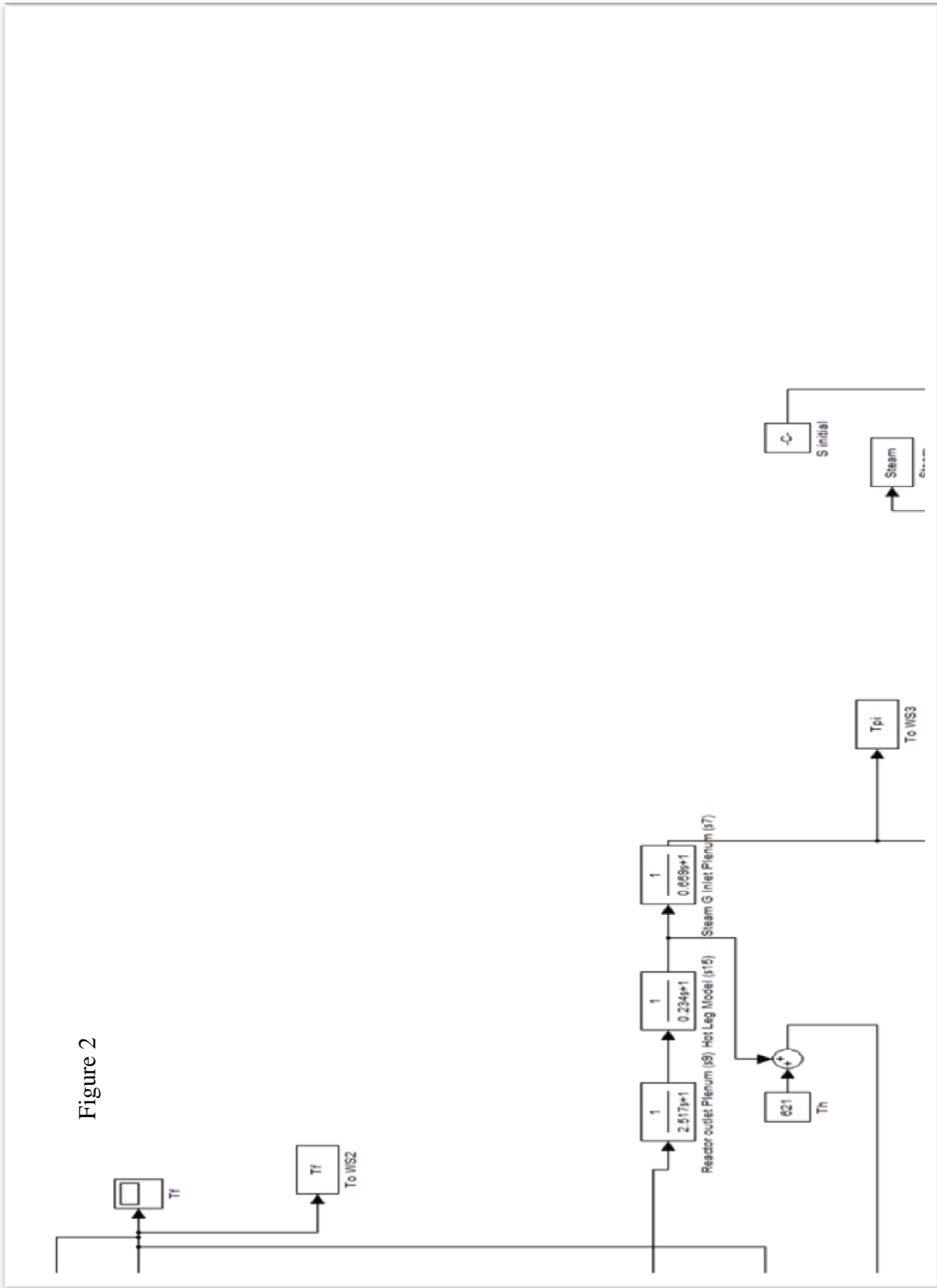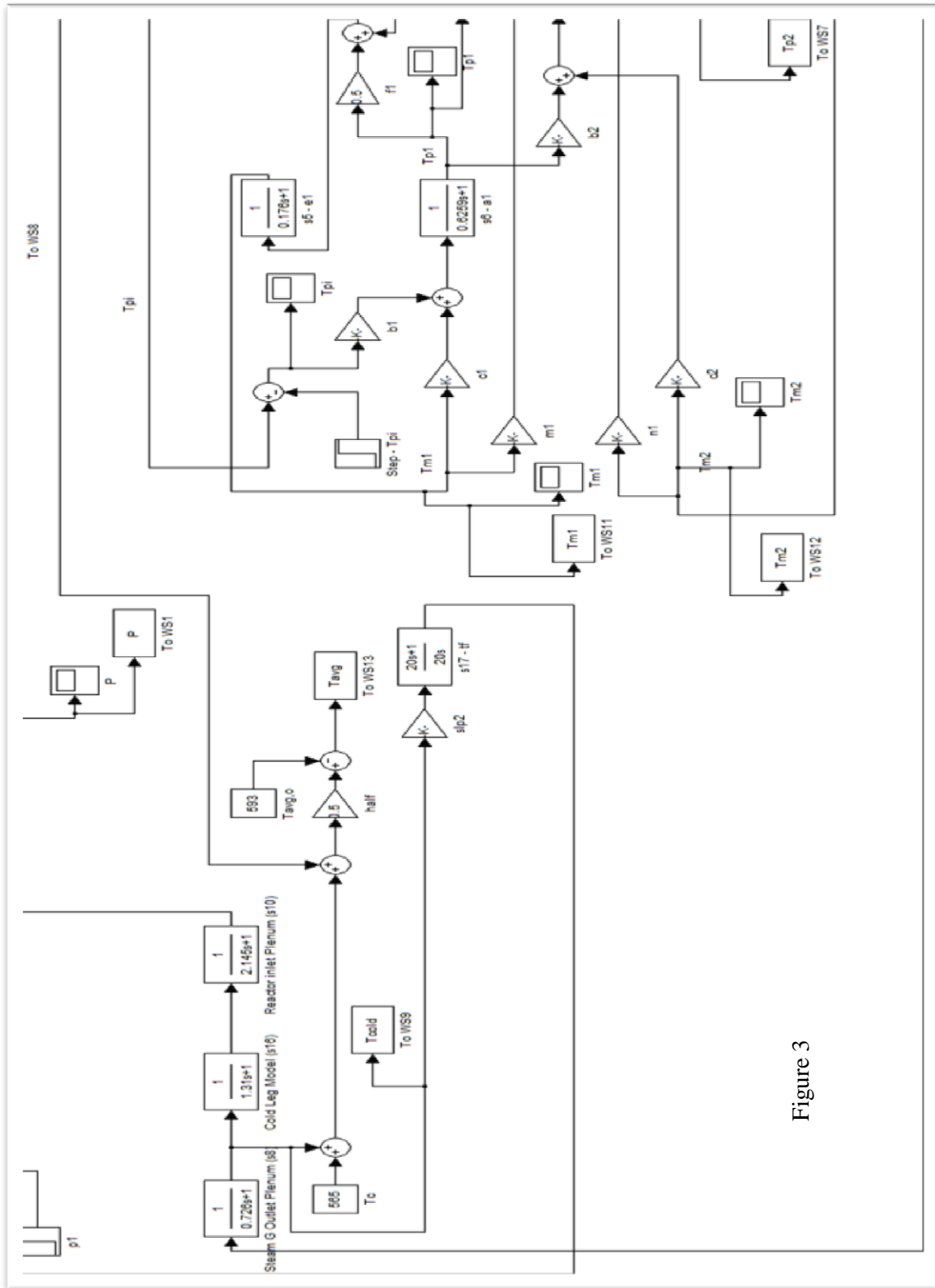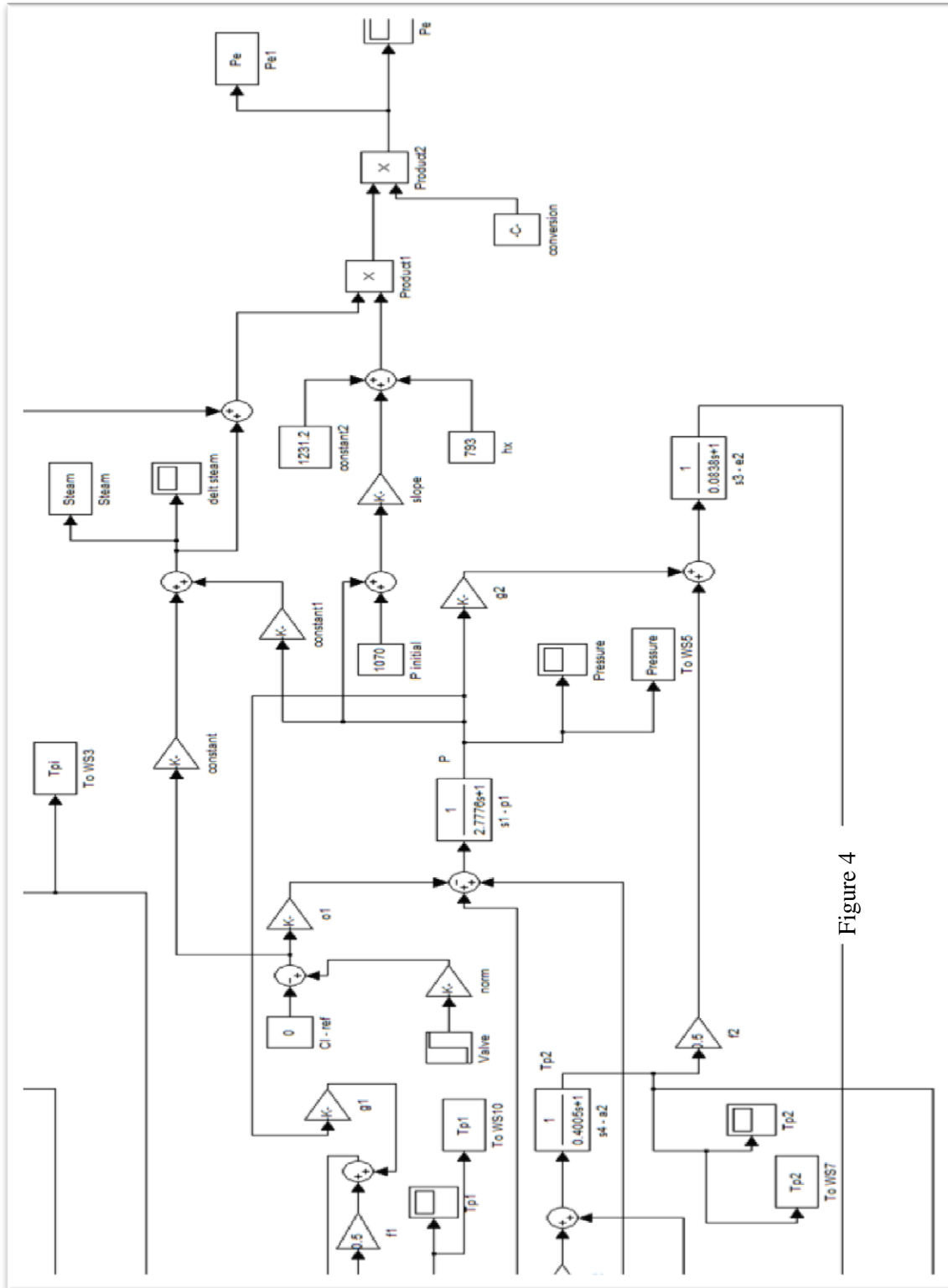
Figure 2

Figure 3

Figure 4

APPENDIX D

PSLF FILES

D.1 PSLF Code for Electrical Network

```
# history file date Fri Nov 30 14:24:31 2012
# present file date Wed Dec 12 16:09:11 2012
# Version 18.1_00
title
A small grid representing Turkey for the simulation
!
comments
!
solution parameters
tap    0   tcul  enabled/disabled
phas   0   ps    enabled/disabled
area   0   area  enabled/disabled
svd    0   svd   enabled/disabled
dctap  0   dc    enabled/disabled
gcd    0   gcd   enabled/disabled
jump  0.000500   jumper threshold
toler  1.0000   newton tolerance
sbase 10000.0000   system mva base
!
bus data [  10]           ty vsched  volt    angle   ar zone  vmax   vmin   date_in date_out pid L  own st  latitude
longitude island   sdmon   vmax1     vmin1      dvmax
    1 "Load_bus  " 400.0000 : 1 1.00000 1.021292 -14.79454  1   1 1.1000 0.9000  400101  391231  0 0  0 0
0.00000  0.00000 0  0.00000   0.00000   0.00000
    2 "bus_2     " 400.0000 : 1 1.00000 1.050003  -6.66732  1   1 1.1000 0.9000  400101  391231  0 0  0 0
0.00000  0.00000 0  0.00000   0.00000   0.00000
    3 "bus_3     " 400.0000 : 1 1.00000 1.059280  -9.30998  1   1 1.1000 0.9000  400101  391231  0 0  0 0
0.00000  0.00000 0  0.00000   0.00000   0.00000
    4 "bus_4     " 400.0000 : 1 1.00000 1.053511  -3.99364  2   1 1.1000 0.9000  400101  391231  0 0  0 0
0.00000  0.00000 0  0.00000   0.00000   0.00000
    5 "bus_5     " 400.0000 : 1 1.00000 1.045948  -5.62386  1   1 1.1000 0.9000  400101  391231  0 0  0 0
0.00000  0.00000 0  0.00000   0.00000   0.00000
    6 "bus_6     " 400.0000 : 1 1.00000 1.025220 -14.65226  3   1 1.1000 0.9000  400101  391231  0 0  0 0
0.00000  0.00000 0  0.00000   0.00000   0.00000
  101 "N_gas_2   "  16.0000 : 2 1.00000 1.000000  1.58972  2   1 1.0500 0.9500  400101  391231  0 0  0 0
0.00000  0.00000 0  0.00000   0.00000   0.00000
  102 "N_gas     "  16.0000 : 0 1.00000 1.000000  0.00000  1   1 1.0500 0.9500  400101  391231  0 0  0 0
0.00000  0.00000 0  0.00000   0.00000   0.00000
  103 "NPP       "  16.0000 : 2 1.00000 1.000000 -7.18428  3   1 1.0500 0.9500  400101  391231  0 0  0 0
0.00000  0.00000 0  0.00000   0.00000   0.00000
  104 "Hydro     "  16.0000 : 2 1.00000 1.000000  1.58972  2   1 1.0500 0.9500  400101  391231  0 0  0 0
0.00000  0.00000 0  0.00000   0.00000   0.00000
branch data [   6]                  ck se ------------long_id_------------  st resist  react  charge  rate1  rate2
rate3  rate4 aloss  lngth
    1 "Load_bus  " 400.00    2 "bus_2     " 400.00 "1 " 1 "                " : 1 0.000000 0.050000 1.000000
0.0   0.0   0.0   0.0 0.000   0.0 /
    1  1 0.000000 0.000000 0.000000 400101  391231  0 0 0  0.0   0.0   0.0   0.0  0 0.000  0 0.000  0 0.000  0
0.000  0 0.000  0 0.000  0 0.000  0 0.000  0 0
    1 "Load_bus  " 400.00    3 "bus_3     " 400.00 "1 " 1 "                " : 1 0.000000 0.050000 1.000000
0.0   0.0   0.0   0.0 0.000   0.0 /
    1  1 0.000000 0.000000 0.000000 400101  391231  0 0 0  0.0   0.0   0.0   0.0  0 0.000  0 0.000  0 0.000  0
0.000  0 0.000  0 0.000  0 0.000  0 0.000  0 0
    2 "bus_2     " 400.00    4 "bus_4     " 400.00 "1 " 1 "                " : 1 0.000000 0.050000 1.000000
0.0   0.0   0.0   0.0 0.000   0.0 /
    2  1 0.000000 0.000000 0.000000 400101  391231  0 0 0  0.0   0.0   0.0   0.0  0 0.000  0 0.000  0 0.000  0
0.000  0 0.000  0 0.000  0 0.000  0 0.000  0 0
    3 "bus_3     " 400.00    4 "bus_4     " 400.00 "1 " 1 "                " : 1 0.000000 0.050000 1.000000
0.0   0.0   0.0   0.0 0.000   0.0 /
```

```
   2   1 0.000000 0.000000 0.000000 400101 391231  0 0 0   0.0   0.0   0.0   0.0  0 0.000  0 0.000  0 0.000  0
0.000  0 0.000  0 0.000  0 0.000  0 0.000 0 0
   5 "bus_5      " 400.00    2 "bus_2      " 400.00 "1 " 1 "                    " : 1 0.000000 0.010000 0.200000
0.0   0.0   0.0   0.0 0 0.000   0.0 /
   1   1 0.000000 0.000000 0.000000 400101 391231  0 0 0   0.0   0.0   0.0   0.0  0 0.000  0 0.000  0 0.000  0
0.000  0 0.000  0 0.000  0 0.000  0 0.000 0 0
   6 "bus_6      " 400.00    1 "Load_bus   " 400.00 "1 " 1 "                    " : 1 0.000000 0.020000 0.400000
0.0   0.0   0.0   0.0 0 0.000   0.0 /
   3   1 0.000000 0.000000 0.000000 400101 391231  0 0 0   0.0   0.0   0.0   0.0  0 0.000  0 0.000  0 0.000  0
0.000  0 0.000  0 0.000  0 0.000  0 0.000 0 0
transformer data [  4]                   ck ------------long_id_------------   st ty --no---   reg_name        zt
int              tert                ar zone tbase ps_r  ps_x  pt_r  pt_x  ts_r  ts_x
   4 "bus_4      " 400.00   101 "N_gas_2    " 16.00 "1 " "                    " : 1 1     0 "        " 0.00 0     0 "
"  0.00     0 "         " 0.00  2   1 1000.000000 0.000000e+000 1.000000e-001 0.000000e+000 0.000000e+000
0.000000e+000 0.000000e+000 /
 400.000000 16.000000 0.000000 0.000000 0.000000e+000 0.000000e+000 1000.0   0.0   0.0   0.0 0.000 0.000000
0.000000 0.000000 0.000000 0.000000 1.025000 1.000000 1.000000 1.000000  400101  391231  0 0    0.0   0.0
0.0   0.0 /
  0 0.000   0 0.000   0 0.000   0 0.000   0 0.000   0 0.000   0 0.000   0 0.000   0 /
  0.000000 0.000000 0.000000 0.000000   0.0   0.0   0.0   0.0   0.0   0.0 0.000 0.000 0 0  0 0 0.0000 0.0000 0
   4 "bus_4      " 400.00   104 "Hydro      " 16.00 "1 " "                    " : 1 1     0 "        " 0.00 0     0 "
"  0.00     0 "         " 0.00  2   1 30000.000000 0.000000e+000 1.000000e-001 0.000000e+000 0.000000e+000
0.000000e+000 0.000000e+000 /
 400.000000 16.000000 0.000000 0.000000 0.000000e+000 0.000000e+000 30000.0   0.0   0.0   0.0 0.000
0.000000 0.000000 0.000000 0.000000 0.000000 1.025000 1.000000 1.000000 1.000000  400101  391231  0 0
0.0   0.0   0.0   0.0 /
  0 0.000   0 0.000   0 0.000   0 0.000   0 0.000   0 0.000   0 0.000   0 0.000   0 /
  0.000000 0.000000 0.000000 0.000000   0.0   0.0   0.0   0.0   0.0   0.0 0.000 0.000 0 0  0 0 0.0000 0.0000 0
   5 "bus_5      " 400.00   102 "N_gas      " 16.00 "1 " "                    " : 1 1     0 "        " 0.00 0     0 "
"  0.00     0 "         " 0.00  1   1 20000.000000 0.000000e+000 1.000000e-001 0.000000e+000 0.000000e+000
0.000000e+000 0.000000e+000 /
 400.000000 16.000000 0.000000 0.000000 0.000000e+000 0.000000e+000 20000.0   0.0   0.0   0.0 0.000
0.000000 0.000000 0.000000 0.000000 0.000000 1.025000 1.000000 1.000000 1.000000  400101  391231  0 0
0.0   0.0   0.0   0.0 /
  0 0.000   0 0.000   0 0.000   0 0.000   0 0.000   0 0.000   0 0.000   0 0.000   0 /
  0.000000 0.000000 0.000000 0.000000   0.0   0.0   0.0   0.0   0.0   0.0 0.000 0.000 0 0  0 0 0.0000 0.0000 0
   6 "bus_6      " 400.00   103 "NPP        " 16.00 "1 " "                    " : 1 1     0 "        " 0.00 0     0 "
"  0.00     0 "         " 0.00  3   1 1000.000000 0.000000e+000 1.000000e-001 0.000000e+000 0.000000e+000
0.000000e+000 0.000000e+000 /
 400.000000 16.000000 0.000000 0.000000 0.000000e+000 0.000000e+000 1000.0   0.0   0.0   0.0 0.000 0.000000
0.000000 0.000000 0.000000 0.000000 1.025000 1.000000 1.000000 1.000000  400101  391231  0 0    0.0   0.0
0.0   0.0 /
  0 0.000   0 0.000   0 0.000   0 0.000   0 0.000   0 0.000   0 0.000   0 0.000   0 /
  0.000000 0.000000 0.000000 0.000000   0.0   0.0   0.0   0.0   0.0   0.0 0.000 0.000 0 0  0 0 0.0000 0.0000 0
generator data [  4]      id ------------long_id_------------   st ---no--   reg_name        prf qrf ar zone pgen  pmax
pmin qgen  qmax  qmin  mbase  cmp_r cmp_x gen_r gen_x         hbus             tbus             date_in
date_out pid N
  101 "N_gas_2    " 16.00 "n1" "                    " : 1   101 "N_gas_2    " 16.00 1.000000 1.000000  2   1
1000.000000  0.000000   0.000000 -229.392059 1000.000000 -1000.000000 1100.0000 0.000 0.000 0.000 0.000     0
"         " 0.00     0 "         " 0.00  400101  391231  0 0 /
 0.0000 0.0000 1.0000  0 0.000  0 0.000  0 0.000  0 0.000  0 0.000  0 0.000  0 0.000  0 0.000   0  0  0  0  0  0  0
0.0 0 0  0.000000
  102 "N_gas      " 16.00 "ng" "                    " : 1   102 "N_gas      " 16.00 1.000000 1.000000  1   1
20000.000000  0.000000   0.000000 -3105.062256 10000.000000 -10000.000000 22000.0000 0.000 0.000 0.000 0.000
  0 "         " 0.00     0 "         " 0.00  400101  391231  0 0 /
 0.0000 0.0000 1.0000  0 0.000  0 0.000  0 0.000  0 0.000  0 0.000  0 0.000  0 0.000  0 0.000   0  0  0  0  0  0  0
0.0 0 0  0.000000
```

```
   103 "NPP       " 16.00 "nr" "                    " : 1   103 "NPP       " 16.00 1.000000 1.000000  3   1
1300.000000  0.000000  0.000000 82.699013 1000.000000 -1000.000000 1333.0000 0.000 0.000 0.000 0.000     0 "
"  0.00    0 "       " 0.00  400101  391231  0 0 /
 0.0000 0.0000 1.0000  0 0.000  0 0.000  0 0.000  0 0.000  0 0.000  0 0.000  0 0.000  0 0.000  0  0  0  0  0  0  0
0.0 0 0  0.000000
   104 "Hydro     " 16.00 "hy" "                    " : 1   104 "Hydro     " 16.00 1.000000 1.000000  2   1
30000.000000  0.000000  0.000000 -6881.761719 15000.000000 -15000.000000 33000.0000 0.000 0.000 0.000 0.000
0 "       " 0.00    0 "       " 0.00  400101  391231  0 0 /
 0.0000 0.0000 1.0000  0 0.000  0 0.000  0 0.000  0 0.000  0 0.000  0 0.000  0 0.000  0 0.000  0  0  0  0  0  0  0
0.0 0 0  0.000000
load data  [  1]        id ------------long_id_------------  st    mw     mvar   mw_i   mvar_i   mw_z    mvar_z  ar
zone  date_in date_out pid N own M nonc  thr_bus flg
   1 "Load_bus  " 400.00 "1 " "                    " : 1 52300.000000 25000.000000 0.000000 0.000000 0.000000
0.000000  1  1  400101  391231  0 0  0 0  0    0 "       " 0.00  0
shunt data  [  8]        id             ck se ------------long_id_------------    st ar  zone   pu_mw  pu_mvar
date_in date_out pid N own part1 own part2 own part3 own part4 --num-- ----name---- --kv-- M --num-- ----name----
--kv--  ID  st
   1 "Load_bus  " 400.00 "f "    2 "bus_2     " 400.00 "1 "  1 "                    " : 0  1   0 0.000000 1.000000
400101  391231  0 0  0 0.000  0 0.000  0 0.000  0 0.000     0 "       " 0.00 " " 0 0
   1 "Load_bus  " 400.00 "t "    2 "bus_2     " 400.00 "1 "  1 "                    " : 0  1   0 0.000000 1.000000
400101  391231  0 0  0 0.000  0 0.000  0 0.000  0 0.000     0 "       " 0.00 " " 0 0
   1 "Load_bus  " 400.00 "f "    3 "bus_3     " 400.00 "1 "  1 "                    " : 0  1   0 0.000000 1.000000
400101  391231  0 0  0 0.000  0 0.000  0 0.000  0 0.000     0 "       " 0.00 " " 0 0
   1 "Load_bus  " 400.00 "t "    3 "bus_3     " 400.00 "1 "  1 "                    " : 0  1   0 0.000000 1.000000
400101  391231  0 0  0 0.000  0 0.000  0 0.000  0 0.000     0 "       " 0.00 " " 0 0
   2 "bus_2     " 400.00 "f "    4 "bus_4     " 400.00 "1 "  1 "                    " : 0  2   0 0.000000 1.000000
400101  391231  0 0  0 0.000  0 0.000  0 0.000  0 0.000     0 "       " 0.00 " " 0 0
   2 "bus_2     " 400.00 "t "    4 "bus_4     " 400.00 "1 "  1 "                    " : 0  2   0 0.000000 1.000000
400101  391231  0 0  0 0.000  0 0.000  0 0.000  0 0.000     0 "       " 0.00 " " 0 0
   3 "bus_3     " 400.00 "f "    4 "bus_4     " 400.00 "1 "  1 "                    " : 0  2   0 0.000000 1.000000
400101  391231  0 0  0 0.000  0 0.000  0 0.000  0 0.000     0 "       " 0.00 " " 0 0
   3 "bus_3     " 400.00 "t "    4 "bus_4     " 400.00 "1 "  1 "                    " : 0  2   0 0.000000 1.000000
400101  391231  0 0  0 0.000  0 0.000  0 0.000  0 0.000     0 "       " 0.00 " " 0 0
area data  [  3]              swing  desired   tol   pnet    qnet
   1 "AREA 1             "  101   0.000   5.000 -32300.000 -9349.500 0
   2 "AREA 2             "  104   0.000   5.000 31000.000 9436.474 0
   3 "AREA 3             "  103   0.000   5.000 1300.000  -86.985 0
zone data  [  1]              pnet    qnet
   1 "Turkey          "   0.000   -0.012 0
end
#
#
#
#This file was written by General Electric International, Inc.
#  PSLF load flow program on Wed Dec 12 16:09:11 2012
#
```

D.2 Dynamic Data for Power Plants

```
#
#          title
#          A small grid representing Turkey for the simulation
#
#
#          area 3 [AREA 3              ]
#
gentpj     103 "NPP"   16.00 "nr" : #9 mva=1333.00 7.0 0.035 0.75 0.035 3.0 0.0 2.1 2.04 0.21 0.4 0.18 0.18 0.12 0.05
0.4 0.0 0.0 -0.01 /
0.5 0.5 0.5
sexs    103 "NPP"   16.00 "nr" : #9 0.1 10.0 100.0 0.05 -5.0 5.0 0.08 0.0 -5.0 5.0 0.0
epcmod  103 "NPP"   16.00 "nr" : #9 "tgov1.p"  3.0000  "ac" -1e-4 "R" 0.0 "beta" 0.0073 "af" -1.2e-5 "A" 1.200926e11
"x" 1.5715e-4 "Tf" 4.376 "d" 0.955 /
          "b" 1.81e-7 "c" 0.045 "T1" 0.322 "h" 0.953 "k" 1.895e-7 "g" 0.047 "T2" .3372 "Trxo" 2.517 "Ti" 2.145
"Trxi" 1.31 "Thl" 0.234 "Tcl" 0.726 "Tpi" 0.659 "b1" /
          0.4884 "c1" 0.5116 "Tp1" 0.6259 "b2" 0.3125 "c2" 0.6875 "Tp2" 0.4005 "f1" 0.5 "g1" 0.0588 "Tm1" 0.176
"f2" 0.5 "g2" 0.0588 "Tm2" .0838 "m1" 2.4249 "n1"    /
          5.0921 "norm" 16091 "o1" 0.0082 "tp" 2.7776 "r" 0.05 "t1" 0.2 "Po" 1070 "SVCo" 16091 "stmo" 17.18e+6
"slp" -0.0385 "conv" 1.906e-7 "B1" 4.108e-4  /
          "Vmax" 0.2 "Vmin" -0.2 "To" 20 "Tci" 565 "Thi" 621 "slp2" 0.0241
#
#
#          area 1 [AREA 1              ]
#
gentpj     102 "N_gas" 16.00 "ng" : #9 mva=22000.00 7.0 0.035 0.75 0.035 3.0 0.0 2.1 2.04 0.21 0.4 0.18 0.18 0.12
0.05 0.4 0.0 0.0 -0.01 /
0.5 0.5 0.5
sexs    102 "N_gas" 16.00 "ng" : #9 0.1 10.0 100.0 0.05 -5.0 5.0 0.08 0.0 -5.0 5.0 0.0
ggov3      102 "N_gas" 16.00 "ng" : #9 mwcap=20000.00 0.04 1.0 1.0 0.1 -0.1 10.0 1.0 0.0 1.0 1.0 0.155 0.5 1.6 0.18
0.2 0.0 1.0 0.0 3.0  /
3.0 1.0 1.0 -2.0 3.3 -3.3 0.0 0.0 0.01 10.0 0.2 0.0 4.0 5.0 99.0 -99.0 0.0 0.0 0.0 0.0 0.0 0.0002 0.1 -0.1 0.00 0.00 0.00
0.00 0.00 0.00  /
0.00 0.00 0.00 0.00
#
#          area 2 [AREA 2              ]
#
gentpj     104 "Hydro" 16.00 "hy" : #9 mva=33000.00 7.0 0.035 0.75 0.035 3.0 0.0 2.1 2.04 0.21 0.4 0.18 0.18 0.12
0.05 0.4 0.0 0.0 -0.01 /
0.5 0.5 0.5
gentpj     101 "N_gas_2" 16.00 "n1" : #9 mva=1100.00 7.0 0.035 0.75 0.035 3.0 0.0 2.1 2.04 0.21 0.4 0.18 0.18 0.12
0.05 0.4 0.0 0.0 -0.01 /
0.5 0.5 0.5
sexs       104 "Hydro" 16.00 "hy" : #9 0.1 10.0 100.0 0.05 -5.0 5.0 0.08 0.0 -5.0 5.0 0.0
sexs    101 "N_gas_2" 16.00 "n1" : #9 0.1 10.0 100.0 0.05 -5.0 5.0 0.08 0.0 -5.0 5.0 0.0
hygov      104 "Hydro" 16.00 "hy" : #9 mwcap=30000.00 0.04 0.3 5.0 0.05 0.5 0.2 1.0 0.0 1.0 1.2 0.5 0.08 0 0 0 0 0 0 0
0 0 0 0 0 0 0 0 0 /
0 0 1.0 0 0 0 0 0 0 0 0 100.0
ggov3      101 "N_gas_2" 16.00 "n1" : #9 mwcap=1000.00 0.04 1.0 1.0 0.1 -0.1 10.0 1.0 0.0 1.0 1.0 0.155 0.5 1.6 0.18
0.2 0.0 1.0 0.0 3.0  /
3.0 1.0 1.0 -2.0 3.3 -3.3 0.0 0.0 0.01 10.0 0.2 0.0 4.0 5.0 99.0 -99.0 0.0 0.0 0.0 0.0 0.0 0.0002 0.1 -0.1 0.00 0.00 0.00
0.00 0.00 0.00  /
0.00 0.00 0.00 0.00
list of out of service models
```

D.3 PSLF Code for Complete PWR Model

```
/***************************************************/
/********  ©2013 Samet Egemen ARDA *****/
/********  All Rights Reserved *****/
/***************************************************/
```

/***** Model comments and data description follow *****

Model input parameters:

epcmod[@mx].ac	moderator temperature coefficient of reactivity
epcmod[@mx].R	reactivity induced by control rods
epcmod[@mx].beta	delayed neutron fraction
epcmod[@mx].af	fuel temperature coefficient of reactivity
epcmod[@mx].A	gain (from reactivity to power)
epcmod[@mx].B1	gain (from reactivity to power)
epcmod[@mx].x	gain (from power to fuel temperature)
epcmod[@mx].Tf	fuel temperature time constant
epcmod[@mx].d	gain (from reactor inlet temperature to coolant node 1 temperature)
epcmod[@mx].b	gain (from reactor power to coolant node 1 temperature)
epcmod[@mx].c	gain (from fuel temperature to coolant node 1 temperature)
epcmod[@mx].T1	coolant node 1 temperature time constant
epcmod[@mx].h	gain (from coolant node 1 temperature to core outlet temperature)
epcmod[@mx].k	gain (from reactor power to core outlet temperature)
epcmod[@mx].g	gain (from fuel temperature to core outlet temperature)
epcmod[@mx].T2	core outlet temperature time constant
epcmod[@mx].Trxo	reactor outlet temperature time constant
epcmod[@mx].Ti	core inlet temperature time constant
epcmod[@mx].Trxi	reactor inlet temperature time constant
epcmod[@mx].Thl	hot leg temperature time constant
epcmod[@mx].Tcl	cold leg temperature time constant
epcmod[@mx].Tci	initial value of cold leg temperature
epcmod[@mx].Thi	initial value of hot leg temperature
epcmod[@mx].slp2	slope of the equation $R = 0.0241*Tavg - 13.619$
epcmod[@mx].To	
epcmod[@mx].Tpi	steam generator inlet temperature time constant
epcmod[@mx].b1	gain (from steam generator inlet temperature to primary lump 1 temperature)
epcmod[@mx].c1	gain (from metal lump 1 temperature to primary lump 1 temperature)
epcmod[@mx].Tp1	primary lump 1 temperature time constant
epcmod[@mx].b2	gain (from primary lump 1 to primary lump 2)
epcmod[@mx].c2	gain (from metal lump 2 to primary lump 2)
epcmod[@mx].Tp2	primary lump 2 temperature time constant
epcmod[@mx].f1	gain (from primary lump 1 to metal lump 1)
epcmod[@mx].g1	gain (from steam pressure to metal lump 1)
epcmod[@mx].Tm1	metal lump 1 temperature time constant
epcmod[@mx].f2	gain (from primary lump 2 to metal lump 2)
epcmod[@mx].g2	gain (from steam pressure to metal lump 2)
epcmod[@mx].Tm2	metal lump 2 temperature time constant
epcmod[@mx].m1	gain (from metal lump 1 to steam pressure)
epcmod[@mx].n1	gain (from metal lump 2 to steam pressure)
epcmod[@mx].norm	valve stroke normalization factor
epcmod[@mx].o1	gain (from steam valve coefficient to steam pressure)
epcmod[@mx].tp	steam pressure time constant
epcmod[@mx].Vmax	maximum steam valve opening
epcmod[@mx].Vmin	minimum steam valve opening

```
epcmod[@mx].r                 droop
epcmod[@mx].t1                valve time constant
epcmod[@mx].Po                initial value of steam pressure
epcmod[@mx].SVCo              initial value of steam valve coefficient
epcmod[@mx].stmo             initial value of steam flow rate
epcmod[@mx].slp               slope of the equation hg = slp*p + 1231.2, hx = 793
epcmod[@mx].conv             power conversion factor
```

invocation in dyd file:

```
epcmod  bus_number bus_name bus_kv model_id : #9  "tgov1.p"  3.0  "ac" -1e-4 "R" 0.0 "beta" 0.0073 "af" -1.2e-5
"A" 1.200926e11 "x" 1.5715e-4 "Tf" 4.376 "d" 0.955 /
        "b" 1.81e-7 "c" 0.045 "T1" 0.322 "h" 0.953 "k" 1.895e-7 "g" 0.047 "T2" .3372 "Trxo" 2.517 "Ti" 2.145
"Trxi" 1.31 "Thl" 0.234 "Tcl" 0.726 "Tpi" 0.659 "b1" /
        0.4884 "c1" 0.5116 "Tp1" 0.6259 "b2" 0.3125 "c2" 0.6875 "Tp2" 0.4005 "f1" 0.5 "g1" 0.0588 "Tm1" 0.176
"f2" 0.5 "g2" 0.0588 "Tm2" .0838 "m1" 2.4249 "n1"    /
        5.0921 "norm" 16091 "o1" 0.0082 "tp" 2.7776 "r" 0.05 "t1" 0.2 "Po" 1070 "SVCo" 16091 "stmo" 17.18e+6
"slp" -0.0385 "conv" 1.906e-7 "B1" 4.108e-4  /
        "Vmax" 0.2 "Vmin" -0.2 "To" 20 "Tci" 565 "Thi" 621 "slp2" 0.0241
```

*** ** End of Model Comments and Data Description *********/

```
define INIT  2
define SORC  3
define ALGE  4
define RATE  5
define OUTP  7
define NETW  8

@mode = dypar[0].mode

@mx   = dypar[0].cmi
@k    = model[@mx].k
@kgen = genbc[@k].kgen

@l = model[@mx].bus

/* end of mandatory setup code */
switch (@mode)

   case SORC:
   break

   case ALGE:
        @dTavg = ((epcmod[@mx].s8) + (epcmod[@mx].s15))/2
        @in =-epcmod[@mx].s8*epcmod[@mx].slp2
        @Ro = @in + epcmod[@mx].s17
        epcmod[@mx].R = @Ro

        @dvsp = epcmod[@mx].s0*epcmod[@mx].Po*epcmod[@mx].norm
        @dpvs = epcmod[@mx].s1*epcmod[@mx].SVCo
        @dstm = @dvsp + @dpvs
        @steam = @dstm + epcmod[@mx].stmo
        @press = epcmod[@mx].s1 + epcmod[@mx].Po
        @dh = @press*epcmod[@mx].slp + 1231.2 - 793
        @btu = @steam * @dh
        genbc[@k].pmech = @btu*epcmod[@mx].conv/gens[@kgen].mbase
   break
```

```
case RATE:
        epcmod[@mx].ds14 =
((epcmod[@mx].ac*epcmod[@mx].s13)+(epcmod[@mx].R*epcmod[@mx].beta)+(epcmod[@mx].af*epcmod[@mx].
s12))*epcmod[@mx].A*epcmod[@mx].B1

        @P =
((epcmod[@mx].ac*epcmod[@mx].s13)+(epcmod[@mx].R*epcmod[@mx].beta)+(epcmod[@mx].af*epcmod[@mx].
s12))*epcmod[@mx].A*epcmod[@mx].B1*10 + epcmod[@mx].s14

        epcmod[@mx].ds12 = ((@P*epcmod[@mx].x) + epcmod[@mx].s13 -
epcmod[@mx].s12)/epcmod[@mx].Tf

        epcmod[@mx].ds13 = (epcmod[@mx].s10*epcmod[@mx].d + @P*epcmod[@mx].b +
epcmod[@mx].s12*epcmod[@mx].g - epcmod[@mx].s13)/epcmod[@mx].T1

        epcmod[@mx].ds11 = (epcmod[@mx].s13*epcmod[@mx].h + @P*epcmod[@mx].k +
epcmod[@mx].s12*epcmod[@mx].g - epcmod[@mx].s11)/epcmod[@mx].T2

        epcmod[@mx].ds10 = (epcmod[@mx].s16 - epcmod[@mx].s10)/epcmod[@mx].Ti

        epcmod[@mx].ds9 = (epcmod[@mx].s11 - epcmod[@mx].s9)/epcmod[@mx].Trxo

        epcmod[@mx].ds16 = (epcmod[@mx].s8 - epcmod[@mx].s16)/epcmod[@mx].Trxi

        epcmod[@mx].ds15 = (epcmod[@mx].s9 - epcmod[@mx].s15)/epcmod[@mx].Thl

        epcmod[@mx].ds17 = @in/epcmod[@mx].To

        epcmod[@mx].ds8 = (epcmod[@mx].s4 - epcmod[@mx].s8)/epcmod[@mx].Tcl

        epcmod[@mx].ds7 = (epcmod[@mx].s15 - epcmod[@mx].s7)/epcmod[@mx].Tpi

        epcmod[@mx].ds6 = (epcmod[@mx].b1*epcmod[@mx].s7 + epcmod[@mx].c1*epcmod[@mx].s5 -
epcmod[@mx].s6)/epcmod[@mx].Tp1

        epcmod[@mx].ds4 = (epcmod[@mx].b2*epcmod[@mx].s6 + epcmod[@mx].c2*epcmod[@mx].s3 -
epcmod[@mx].s4)/epcmod[@mx].Tp2

        epcmod[@mx].ds5 = (epcmod[@mx].f1*epcmod[@mx].s6 + epcmod[@mx].g1*epcmod[@mx].s1 -
epcmod[@mx].s5)/epcmod[@mx].Tm1

        epcmod[@mx].ds3 = (epcmod[@mx].f2*epcmod[@mx].s4 + epcmod[@mx].g2*epcmod[@mx].s1 -
epcmod[@mx].s3)/epcmod[@mx].Tm2

        if ( epcmod[@mx].s0 > epcmod[@mx].Vmax )
                epcmod[@mx].s0 = epcmod[@mx].Vmax
                epcmod[@mx].zs0 = epcmod[@mx].s0
        endif
        if ( epcmod[@mx].s0 < epcmod[@mx].Vmin )
                epcmod[@mx].s0 = epcmod[@mx].Vmin
                epcmod[@mx].zs0 = epcmod[@mx].s0
        endif

        epcmod[@mx].ds0 = ((( genbc[@k].pref - genbc[@k].speed ) / epcmod[@mx].r) - epcmod[@mx].s0 ) /
epcmod[@mx].t1

        if (( epcmod[@mx].ds0 > 0 ) and ( epcmod[@mx].s0 >= epcmod[@mx].Vmax ))
                epcmod[@mx].ds0 = 0
```

```
            endif
            if (( epcmod[@mx].ds0 < 0 ) and ( epcmod[@mx].s0 <= epcmod[@mx].Vmin ))
                    epcmod[@mx].ds0 = 0
            endif

            if ( epcmod[@mx].ds0 >= 0.005)
                    epcmod[@mx].ds0 = 0.005
            endif
            if ( epcmod[@mx].ds0 <= -0.005)
                    epcmod[@mx].ds0 = -0.005
            endif

            epcmod[@mx].ds1 = (epcmod[@mx].m1*epcmod[@mx].s5 + epcmod[@mx].n1*epcmod[@mx].s3 -
epcmod[@mx].norm*epcmod[@mx].o1*epcmod[@mx].s0 - epcmod[@mx].s1)/epcmod[@mx].tp

        break

    case INIT:
            epcmod[@mx].v0 = gens[@kgen].pgen / gens[@kgen].mbase                    /*turbine power*/
            channel_head[0].type = "pm"
            channel_head[0].cmin =  1100
            channel_head[0].cmax = 1500

            epcmod[@mx].s1 = 0                                                       /*pressure*/
            epcmod[@mx].v1 = epcmod[@mx].s1
            channel_head[1].type = "p"
            channel_head[1].cmin = -50
            channel_head[1].cmax = 50

            epcmod[@mx].s0 = 0
            genbc[@k].speed = 1. + epcmod[@mx].r * epcmod[@mx].s0                    /*valve stroke*/
            genbc[@k].pref = genbc[@k].speed
            epcmod[@mx].v2 = epcmod[@mx].s0
            channel_head[2].type = "vs"
            channel_head[2].cmin = -0.2
            channel_head[2].cmax = 0.2

            epcmod[@mx].s3 = 0                                                       /*metal lump 2*/

            epcmod[@mx].s4 = 0                                                       /*primary lump1*/

            epcmod[@mx].v3 = 0                                              /*reactivity change*/
            channel_head[3].type = "ro"
            channel_head[3].cmin = -0.2
            channel_head[3].cmax = 0.2

            epcmod[@mx].s5 = 0                                                       /*metal lump 1*/

            epcmod[@mx].v4 = 0
            channel_head[4].type = "tav"                                   /*average temperature*/
            channel_head[4].cmin = -10
            channel_head[4].cmax = 10

            epcmod[@mx].s6 = 0
            epcmod[@mx].v5 = epcmod[@mx].s6                                          /*primary lump 1*/
            channel_head[5].type = "tp1"
            channel_head[5].cmin = -10
            channel_head[5].cmax = 10
```

```
        epcmod[@mx].s7 = 0                                              /*steam generator inlet temp*/


        epcmod[@mx].s8 = 0                                              /*cold leg temperature*/

        epcmod[@mx].v6 = epcmod[@mx].s8
        channel_head[6].type = "tc"
        channel_head[6].cmin = -10
        channel_head[6].cmax = 10

        epcmod[@mx].s17 = 0                                                 /*controller state*/

        epcmod[@mx].s15 = 0                                              /*hot leg temperature*/

        epcmod[@mx].s16 = 0                                              /*reactor inlet temperature*/

        epcmod[@mx].s9 = 0                                               /*reactor outlet temperature*/

        epcmod[@mx].s10 = 0                                              /*core inlet temperature*/

        epcmod[@mx].s11 = 0                                              /*core outlet temperature*/
        epcmod[@mx].v7 = epcmod[@mx].s11
        channel_head[7].type = "t2"
        channel_head[7].cmin = -10
        channel_head[7].cmax = 10

        epcmod[@mx].s13 = 0                                              /*coolant node 1 temp*/

        epcmod[@mx].s12 = 0
        epcmod[@mx].v8 = epcmod[@mx].s12                                 /* fuel temperature*/
        channel_head[8].type = "tf"
        channel_head[8].cmin = -40
        channel_head[8].cmax = 40

        epcmod[@mx].s14 = 0

        epcmod[@mx].v9 = 0                                               /*reactor thermal power*/
        channel_head[9].type = "P"
        channel_head[9].cmin = -500
        channel_head[9].cmax = 500
    break

    case OUTP:
        epcmod[@mx].v0 = genbc[@k].pmech*gens[@kgen].mbase
        epcmod[@mx].v1 = epcmod[@mx].s1
        epcmod[@mx].v2 = epcmod[@mx].s0
        epcmod[@mx].v3 = @Ro
        epcmod[@mx].v4 = @dTavg
        epcmod[@mx].v5 = epcmod[@mx].s6
        epcmod[@mx].v6 = epcmod[@mx].s8
        epcmod[@mx].v7 = epcmod[@mx].s11
        epcmod[@mx].v8 = epcmod[@mx].s12
        epcmod[@mx].v9 = @P*1.055056e-3                                  /* to convert BTU/s to MW*/
    break

endcase
end
```

APPENDIX E

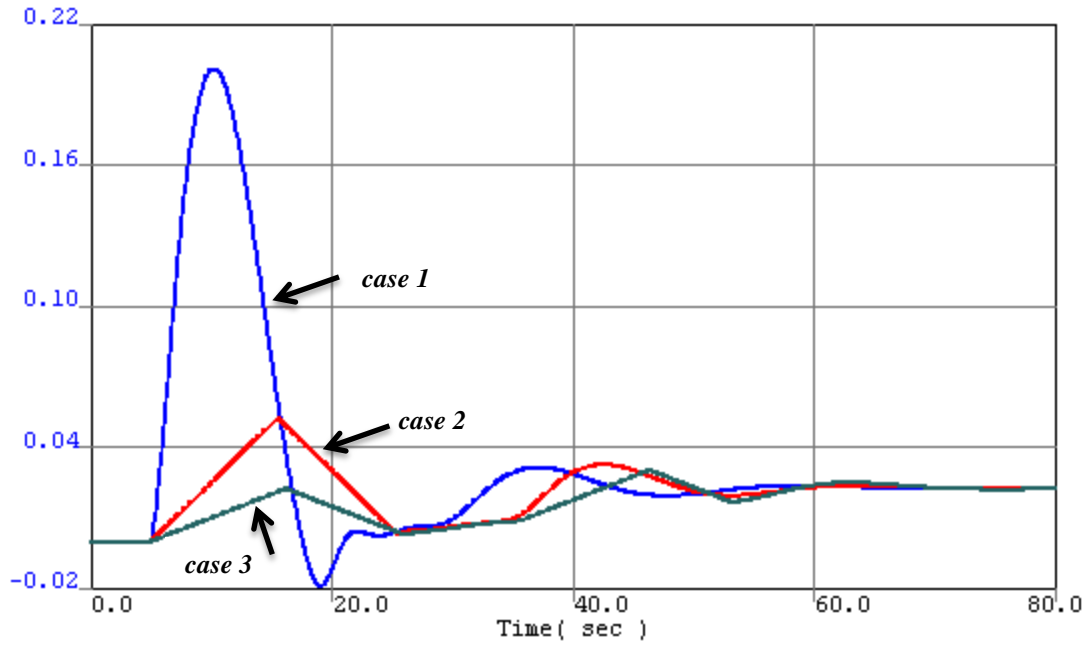ADDITIONAL FIGURES FOR EFFECT OF TURBINE CONTROL

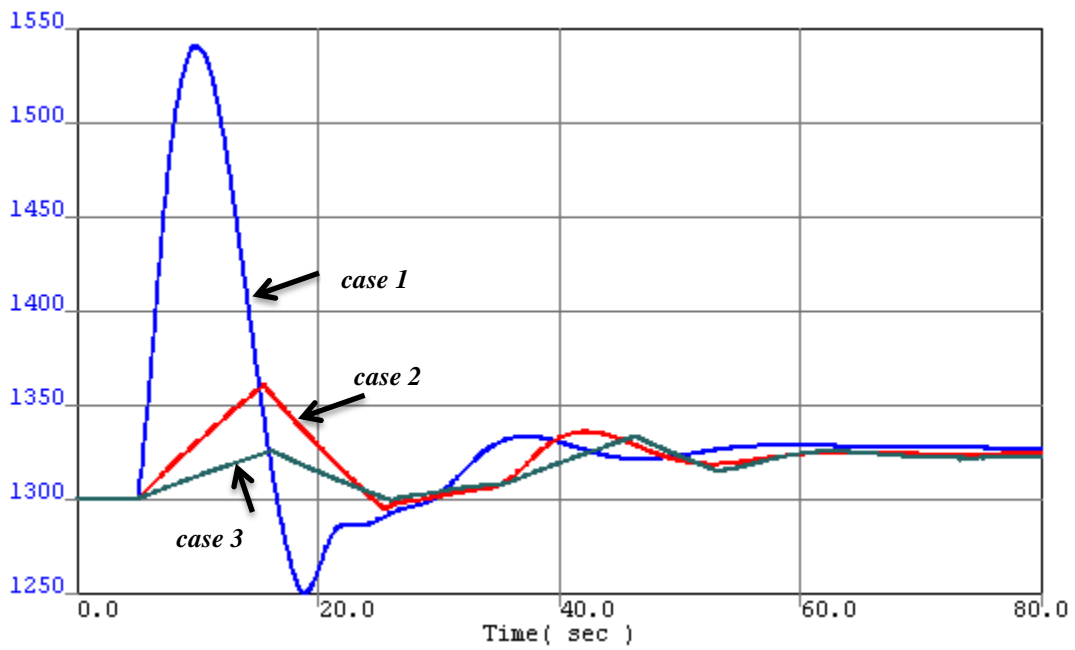Figure E.1Change in the steam valve opening (p.u.).

Figure E.2 Change in the NPP mechanical power (MW).
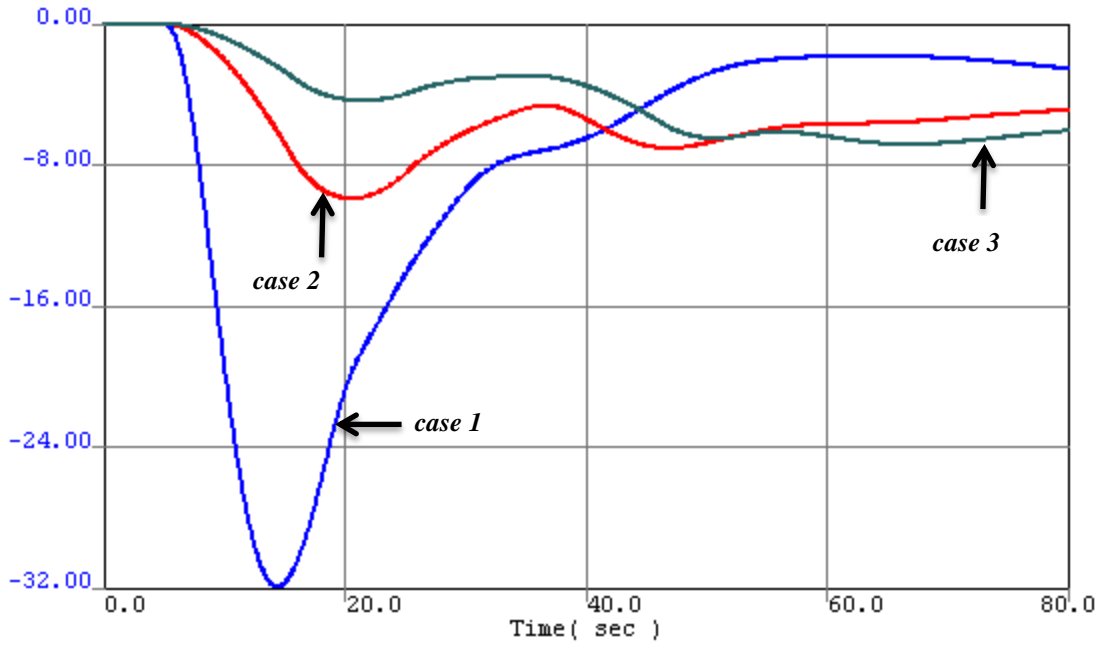
99

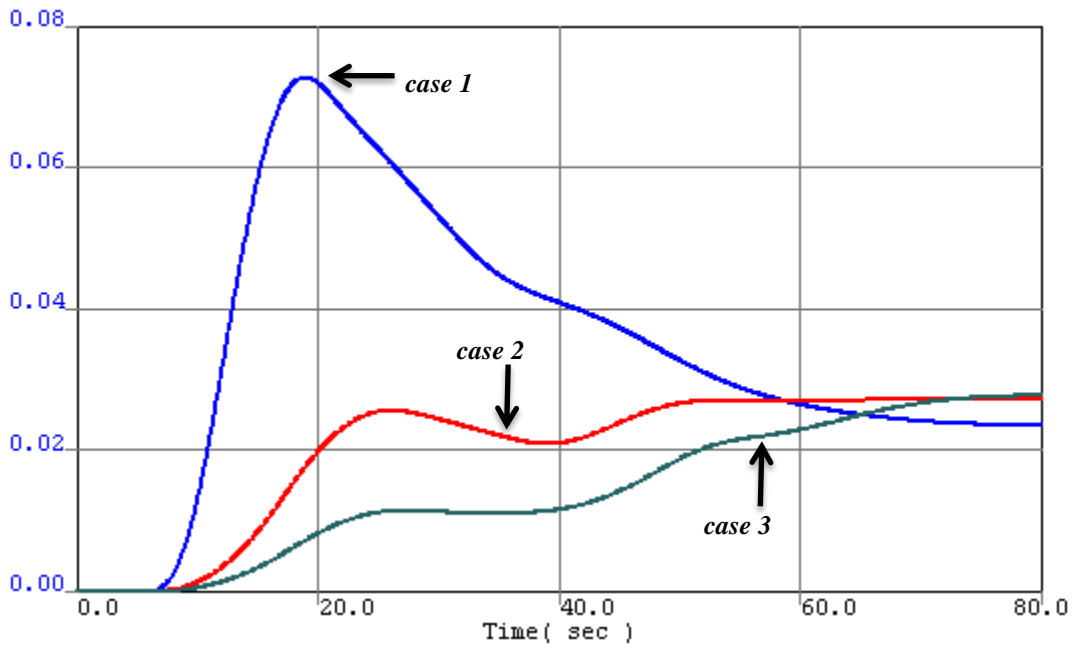Figure E.3 Change in the steam pressure (psi).

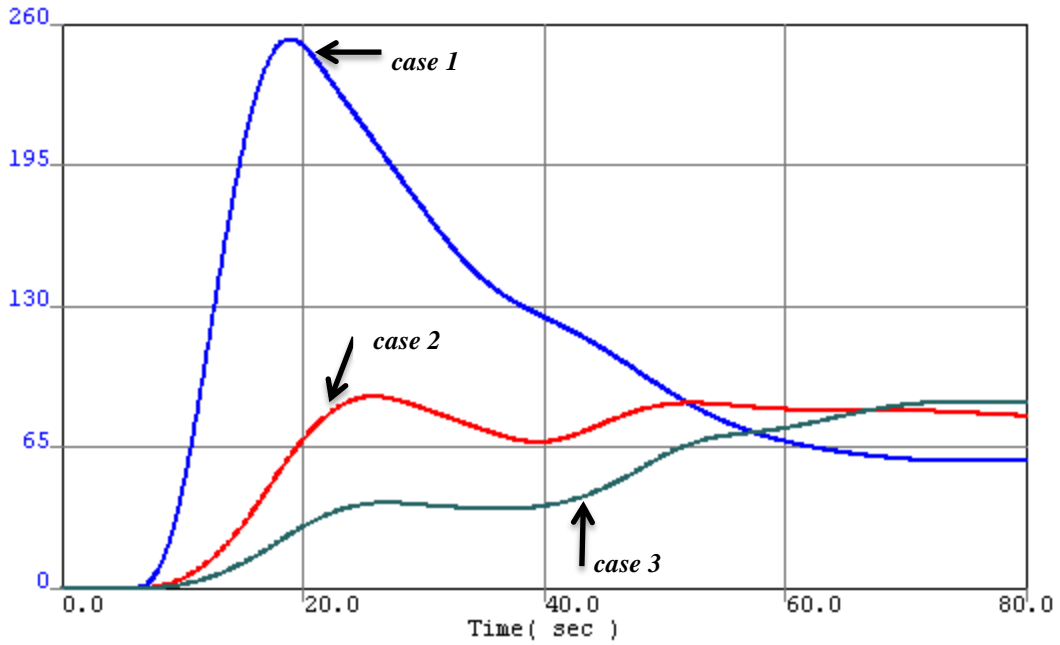Figure E.4 Change in the external reactivity.
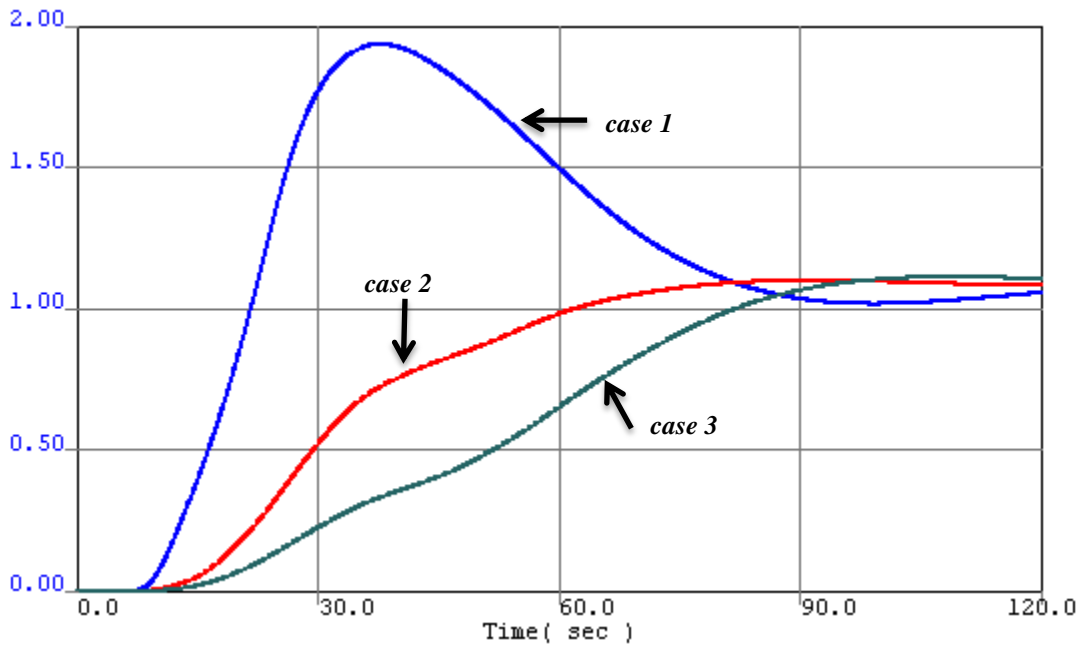
Figure E.5. Change in the reactor thermal power (MW).

Figure E.6 Change in the hot leg temperature (°F).